

# Attempting to enhance sugarcane growth through genetic modification

by

Suzane van der Merwe

*Thesis presented in partial fulfilment of the requirements for the degree Master of Science in  
Plant Biotechnology at the University of Stellenbosch*



Supervisors: Dr Paul N Hills and Dr Christell van der Vyver

Institute for Plant Biotechnology

Department Genetics

March 2016

## **DECLARATION**

By submitting this dissertation electronically, I declare that the entirety of the work contained therein is my own, original work, that I am the sole author thereof (save to the extent explicitly stated), that reproduction and publication thereof by Stellenbosch University will not infringe any third party rights and that I have not previously in its entirety or in part submitted it for obtaining any qualification.

Suzane van der Merwe

March 2016

# Table of Contents

PREFACE .....	IV
Abstract .....	v
Samevatting .....	vi
Part 1 .....	viii
Silencing of the <i>CKX</i> gene family and effects on plant growth .....	viii
Part 2 .....	ix
The effects of acetoin and 2,3-butanediol on disease resistance .....	ix
Thesis outline .....	x
Acknowledgments .....	xi
List of Figures .....	xii
List of Tables .....	xv
List of Abbreviations .....	xvi
CHAPTER 1 .....	2
1.1 Introduction .....	3
1.2 Cytokinin, an important plant phytohormone .....	4
1.2.1 The role of cytokinin in plant growth and development .....	4
1.2.2 Cytokinin metabolism .....	6
1.3 Enhancing plant growth through volatile organic compounds .....	11
1.3.1 Plant growth promoting bacteria .....	11
1.3.2 Different mechanisms to promote growth .....	12
1.3.3 Plant immune responses .....	13
1.3.4 Volatile Organic Compounds .....	16
1.3.5 Acetoin and 2,3-butanediol biosynthesis .....	17
1.4 Project Rationale .....	19
CHAPTER 2 .....	20
2.1 Introduction .....	21
2.1.1 The increase of sugarcane plant growth .....	21
2.1.2 RNA-interference based silencing .....	22

<b>2.2 METHODOLOGY .....</b>	<b>24</b>
2.2.1 Chemicals .....	24
2.2.2 Bacterial growth conditions .....	24
2.2.3 Isolating partial CKX sequences from sugarcane .....	25
2.2.4 Phylogenetic analysis .....	27
2.2.5 Hairpin RNA-interference (hpRNAi) cassette construction .....	28
<b>2.3 RESULTS .....</b>	<b>34</b>
2.3.1 Isolation of partial sugarcane CKX coding sequences .....	34
2.3.2 Phylogenetic analysis .....	35
2.3.3 RNAi assembly attempts .....	38
<b>2.4 DISCUSSION .....</b>	<b>49</b>
2.4.1 Gene silencing in sugarcane .....	49
<b>2.5 CONCLUSIONS .....</b>	<b>55</b>
<b>2.5 ANNEXURES .....</b>	<b>56</b>
Annexure A .....	56
Annexure B .....	58
Annexure C .....	59
Annexure D .....	61
<b>CHAPTER 3 .....</b>	<b>62</b>
<b>3.1 INTRODUCTION .....</b>	<b>63</b>
<b>3.2 MATERIALS AND METHODS .....</b>	<b>64</b>
3.2.1 Bacterial growth conditions and transformations .....	64
3.2.2 Plant growth conditions .....	64
3.2.3 <i>Agrobacterium</i> -mediated plant transformation .....	64
3.2.4 <i>In vitro</i> screening for primary <i>Arabidopsis</i> transformants .....	65
3.2.5 Genotyping putative transformants .....	66
3.2.6 Expression analysis .....	67
3.2.8 VOC Exposure experiments .....	69
3.2.9. Disease development assessments .....	71
3.2.10 Gene marker profile analysis .....	72
3.2.11 Preparation of sugarcane transformation constructs .....	74
3.2.12 Microprojectile Bombardment of Sugarcane Callus .....	75
<b>3.3 RESULTS .....</b>	<b>77</b>
3.3.1 Marker gene selection for sqRT-PCR analysis of ISR .....	77

3.3.2 Confirmation of transgenic <i>Arabidopsis</i> lines	78
3.3.3 Trials with acetoin and 2,3-butanediol	79
3.3.4 Phenotypic response of transgenic lines to <i>Botrytis cinerea</i> inoculation	82
3.3.5 Disease development	87
3.3.6 Gene infection profiling of <i>Botrytis cinerea</i> infected double transgenic AB2 lines	89
3.3.7 Gene expression analysis of single transgenic <i>ALDC</i> plants	90
3.3.8 Expression of <i>ALDC</i> and <i>BDH1</i> in sugarcane	92
<b>3.4 DISCUSSION .....</b>	<b>94</b>
3.4.2 Gene response to fungal infections	96
3.4.3 Exposure to Acetoin and 2,3-butanediol prime certain defence related genes	98
3.4.4 Double transgenic plants exhibit lower resistance	100
<b>3.5 CONCLUSIONS .....</b>	<b>102</b>
<b>3.6 ANNEXURES .....</b>	<b>103</b>
Annexure A	104
Annexure B	105
Annexure C	106
Annexure D	107
<b>CHAPTER 4 .....</b>	<b>108</b>
<b>LITERATURE CITED .....</b>	<b>112</b>

# **PREFACE**

## **Project aim and thesis outline**

## **Abstract**

The current focus of plant breeding is to increase yield and meet the food and energy demands of a growing global population. Progress in this field of study is slow due to the complexity of yield, which is a complex trait governed by an array of different genes and various metabolic pathways. The progress falls drastically short of the increasing commercial demands. Biotechnological approaches can act as an alternative to traditional breeding, to help achieve yield increases that will meet the food and energy demands modern society faces. The purpose of this study was therefore to apply two separate biotechnological methods with the ultimate goal to promote growth in sugarcane.

The well-studied plant phytohormone, cytokinin, has a pivotal role in plant development. Levels of the hormone are regulated by the cytokinin oxidase/dehydrogenase (*CKX*) gene family. The cytokinin oxidase/dehydrogenase enzyme carries the sole responsibility for cytokinin breakdown. This study, therefore, aimed at silencing the *CKX* genes present in sugarcane. The silencing attempt would ideally result in a higher cytokinin level being present in the transgenic plants. In turn, the higher cytokinin levels would then allow for increased plant growth, with the ultimate goal of increasing crop yield. It has been previously reported that silencing of only one of the genes, present in the *CKX* gene family, increases shoot and root weight. In order to silence one, or the majority of the *CKX* gene family, a novel RNA interference-based technology was employed. The method, referred to as the isothermal *in vitro* recombination system (IR-hpRNAi), allows for the assembly of a hairpin containing RNA vector in a single cloning step. It also allowed for the benefit of using the traditional sugarcane transformation vector, pUBI510+, containing an ubiquitin promoter and *CamV* terminator. Due to the novelty of the method in our laboratory, optimization was required. In addition to the IR-hpRNAi method, the traditional GATEWAY® cloning system was also successfully employed for the construction of a hairpin cassette.

The second method employed was based on the introduction of the *ALDC* and *BDH1* gene into *Arabidopsis thaliana* and subsequently into sugarcane. Certain rhizobacterial strains provide plants with enhanced plant health and increased growth. These beneficial rhizobacteria are known as plant growth-promoting rhizobacteria (PGPR). The PGPR are able to do provide the plant with beneficial effects via the release of specific volatile organic compounds (VOCs), amongst other mechanisms. Acetoin and 2,3-butanediol are two of the VOCs known to increase plant growth and disease resistance. To elicit ISR, the volatiles prime expression of specific ethylene- and jasmonic acid-response genes. The *ALDC* and *BDH1* genes are responsible for the synthesis of the two respective VOCs. Increased disease resistance is caused by eliciting an induced systemic response (ISR) in the plant, which in turn

allows the plant to respond quickly and efficiently to infection. An increase in disease resistance links closely to an increase in overall plant growth as it prevents any inhibition or limitation that would have been enforced through successful infection.

Previous research demonstrated an increase in plant growth when transgenic lines, expressing *ALDC* and *BDH1*, were produced. During this study, transgenic *Arabidopsis thaliana* lines were created, expressing the *ALDC* and *BDH1* genes, with the ultimate aim of producing plants with a more effective immune system. To test if the transgenic plants exhibit an increase in pathogen resistance infection trials were conducted by infecting the transgenic AB2 and A3 lines with the necrotrophic, fungal pathogen, *Botrytis cinerea*. Plant resistance was assessed quantitatively by assessing lesion development, and conducting sqRT-PCR analysis on several ISR-related genes. The A3 line, containing only the *ALDC* gene, exhibited a slight increase in disease resistance, while the *ALDC* and *BDH1* containing AB2 line showed a decreased resistance. The study additionally aimed to produce *ALDC* and *BDH1* expressing sugarcane lines that exhibit increased disease resistance, along with plant growth.

## **Samevatting**

Tans is die fokus van plantteling om oes opbrengste van gewasse te verhoog. Daar is 'n sterk toename in voedsel aanvraag as gevolg van die groeiende globale bevolking. Vordering in hierdie studieveld is egter stadig, omdat die genetiese eienskappe wat die metabolismiese prosesse vir opbrengs en groei beheer, baie kompleks is. Die vordering val dus kort van die eise wat die moderne samelewing op die voedsel industrie plaas. Biotegnologie dien as 'n alternatiewe metode vir tradisionele teling. Dit kan moontlik help om voedsel opbrengste te verhoog tot op so 'n punt dat dit voldoende sal wees vir die eise wat moderne samelewing stel. Die doel van hierdie studie was dus om twee afsonderlike biotegnologiese metodes te gebruik om plante groei te verbeter en uiteindelik oes opbrengste te verhoog.

Sedert die ontdekking van sitokinien, is die planthormoon deeglik bestudeer en het dit bekend geraak vir sy sleutelrol in die ontwikkeling van plante. Dit is nou welbekend dat interne sitokinien hormoonvlakke gereguleer word deur die sitokinien oksidase/dehidrogenase (*CKX*) geen-familie. Die sitokinien oksidase/dehidrogenase ensieme wat geproduseer word, is alleenlik verantwoordelik vir die afbreek van sitokinien in plante. Ons studie was dus daarop gemik om *CKX* geenuitdrukking teenwoordig in suikerriet te stil. Dit is gedoen met die doel om 'n hoër vlak sitokiniene te bewerkstellig. Op sy beurt sou die hoër vlakke van sitokinien teenwoordig in die transgeniese suikerriet lei tot verbeterde groei en hoër gewas opbrengste.



Dit is vroeër bewys dat wanneer een van die gene teenwoordig in die CKX geenfamilie verstil word, veroorsaak dit verhoging in plantmasse en wortel gewig. Verstillings van die geen was moontlik met 'n biotegnologies-ontwerpte haarnaald (RNA-georiënteerde inmenging). Die metode, bekend as die isotermiese *in vitro* rekombinasie stelsel (IR-hpRNAi), maak voorsiening vir die bou van 'n haarnaald in 'n toepaslike transformasie vektor. In hierdie spesifieke geval, vir ons studie, het die metode voorsiening gemaak vir die gebruik van die tradisionele suikerriet-transformasie vektor, pUBI510 +, wat 'n *ubiquitine* promotor en *CamV* termineringsgeen insluit. As gevolg van die metode se onbekendheid in ons laboratorium, was die optimalisering daarvan 'n sleutelfaktor. Saam met die IR-hpRNAi metode, is die tradisionele GATEWAY® kloneringsstelsel ook toegepas.

Vir die tweede gedeelte het die studie gefokus op die bevestiging van die *ALDC* en *BDH1* gene in *A. thaliana* en daarna suikerrietplante. Sekere rhizobakterieë verskaf plante met 'n verhoogde immuniteit. Hierdie voordelige rhizobakterieë staan bekend as plant groei-bevorderende rhizobakterieë (PGPR) en laat plante beter groei. Die bakterie verskaf ook 'n versterkte immuunstelsel aan die plant. Een van die maniere waarop hierdie PGPR in staat is om die plante se verbeterde groei en versterkte immuunstelsel te fasiliteer, is deur middel van vlugtige organiese verbindings (VOVs). *Acetoin* en 2,3-butaandiol is twee van die VOVs wat PGPR vrystel. Verhoogde siekteweerstand is die gevolg van 'n geïnduseerde sistemiese immunereaksie (ISR) in die plant. Vir 'n ISR om in die plant plaas te vind moet 'n spesifieke etileen (ET)- en jasmonsuur (JA)-reaksie ontlok word. Vorige studies het bepaal dat die VOVs verantwoordelik is vir die ISR deur die aktivering van spesifieke ET/JA verwante gene (Ryu et al., 2004a; Kwon et al., 2010; Rudrappa et al., 2010). Omdat 'n vorige meestersstudie (Dempers, 2014) reeds 'n toename in plantegroei vasgestel het, toe transgeniese lyne wat die *ALDC* and *BDH1* gene uitdruk bestudeer is, het die huidige studie gefokus op patogeniese weerstand. Gedurende hierdie studie is transgeniese *A. thaliana* lyne geskep, wat die *ALDC* of *BDH1* gene bevat. Hierdie twee gene is verantwoordelik vir acetoin (AC) en 2,3-butaandiol (2,3-BD) produksie. Die uiteindelige doel van die studie was om te toets of die transgeniese plante 'n toename in patogeënweerstand wys. Patogeënweerstand is getoets deur die transgeniese plante te infekteer met die nekrotrofiese swam, *Botrytis cinerea*. Plantweerstand is kwantitatief geassesseer deur die beoordeling van letsel ontwikkeling, asook deur semikwantitatiewe polimerasie-kettingreaksie (skRT-PKR) analise. Die skRT-PKR analise is uitgevoer om die uitdrukkingsvlakke van ISR-verwante gene te bepaal. Die A3 lyn, wat slegs die *ALDC* geen bevat het 'n effense toename in weerstand teen *B. Cinerea* getoon. Aan die ander kant het die AB2 transgeniese lyn, wat albei gene bevat, 'n afname in weerstand getoon.

Hierdie studie was ook daarop gemik om addisionele AB suikerriet lyne, wat beide die *ALDC* en *BDH1* gene uitdruk, te produseer.

## **Part 1**

### **Silencing of the *CKX* gene family and effects on plant growth**

For the first part, the project focused on constructing a RNA-interference vector to silence the expression of sugarcane cytokinin oxidase/dehydrogenase (*CKX*) genes. The *CKX* genes are metabolically responsible for the breakdown of cytokinin in plants. As an important plant hormone that promotes plant growth and development, an increased level of cytokinins would be beneficial for increasing plant growth, and ultimately overall crop yield. A previous study has been conducted in which the *HvCKX1* gene in barley was successfully silenced. A positive correlation between decreased enzyme activity and higher plant mass was observed (Zalewski et al., 2010; Zalewski et al., 2012). The aim of this part of the study was therefore to create a silencing construct with the use of bio-informatical analysis applying a novel method referred to as isothermal *in vitro* recombination (IR-hpRNAi). The silencing construct will then subsequently be used to transform sugarcane. The ultimate goal of this part of the study was to increase plant yield by successfully silencing one or multiple genes from the *CKX* gene family present in sugarcane. This specific method, based on Gibson Assembly® (Gibson, 2011), was applied once before (Jiang et al., 2013), but it was novel to the IPB. This method thus required optimization for future use in the Institute for Plant Biotechnology (IPB) laboratory environment.

*The specific objectives for this part of the study were as follows*

- Employ phylogenetic analysis to identify an appropriate region within *CKX* genes to include in the hairpin construct design.
- Create a *CKX* gene silencing construct through Gibson Assembly® based IR-hpRNAi
- Transform sugarcane and successfully silence one or multiple genes from the *CKX* gene family in sugarcane

## **Part 2**

### **The effects of acetoin and 2,3-butanediol on disease resistance**

Although the beneficial effects of the addition of plant growth-promoting rhizobacteria (PGPR) to the soil in which crops are grown, have been well known for many years, the mechanism through which they interact with the plant have only recently been discovered (Ryu et al., 2004a). Limited research has been done to elucidate the mechanisms through which the rhizobacteria are able to interact with plants and why this is such a successful symbiotic relationship. Recently it has, however, been shown for some strains of PGPR, that communication between plant and bacteria occurs via the release of volatile organic compounds (VOCs) like acetoin and 2,3-butanediol, by the bacteria.

Further research was therefore conducted to determine what would happen if the crop plant was to produce the volatile on its own, cutting out the necessity of additional PGPR application in agriculture. Previous research on transgenic lines confirmed that when *Arabidopsis* was engineered to produce acetoin and 2,3-butanediol, an increase in overall plant growth was found (Dempers, 2014). For this study the focus was on determining how the introduction of the *ALDC* and *BDH1* genes, responsible for volatile production, would influence plant resistance and how increased resistance benefits plant growth.

The second part of this project focused on investigating the disease resistance in transgenic *Arabidopsis thaliana* plants overexpressing the bacterial volatiles acetoin and 2,3-butanediol, before attempting to produce transgenic sugarcane lines overexpressing the relevant *ALDC* and *BDH1* genes.

*The objectives for this part of the study were as follows*

- Produce double transgenic *A. thaliana* plants containing both the *ALDC* (for acetoin production) and *BDH1* (for 2,3-butanediol production) genes.
- Investigate disease resistance, with a particular focus on ISR in double transgenic *Arabidopsis thaliana* plants. This would occur through the infection of plantlets with *Botrytis cinerea* and comparing the disease development between transgenic and wild-type plants.
- Construct appropriate expression vectors containing the *ALDC* and *BDH1* genes respectively, for the generation of transgenic sugarcane lines producing acetoin and 2,3-butanediol.

## **Thesis outline**

### **This thesis is divided into the following chapters:**

- Chapter 1:* In the first chapter a literature overview is given firstly on cytokinin and the discovery, function and biochemistry of cytokinin oxidase/dehydrogenase genes. It discusses sugarcane as an important global crop and how higher levels of cytokinin present in the plant can aid in achieving increased yields. The second part introduces plant growth promoting rhizobacteria, the volatile organic compounds they produce and studies that have shown the effects of these volatiles on plant growth and disease resistance. It also discusses acetoin and 2,3-butanediol as commercial compounds and why these volatiles are thought to be beneficial for plants.
- Chapter 2:* The chapter consists of a short Introduction, Materials and Methods, as well as a Results section. This is followed by a Discussion of the results and a brief Conclusion. The focus is on the work done to establish the Gibson Assembly® IR-hpRNAi method as a means of creating a silencing gene cassette, as well as the phylogenetic analysis of the *CKX* gene family.
- Chapter 3:* The chapter consists of a short Introduction, Materials and Methods, as well as a Results section. This is followed by a Discussion of the results and a brief Conclusion. In this chapter, the focus is specifically on investigating enhanced disease resistance in the transgenic *Arabidopsis* plants expressing the *ALDC* and *BDH1* genes. The results observed whilst investigating a disease in resistance in transgenic *Arabidopsis* plants are discussed. The process of producing transgenic sugarcane plants containing the *ALDC* and *BDH1* genes responsible for volatile production is also initiated.
- Chapter 4:* General conclusions are made from the results presented in Chapters 2 and 3. Future work which will aid in filling the gaps identified in this study is also discussed.

## **Acknowledgments**

The study benefited from various inputs throughout its course and it is my honour to acknowledge the following people for their contribution to this study.

- I would like to start by thanking both my supervisors, Dr Paul N. Hills and Dr Christell van der Vyver for their advice and patience during this study. Thank you for believing in me, even when I didn't believe in myself.
- To Dr Kenneth Oberlander for assisting me with the phylogenetic analysis.
- To Benjamin Cloete from the Department of Plant Pathology for his assistance in optimizing my *B. cinerea* infection protocol.
- To both my parents. For all that you have done, may God bless you both.
- A word of thanks for Dr Inonge Mulako and Ruan De Villiers for helping me stay motivated when the mountains I faced seemed too overwhelming to climb.
- A special word of thanks to Dr Lynn Hoffman for encouraging me to follow my dreams, always believing in me and acting as a perfect role model to a young female scientist, like myself.
- Thank you to Prof Jens Kossmann for allowing me the opportunity to complete my Master's thesis at the Institute for Plant Biotechnology.
- A word of acknowledgement to the National Research Fund, as well as the Erasmus Trust for financial support.
- Finally, I dedicate this thesis to Helenius Postma, Senior, my loving grandfather in all but blood. I miss you every single day, Oupa. I wish with all my heart for another Friday evening, laughing in the Wimpy with you next to me. I know you are keeping God busy with your philosophy in heaven and I hope to join you at His feet one day. I hope this thesis testifies of the immeasurable impact you had on my life.

## **List of Figures**

### **Chapter 1**

Figure 1.1	Different chemical structures of naturally occurring cytokinins and synthetic cytokinins	4
Figure 1.2	The MonoQ figure as presented in Bileyu et al., (2001)	8
Figure 1.3	The acetoin and 2,3-butanediol biosynthesis pathway, present during bacterial fermentation	17

### **Chapter 2**

Figure 2.1	A visual representation of the 4 sugarcane partial <i>CKX</i> gene fragments through amplification with the sorghum-based primers	34
Figure 2.2	A phylogenetic tree representing 57 coding sequences of plant cytokinin dehydrogenases (CKXs), from 11 different plant species	36
Figure 2.3	The newly isolated SugarcaneCTKD sequence included in RNAi vector design	37
Figure 2.4	PCR amplification of the sense and anti-sense gene specific fragments used for creating the hpRNAi construct	39
Figure 2.5	The colony PCR conducted on 7 colonies produced after the first cloning attempt of the hairpin cassette	40
Figure 2.6	Gel electrophoresis of assembly attempt with sense and antisense fragments for different time intervals	40
Figure 2.7	Analysis of the isothermal in vitro recombination - attempt 3	41
Figure 2.8	Analysis of the Gibson assembly cloning kit reaction	42
Figure 2.9	Analysis of isolated plasmid DNA from 3 separate colonies generated by the Gibson assemble kit	42
Figure 2.10	<i>Bam</i> HI restriction on the 9 remaining colonies from attempt 3	44
Figure 2.11	Transformation of the positive control, included in attempt 4	45
Figure 2.12	A visualisation of the successful Gibson Assembly reaction (attempt 6) on a 2% agarose gel	46
Figure 2.13	A visual representation of the <i>Xho</i> I digestion to confirming A and C as positive clones	47

Figure 2.14	Insert confirmation of possible positive RNAi vector clones, with restriction digest	48
Figure 2.15	PCR confirmation of potentially positive RNAi hairpin constructs, A and C	49

### Chapter 3

Figure 3.1	An example of the <i>in vitro</i> screening for transformants	66
Figure 3.2	Assessment of the effects of volatile acetoin and 2,3-butanediol on <i>B. cinerea</i> growth directly	70
Figure 3.3	A visual representation of the predesigned lesion scoring system used during lesion evaluation	71
Figure 3.4	sqRT-PCR results illustrating gene response profiles	78
Figure 3.5	Confirmation of gene expression for the <i>ALDC</i> and <i>BDH1</i> genes in putative transgenic <i>A. thaliana</i> plants.	79
Figure 3.6	<i>Botrytis</i> infected <i>Arabidopsis</i> leaves from acetoin and 2,3-butanediol treated plants	79
Figure 3.7	sqRT-PCR analysis on the water, acetoin and 2,3-butanediol treated <i>Arabidopsis</i> plants, 24 and 48 hours post inoculation with <i>B. cinerea</i>	80
Figure 3.8	<i>B. cinerea</i> disease development of double transgenic <i>Arabidopsis</i> plants containing the <i>ALDC</i> and <i>BDH1</i> genes (Line AB2), as seen on Day 1, 2, 5 and 7 post inoculation	84
Figure 3.9	Disease development in the single expressing <i>ALDC</i> -line, A3 and the single expressing <i>BDH1</i> -line, B8 post infection with <i>B. cinerea</i>	85
Figure 3.10	Close up example of <i>Arabidopsis</i> leaves with different diseased phenotypes post <i>B. cinerea</i> inoculation.	86
Figure 3.11	The lesion diameter for the AB2, A3, B8 and WT lines, 24 h (Day 1), 48 h (Day 2) and 72 h (Day 3) post inoculation with <i>B. cinerea</i> , is plotted	88
Figure 3.12	A score was awarded for the AB2, A3, B8 and WT lines, 24 h (Day 1), 48 h (Day 2) and 72 h (Day 3) post inoculation with <i>B. cinerea</i>	88
Figure 3.13	Semi-quantitative RT-PCR analysis of <i>B. cinerea</i> infected double expressing <i>ALDC</i> and <i>BDH1</i> AB2 line	91

Figure 3.14	Semi-quantitative RT-PCR analysis of <i>B. cinerea</i> infected transgenic line A3 plants	92
Figure 3.15	<i>pUBI::FNR:ALDC</i> and <i>pUBI::FNR:BDH1</i> positive transformants	93



## **List of Tables**

### **Chapter 2**

Table 2.1	Primer pairs for the amplification of the partial sugarcane <i>CKX</i> gene fragments	25
Table 2.2	General PCR conditions used during <i>CKX</i> gene fragment isolations	26
Table 2.3	Primer sequences, as designed for sense and antisense hairpin fragment amplification	28
Table 2.4	General PCR conditions for the use of Q5® High-Fidelity DNA Polymerase	30
Table 2.5	pUBI510+ sugarcane transformation vector specific primers	31
Table 2.6	All the different chemicals, with the respective concentrations that were combined to create the Gibson Assembly One-Step 5x ISO Buffer	32
Table 2.7	The different components required for a 2x IR reaction buffer according to Gibson (2011)	33
Table 2.8	The different DNA concentrations added for Attempt 3 at an isothermal <i>in vitro</i> recombination and assembly of an hpRNAi construct	40
Table 2.9	Attempt 4 experimental set up	45

### **Chapter 3**

Table 3.1	Gene specific primers for genotyping of potential transgenic plants	68
Table 3.2	The specific primers that were designed to amplifying a 500 bp fragment during sqRT-PCR analysis	73
Table 3.3	The average lesion development observed in <i>B. cinerea</i> infected plants for each time point	81

## **List of Abbreviations**

2,3-BD	2,3-butanediol
°C	Degrees Celsius
µg	Microgram
µm	Micrometer
µmol	Micromole
µg/mL	Microgram per milliliter
µL	Microliter
µmoles	Micromoles
AC	Acetoin
ALDC	α-Acetolactate decarboxylase
AHLs	Acyl-homoserine lactones
Avr	Avirulence
BDH1	Acetoin reductase/2,3-butanediol dehydrogenase
bp	Base pair
CaMV	Cauliflower mosaic virus
cDNA	Complementary deoxyribonucleic acid
CKX	Cytokinin oxidase/dehydrogenase
cm	Centimeter
CMV	Cucumber mosaic virus
CPPU	N-(chloro-4-pyridil)-N-phenylurea
d	Day
dH <sub>2</sub> O	Distilled water
DNA	Deoxyribonucleic acid
dNTP	Deoxynucleotide triphosphate
DPI	Diphenyliodonium
dpi	Days post inoculation

DZ	Dihydrozeatin
EDTA	Ethylene diaminetetra acetic acid
epsp	5-enolpyruvylshikimate-3-phosphate synthase
ÉT	Ethylene
FAD	Ferredoxin reductase binding domain
FMN	Flavin mononucleotide
FNR	Ferredoxin-NADP <sup>+</sup> reductase
gDNA	Genomic deoxyribonucleic acid
g/L	Grams per liter
GUS	B-glucuronidase
h	Hour
HCl	Hydrogen chloride
hpi	Hours post inoculation
HR	Hypersensitive response
IM	Isomaltulose
iP	Isopentenyladenine
IPB	Institute for Plant Biotechnology
IR	<i>In vitro</i> recombination
ISR	Induced systemic resistance
JA	Jasmonic acid
kDA	Kilodalton
KOH	Potassium hydroxide
kPa	Kilopascal
LB	Luria-Bertani (medium)
m	Meter
M	Molar
mg/L	Milligram per liter
ml	Milliliters

mm	Millimeters
MS	Murashige and Skoog (medium)
m/v	Mass per volume
NaCl	Sodium chloride
NahG	Salicylate hydroxylase
NEB	New England Biolabs
ng	Nanogram
OD	Optical density
PCR	Polymerase Chain Reaction
pg	Picogram
QS	Quorum sensing
R	Plant-encoded resistance
PCR	Polymerase chain reactions
PDA	Potato dextrose agar
PGPR	Plant growth promoting rhizobacteria
PR	Pathogenesis-related
RACE	Rapid Amplification of cDNA Ends
RNA	Ribonucleic acid
rpm	Revolutions per minute
s	Second
SA	Salicylic acid
SAR	Systemic Acquired Resistance
SDS	Sodium dodecyl sulfate
sqRT-PCR	Semiquantitative reverse-transcription polymerase chain reaction
T <sub>m</sub>	Melting temperature
TMV	Tobacco mosaic virus
TNV	Tobacco necrosis virus
U/μL	Units per microliter

UV	Ultra violet
VOC	Volatile organic compound
WT	Wild-type
z	Zeatin
ZR	Zeatin riboside

# **CHAPTER 1**

## **Literature Review**

## **1.1 Introduction**

Approximately 75% of the world's sugar harvested for human consumption originates from the sugarcane crop (Falco et al., 2000; Wu and Birch, 2007). In tropical and sub-tropical countries sugarcane production plays a vital economic role. Apart from sugar beet, sugarcane is unique amongst plants as it stores sucrose instead of a polymeric compound. Recently the crop increased in importance due to its potential use as a second generation biofuel. Sugarcane was shown to be the industrial crop with the highest potential to act as a renewable energy source (Pimentel and Patzek, 2005). It is now regarded as one of the most important cash crops in the world. Sugar yield from this crop is therefore a key determinant of its economic value and environmental sustainability. Consequently, research is focussing on sugarcane crop improvement. The hope is that cultivars can be produced for higher sucrose yields, without having to increase marginal costs related to harvesting and milling of the crop.

Both traditional breeding and molecular approaches have been applied to try and increase the sucrose levels and improve plant growth. Slow progress was seen in the attempt to increase the stored sucrose levels. Despite an intense focus on this, research has not been able to increase the endogenous sucrose levels in elite sugarcane cultivars for the past decade. Due to the slow progress, genetic engineering is currently employed in sugarcane crop improvement. Attempts to alter sugar metabolism in the plant through the modification of plant genes have been troublesome (Wu and Birch, 2007). Elite cultivars seem to be able to counter the increase with sufficient control mechanisms, when single sugarcane genes are manipulated. A different approach was attempted by a research group from Brisbane, Australia. The aim was to modify the sugarcane by introducing a bacterial isomerase enzyme into the plant system. The plant system then produces isomaltulose (IM) from sucrose, which is only metabolized by humans, but not the plant itself. The IM also contain various health benefits above those of sucrose. It is digested more slowly, because it is resistant to breakdown by a salivary invertase. Rather, it is digested by an intestinal disaccharidase. This allows for less of a fluctuation in blood sugar levels and insulin concentrations (Lina et al., 2002; Wu and Birch, 2007). The study showed that the IM is accumulated in storage organs and resulted in twice the sugar yield when harvested. It was therefore possible to lift the former ceiling of sugar storage in sugarcane cultivars (Wu and Birch, 2007).

Over the past two decades various different transgenic sugarcane lines have been produced, with plants now containing transgenes to improve sugarcane mosaic virus resistance, insect resistance and herbicide resistance (Falco et al., 2000). Examples of these successes include the introduction of the *bar* gene that produce transgenic lines tolerant to glufosinate ammonium containing herbicides (Falco et al., 2000). In a separate study conducted more

recently, the *cry1A* gene was introduced, conferring insect resistance (Rapulana and Bouwer, 2013). The successful introduction of the synthetic CP4 *epsps* gene (5-enolpyruvylshikimate-3-phosphate synthase from *Agrobacterium* sp. strain CP4), enabling glyphosate tolerance, from *Agrobacterium* was shown, conferring herbicide resistance (Noguera et al., 2015). The Argentinian research group successfully produced six lines that showed stable inheritance of the *epsps* gene and was also able to conduct field tests on these lines. All of these genes hold commercial interest for the sugarcane industry. Despite all the progress, only one genetically engineered sugarcane cultivar has officially been released for commercial use. This transgenic sugarcane was released in Indonesia in 2013, and is a variety with increased drought resistance (Noguera et al., 2015).

## **1.2 Cytokinin, an important plant phytohormone**

### **1.2.1 The role of cytokinin in plant growth and development**

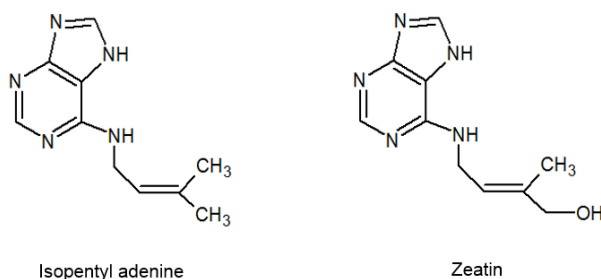
More than half a century ago, cytokinin was identified as a plant hormone involved in plant cell division. The discovery of the hormone occurred by accident after a compound was identified that positively regulated cell division, a process now referred to as cytokinesis. It was discovered shortly after the identification of kinetin in autoclaved herring sperm (Miller et al., 1956). The discovery of kinetin was followed by that of isoprenoid cytokinins and their derivatives modified at the second carbon of the aromatic ring (Yuldashev et al., 2012). After its discovery, the hormone was intensively studied and has been linked to the regulation of cell division, the stimulation of leaf expansion, seed dormancy and senescence (Mok et al., 2000). Recent studies have shown that cytokinin is able to influence plant physiology in such a broad way due to its regulation of the cell-cycle (Werner et al., 2001; Schmölling et al., 2003; Malito et al., 2004).

This hormone family is chemically described as N<sub>6</sub>-substituted purine derivatives, consisting of three predominant natural forms namely isopentenyladenine (iP), zeatin (Z) and dihydrozeatin (DZ). Various synthetic structures also exist including kinetin and benzyladenine (Figure 1.1). Different types of the hormone are formed by different substitutions at the 6<sup>th</sup> position in the purine ring. This position is mainly substituted with an isoprenoid or an aromatic side chain. Early in the previous decade, over 35 naturally occurring cytokinins had been identified (Mok and Mok, 2001). The most commonly known physiologically active conjugate with an aromatic side chain is N<sup>6</sup>-benzyladenine (Malito et al., 2004). The isoprenoids can



either be saturated or unsaturated (Spíchal, 2012). Glycosidic conjugates have been shown to inactivate the hormone reversibly, as well as irreversibly and have been shown to aid in the transport of the hormone through the plant system (Werner et al., 2001; Qin et al., 2011)

a.



b.

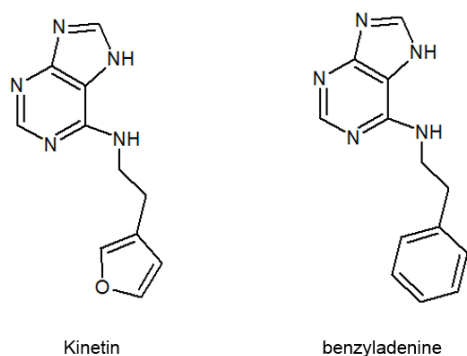


**Figure 1.1:** Different chemical structures of a) naturally occurring cytokinins and b) synthetic cytokinins

Much research has been focused on the stereochemistry of zeatin, with *trans*-zeatin being the first naturally-occurring cytokinin to be identified. Additionally, it was thought to be the most abundant of all the natural cytokinins. During the past 10 years this hypothesis has, however, been challenged with studies finding *cis*-zeatin to be the predominant zeatin in several plant species including potato (Nicander et al., 1995), maize (Mok and Mok, 2001) and rice (Kojima et al., 2009). In a recent review, it was shown that both were abundant in *Arabidopsis* plants but during different stages of growth, with the *trans*-zeatin being more prevalent during active growth and *cis*-zeatin during developmental stages (Murai, 2014). Despite the advances made over the past 10 years, the exact physiological function of these zeatin type cytokinins and how this correlates to abundance is not clear. The biosynthetic pathway of *cis*-zeatin is described as a fundamental research question that remains to be answered for crop plants like maize (Murai, 2014).

As mentioned before, cytokinin plays a pivotal physiological role in plant growth and development as demonstrated by Skoog and Miller in 1957. It was established that cytokinin positively influences shoot development, but inhibits the developments of roots. Auxin demonstrated the opposite effect (Miller et al., 1956). The relationship between cytokinin and auxin has been well characterized through a series of classic tissue culture experiments (Hwang et al., 2012). The cross-talk between the two hormone groups plays an especially important role during embryogenesis, where even if they initiate different structure developments, the antagonistic relationship ensures efficient and complete development. Cross-talk has been shown to occur not only throughout embryogenesis; distinct interactions between the two hormones have been identified in the root meristem, as well as the shoot meristem. Additionally the antagonistic relationship has been shown to induce xylem and phloem differentiation (Hwang et al., 2012).

### **1.2.2 Cytokinin metabolism**

Due to the importance of this phytohormone, a finely regulated balance between biosynthesis and degradation is required. Cytokinins have a half-life spanning of a few hours, and the hormone is thus rapidly metabolized endogenously (Suttle and Mornet, 2005). Further investigation indicated that cytokinins are metabolised through both the reversible and irreversible inactivation of the phytohormone (Frébort et al., 2002; Avalbaev et al., 2012). Reversible metabolism of cytokinin produces various metabolites that are still biologically active. However, this is not the case in irreversible metabolism of cytokinin. Two separate pathways have been identified, each unique in the enzyme that catalyses the process, as well as the means of inactivation (Suttle and Mornet, 2005). The first irreversible pathway acts through glucosyl transferase(s) that catalyse N-glucosylation at the 7<sup>th</sup> or 9<sup>th</sup> positions. The pathway seems to differ between species, where the formation of certain conjugates is favoured above others. No matter the conjugate formed, the product remains biologically inactive, and accumulates in various tissues as metabolic end-products (Auer, 1997).

Over the past decade, it was determined that a specific enzyme, referred to as cytokinin oxidase/dehydrogenase (CKX), is responsible for the second pathway (Schmülling et al., 2003). It plays a cardinal role in the degradation of cytokinin because it is able to irreversibly inactivate the hormone in a single biological step (Galuszka et al., 2004). The phytohormone is inactivated when the CKX catalyses the cleavage of the side chain, converting the cytokinins and their ribonucleosides to adenine and adenosine (Galuszka et al., 2004; Frébort et al., 2011). The cleavage event is catalysed by the enzyme when the secondary amine group on the side-chain is oxidized (Malito et al., 2004). Although it was shown that cytokinin free bases

seem to be a preferred substrate for CKX, the enzyme still displays broad specificity. Chemical studies showed that it readily cleaves both *cis*- and *trans*-zeatin type cytokinins, as well as the side chain from isopentenyl type cytokinins (Schmülling et al., 2003). A study by Bileyeu et al. (2001), showed the highest  $K_m$  values for zeatin (Z) and zeatin riboside (ZR). These values were significantly higher than what was measured for N<sup>6</sup>-(2-isopentenyl) adenine and N<sup>6</sup>-(2-isopentenyl) adenosine, with ZR showing a 5 times increase in  $K_m$  value (Bileyeu et al., 2001). It was also concluded from the study that they are not inhibitors of CKX activity, as is the case with phenylurea-type cytokinins. This includes N-(chloro-4-pyridil)-N-phenylurea (CPPU), which has been shown to strongly inhibit CKX activity (Armstrong, 1994). In some plant species the CKX enzymes are however, not the predominant means for cytokinin degradation. The radish, *Raphanus sativus*, shows an alternative pathway where N-conjugates are formed instead (Schmülling et al., 2003). Also, general enzyme activity indicates that it plays a major role in controlling CK homeostasis, but certain species and tissue specific differences are now being discovered (Jones and Barnard, 2005).

CKX enzymes have been identified in a number of different plant tissues and species (Schmülling et al., 2003). This includes maize, wheat, rice and barley (Massonneau et al., 2004), as well as two non-plant species, *Saccharomyces cerevisiae* (Van Kast and Laten, 1987) and *Dictyostelium discoideum* (Armstrong and Firtel, 1989). Although the enzyme was initially classified as an oxygenase, kinetic data gathered from studying the wheat CKX showed that oxygen acts as a very poor electron acceptor. The original hypothesis described a mode of inactivation where oxygen was required as electron acceptor during regeneration of the oxidized flavin during turnover (Galuszka et al., 2004). However, when the enzyme's mode of action was studied in more detail, it was found that for example quinones are more suitable substrates because they are more efficient electron acceptors (Frebort et al., 2011). This has led to a renaming of the enzyme to cytokinin dehydrogenase. For the purpose of this thesis, however, the enzyme will be referred to CKX as in the majority of the available literature.

Although the first CKX was partially purified from wheat by Laloue and Fox in 1989, the first gene could only be isolated a decade later. Laloue and Fox described the general properties of a cytokinin-binding protein which was present at high levels in wheat embryos, but little more was known until two independent research groups simultaneously successfully cloned and characterized the first CKX gene from *Zea mays* (Laloue and Fox, 1989). The gene isolated was designated *ZmCKX1* (Houba-Hérin et al., 1999; Morris et al., 1999). Activity was confirmed by expressing the gene in two heterologous systems, namely *Pichia pastoris* (Morris et al., 1999) and *Physcomitrella patens* (Houba-Hérin et al., 1999).

Houba-Hérin and colleagues were able to purify the native CKX enzyme at low amounts, along with the recombinant protein at higher amounts. The group was able to isolate a peptide sequence and deduce amino acid sequence from the peptide (Houba-Hérin et al., 1999). By using 5'- and 3'-RACE (Rapid Amplification of cDNA Ends) PCR a complete cDNA sequence was obtained. The sequence was subsequently cloned into a plant expression vector, because initial attempts to express the protein in *Escherichia coli* cells were unsuccessful. Transient protein expression was obtained in *Physcomitrella patens* protoplasts. With the help of SDS-PAGE, a protein size of 63 kDa was determined, which differed significantly from the original studies, indicating a smaller protein (Burch and Horgan, 1989; Houba-Hérin et al., 1999; Schreiber et al., 2008). The CKX enzyme is also most likely a flavoprotein, as it was strongly inhibited by diphenyliodonium (DPI), which corresponds with the inhibition of activity in other flavoprotein oxidoreductases. Sequence similarity of 50% to a domain found in FAD-dependent oxidases was also found (Houba-Hérin et al., 1999).

A second research group, led by Roy Morris at the University of Missouri, simultaneously published a paper in which they also described a protein of 57 kDa in size, a conserved FAD binding sequence and eight consensus *N*-glycosylation sequences (Morris et al., 1999). In contrast to the above-mentioned study, Morris and his team expressed the *ZmCKX1* gene in *Pichia*, where an active glycosylated CKX enzyme was obtained. It was confirmed that the gene encoded a flavoprotein oxidase with the help of a recombinant protein absorption spectrum. The absorption coincided with other enzymes containing a substrate reducible-FAD. Sequence analysis revealed homology to two other genes. The first had a 40% homology to a recently deposited *Arabidopsis* BAC clone. The second had a 33.6% similarity to the *fas5* open reading frame from *Rhodococcus fascians*. The study concluded that a CKX gene had been isolated that encoded for a glycosylated FAD-containing oxidoreductase. The protein encoded by this gene had a substrate specificity similar to that of native CKXs (Morris et al., 1999).

Two years later, in 2001, it was confirmed that cytokinin oxidase/dehydrogenases are flavoproteins containing no detectable heavy metals. It still proved difficult to determine whether the cofactor involved was a flavin adenine dinucleotide or a flavin mononucleotide (FMN) (Bilyeu et al., 2001). In order to identify the cofactor covalently bound to the purified CKX enzyme, the distinct chromatographic properties of FMN and FAD on MonoQ, were determined to compare results when the flavin-containing peptide was isolated and treated with a nucleotide pyrophosphatase. When the results were compared with the established Mono Q figure (Cook et al., 1984) (Figure 1.2), it was concluded that FAD covalently binds to the CKX enzyme (Bilyeu et al., 2001). The study also disproved the hypothesis that the CKX

enzymes contained copper or any other heavy metals (Burch and Horgan, 1989; Bilyeu et al., 2001). Expression patterns and distribution in developing maize kernels found high amounts of CKX in the embryo, contrasting the low amounts detected in the endosperm. The resulting data indicated a possible subcellular separation between the cytokinin hormone and CKX enzymes within the maize kernel.

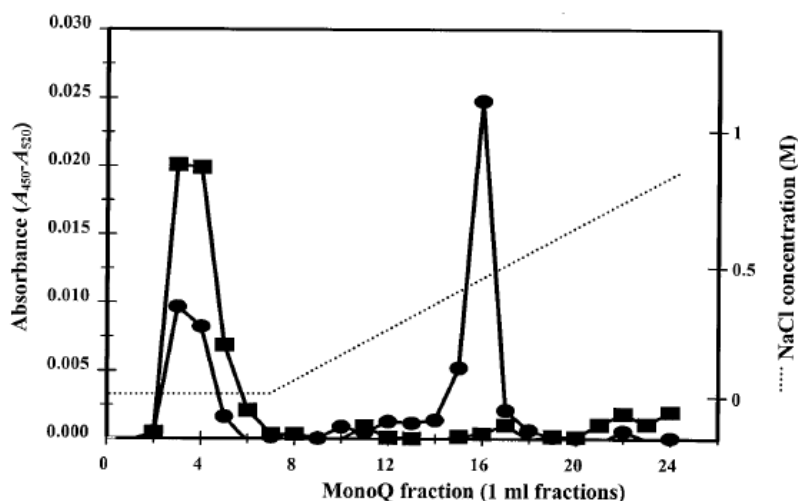


**Figure 1.2:** The MonoQ figure as presented in Bilyeu et al., (2001), indicating the flavin cofactor. A homogenous sample of recombinant CKX1 was purified from a tryptic digest. The plot represents fractionation on MonoQ, before (●) and after (■) nucleotide pyrophosphatase treatment. The  $A_{450} - A_{520}$  value is plotted for each sample (Bilyeu et al., 2001).

In 2004, an Italian research group led by Malito described the crystal structure of recombinant *Zea mays* CKX. The structure was studied in its native state, as well as with a slow-reacting substrate to elucidate more of the enzyme's mode of action. The research concluded that four main steps are involved in the enzyme's mode of action. It identified a plug-into-socket mode that allows for substrate binding and the oxidation of the substrate through a formal transfer of an hydrogen atom (Malito et al., 2004).

Subsequent to the cloning of *ZmCKX1*, the CKX genes from *Arabidopsis thaliana*, rice, *Dendrobium* and barley were cloned and characterized (Bilyeu et al., 2001; Werner et al., 2001; Schmülling et al., 2003; Yang et al., 2003; Galuszka et al., 2004). Additionally, two putative genes were discovered in the cyanobacterium, *Nostoc (Anabaena)* sp. PCC 7120 (Kaneko et al., 2001) and in the phyto-pathogen *Rhodococcus fascians* (Crespi et al., 1994). After a closer look at nucleotide sequences from the various species, it was concluded that CKXs are encoded by a multigene family. The size of the gene family varied greatly between

species, with seven homologs identified in the *Arabidopsis thaliana* genome and at least eleven gene homologs identified in the rice genome. Within the maize genome thirteen different sequences were identified (Schmülling et al., 2003). The presence of the different genes within a specific genome has been shown to be a result of diversity in subcellular localization of the enzyme and has also indicated variation in biochemical features. Various AtCKX proteins encoded for by the seven individual genes can be found in the cytoplasm, apoplast and vacuole. However, a review paper published in 2012 by Avalbaev and colleagues, concluded that more intense genetic studies of these genes were still required to better understand function and enzyme activity. Although the genes from maize and *Arabidopsis* had been well studied at that point, further research focusing on phylogenetic analysis would contribute to the understanding of the evolutionary development of the gene family in different plant species. This will in turn help to classify and characterize the different proteins in terms of their role in plant development, especially during different growth stages (Avalbaev et al., 2012).

The phylogenetic trees drawn thus far have been an invaluable source of information (Avalbaev et al., 2012). One of the first studies by Schmülling et al. (2003), included the available protein sequences from *Zea mays*, *ZmCKX1*, the seven *Arabidopsis AtCKX* sequences and five *OsCKX* sequences from rice. From the tree it could be concluded that the segregation in genes occurred before plants diverged from dicotyledonous to monocotyledonous (Schmülling et al., 2003). More recent research showed that the maize genes formed a part of a completely different cluster of genes, separate from *Arabidopsis*. This was an indication of property differences between the enzymes in monocotyledonous plants versus dicotyledonous plants (Vyrubalova et al., 2009).

## **1.3 Enhancing plant growth through volatile organic compounds**

### **1.3.1 Plant growth promoting bacteria**

The use of naturally occurring soil bacteria in agriculture has been common practise since ancient times, where Theophrastus (372-287 BC) recorded mixing different soil samples to increase plant health (Tisdale and Nelson, 1975). The reason as to why this mixing of soil was beneficial only became clear in 1683 when Anton von Leeuwenhoek discovered the existence of tiny life forms, only visible under a microscope. These microscopic organisms were called bacteria. Hellriegel and Wilforth (1888) then showed that bacteria in soil colonized around plant roots and discovered the ability of the microorganisms to fix atmospheric nitrogen into a form usable by the plants. They also described the rhizosphere as the area of soil occurring in close proximity with plant roots, where the majority of soil bacteria colonized. A century later, Kloepper and Schroth (1978), coined the term rhizobacteria, referring to the bacteria able to successfully colonize plant roots, stimulating growth and reducing plant disease incidence.

A diverse and complex ecosystem exists in the rhizosphere surrounding the roots of plants. Within this ecosystem various microorganisms exist, competing for nutrients and food supplies. It is believed that three types of interaction exist between plants and rhizobacteria, including a neutral, beneficial or detrimental effect. The majority of rhizobacteria have a minimal effect on the plants (Bhattacharyya and Jha, 2012). In certain cases plant growth can be negatively influenced by phytopathogenic rhizobacteria producing phytotoxic substances (e.g. ethylene). On the other hand, there are those that positively influence growth through indirect or direct mechanisms. A specific group of beneficial rhizobacteria known as plant growth-promoting rhizobacteria (PGPR) that produce an array of biologically-active compounds enhancing plant growth and pathogen resistance exist (Bhattacharyya and Jha, 2012; Bashan et al., 2014)

Various different studies have been undertaken to investigate how PGPR elicit these effects and how the benefits can be taken advantage of in an agricultural setting. It was shown that the bacteria increase seed emergence, plant weight, crop yields and disease control in a range of agricultural species (Kloepper, 1980; Zablotowicz et al., 1991). For example, a case of increased seed emergence was reported in canola seeds after they were coated with PGPR and the bacteria allowed to propagate before planting (Zablotowicz et al., 1991). Studies have



been done both in the field and under greenhouse conditions. Although reports vary greatly in terms of results, a yield increase of not lower than 30% and up to 70% was reported in some cases (Ryu et al., 2005). Inconsistent results can be attributed to limited knowledge of the contributing variables in these trials (for example how temperature affects bacterial colonization) and a lack of understanding in regard to how the bacterial mechanisms involved function (Weller, 1988).

Researchers have, however, established that in order for PGPR to be effectively applied in agriculture they need to be in possession of specific traits. If the strain shows good colonization of roots, if it can withstand different temperatures and finally, inhibit a variety of different plant pathogens, it has the necessary traits to act as an effective biocontrol. Another factor recently mentioned to effect the popularity of a strain was its ability to adapt to different agricultural environments, present in the different countries, allowing a standard range of PGPR strains to be optimized and distributed (Bhattacharyya and Jha, 2012; Glick, 2012).

### 1.3.2 Different mechanisms to promote growth

For optimum use as a biocontrol, research over the past two decades has focused on identifying the various mechanisms through which PGPR act on plants. A better understanding will aid in the commercialization of PGPR strains (Glick, 2012). Although plants have been shown to be positively influenced by the PGPR in various different ways, the different modes of action are generally divided into direct and indirect mechanisms (Castor et al., 2009).

Direct mechanisms include aiding in the acquisition of nutrients through nitrogen fixation and the solubilisation of different minerals like phosphate (Bhattacharyya and Jha, 2012; Glick, 2012). In some cases PGPR also secrete plant growth regulators, including phytohormones (like cytokinin and gibberellin), as a strategy to directly influence the plant growth. An example of this is the *Paenibacillus polymyxa* E681 strain that has been shown to produce cytokinin in order to promote plant growth in *Arabidopsis* plants (Timmusk et al., 1999; Ryu et al., 2005). Additionally, it was illustrated that *Paenibacillus polymyxa* strain E681 stunted pathogenic fungal growth *in vitro*. Effective root colonization of the whole root system, including lateral roots and the root tips was illustrated in the same study. The E681 strain also showed a retention of biological activity at 20°C. All of these identified factors, especially when considered in combination with each other, indicated a potential agricultural use (Ryu et al., 2005). An alternative direct approach of the bacteria is where they break down several of the ethylene precursors to reduce the endogenous levels in the subject plant. Indirect stimulation



can be seen as a form of biocontrol that the PGPR enforces on the rhizosphere. The PGPR produce various antibiotics to prevent biofilm formation of pathogens and act to prevent pathogen propagation. The antagonistic mechanism employed also focuses on the induction of plant immune responses (van Loon, 2007; Bhattacharyya and Jha, 2012). PGPR can be divided into three main categories, based on the different mechanism they utilize. The first group includes bio-fertilizers that stimulate plant growth by making more basic nutrients available to the plants. The next category describes phyto-stimulators that produce hormone-like/phytohormone compounds to induce plant growth. The last category includes bio-pesticides that promote growth through the control of phyto-pathogenic agents (Bhattacharyya and Jha, 2012).

### 1.3.3 Plant immune responses

Due to the sessile nature of plants, they have been forced to develop an array of complicated defence systems. Evolution has allowed plants to develop various highly efficient defence mechanisms against pathogenic attack, incorporating various phytohormones and signalling pathways. Plants have developed both a constitutive and an inducible defence response against the onslaught of pathogens they are faced with. As mentioned above, a large portion of PGPR are also known to enhance plant immunity against plant diseases, aiding in their fight.

Often a hypersensitive response (HR) is triggered in plants. This entails the induction of programmed cell death at the site of pathogenic infection. The HR occurs on a gene to gene basis, where the specific gene interactions then leads to systemic acquired resistance (SAR) protecting remote parts of the plant against attack. Induction of SAR is specifically linked to the gene for gene interaction between the plant-encoded resistance (*R*) and corresponding avirulence (*Avr*) gene products. By triggering SAR, the plant obtains a non-specific, long-lasting resistance against bacterial, fungal and viral pathogens (Ryals et al., 1994). The increase of SAR can occur via two different pathways, regulated by either salicylic acid (SA) or jasmonic acid (JA). The first pathway regulated by SA, is specifically linked to the activation of pathogenesis-related proteins (*PRs*) such as *PR-1*, *PR-2* and *PR-5*. This has been illustrated in both *Arabidopsis thaliana* and *Nicotiana tabacum* (tobacco) plants. A great number of other genes are also proposed to be involved in SAR, but the *PR* gene family has become a hallmark for SAR in *Arabidopsis* and tobacco plants (Delaney, 1997; Ryu et al., 2004a; van Loon, 2007). It is also clear that the *NPR1* gene is required for SAR against bacteria and fungi, but an alternative pathway involving the plant mitochondrial enzyme,

alternative oxidase (AOX) was proposed to be involved in triggering SAR against viral infections (Naylor et al., 1998; Wang et al., 2002).

An induced systemic resistance (ISR) is elicited by beneficial soil bacteria and thus is often referred to as the PGPR-elicited immune response. This immune response is described as the opposite of SAR, as it is induced indirectly and heavily relies on the plant-PGPR-pathogen interaction (Duijff et al., 1998). As mentioned before, the immune response is triggered by certain chemicals produced by the PGPR that lead to an increased immunity in aerial parts of the plant. It is phenotypically similar to pathogen-induced SAR and also leads to a reduction/stunting of pathogenic growth. Two different types of ISR have been described. It has been observed that there is an ISR-prime where the immune response is induced by the PGPR prior to infection. A second response is referred to as ISR-boost elicited post inoculation with a pathogen (Verhagen et al., 2004).

A number of studies have shown the induction of ISR by Gram positive *Pseudomonas* spp. and Gram positive *Bacillus* spp., and that the immune response is generally via an SA-independent mechanism (Kwon et al., 2010; Rudrappa et al., 2010). Studies have shown that the response is still *NPR1*-mediated, but without the induction of the *PR* (pathogenesis-related) genes. The ISR response is thought to be regulated by ethylene (ET) and JA-signalling pathways. Certain studies have however, shown the involvement of SA, illustrating how specific PGPR commercial strains elicit ISR through the priming of a SA- and JA-dependent signalling pathway (Kloepper et al., 2004). In 2012, a study investigated the effect *Paenibacillus polymyxa* E681 has on *Pseudomonas syringae* pv. *maculicola* ES4326 challenged *Arabidopsis* plants. The study showed an unexpected result, when it illustrated significant upregulation of the *PR1* gene promoter linked to the GUS gene. As previously mentioned, the *PR* gene family is traditionally linked to SAR and SA-dependent signalling (Lee et al., 2012). In a separate study it was shown that when soil was drenched with the PGPR strains, *Pseudomonas fluorescence* CHAO and *Pseudomonas aeruginosa* 7NSK2, attacks from both Tobacco necrosis virus (TNV) and Tobacco mosaic virus (TMV) were stunted. The ISR elicited was shown to be dependent on SA, as SA-deficient mutants did not show an increased resistance against the two viruses (Maurhofer et al., 1998). This result is closely coupled with viral infection, and the conclusion was made that induced resistance by PGPR is a SA-dependent mechanism (Ryu et al., 2005). Linking to this, a similar study found that *Serratia marcescens* strain 90-166 reduced disease severity and protected against Cucumber mosaic virus (CMV) (Raupach et al., 1996), but *Pseudomonas fluorescence* strain WCS417r could not trigger resistance against TMV, although it was able to reduce disease severity in *Arabidopsis thaliana* against bacterial and fungal pathogens (Ton et al., 2001). Protection

against the fungal and bacterial pathogens was shown to be triggered independently of SA, as *NahG* mutant plants were still shown to be protected (Pieterse, 1998). The *NahG* gene encodes for salicylate hydroxylase that renders SA inactive by converting it to catechol. These mutants, in essence, prevents the SAR from being activated. It was therefore concluded in light of the results obtained from these studies that potentially a different signalling pathway acts against viral infections (Ryu et al., 2004a). Interestingly, it has also been shown that the necrotrophic pathogen *Botrytis cinerea* elicits no SAR in *Arabidopsis* and tomato plants (Govrin and Levine, 2002), but rather an NPR1-mediated ISR, controlled by the ET- and JA-signaling pathways (Verhagen et al., 2004) (Glazebrook, 2005). These findings provide a greater insight into the mechanisms through which ISR is elicited in plants, and hint at the fact that the mechanism could be heavily dependent on not only the PGPR, but also the plant under attack and the pathogen it is being challenged with (Mathys et al., 2012).

PGPR produce a variety of determinants that can elicit a response either through direct or indirect mechanisms. The determinants are produced as siderophores, antibiotics, lipopolysaccharides and even bacterial metabolites (Press et al., 2001; Ryu et al., 2004b; Lee et al., 2012; Pieterse et al., 2014a). Bacterially produced VOCs, like acetoin and 2,3-butanediol, are a recent addition to the different forms these determinants take and are considered an indirect trigger for ISR. Quorum sensing molecules have also been identified to be an important determinant in terms of plant-microbe interactions. Certain quorum sensing molecules, including acyl-homoserine lactones (AHLs) have been shown to trigger ISR. When a PGPR strain, *Serratia liquefaciens* MG1, known to produce 2 AHLs, was applied to the roots of *Solanum lycopersicum* L. (tomatoes) an ISR against *Alternaria alternata* (a leaf fungal pathogen) was observed. This effect was confirmed when no immune response relating to ISR was observed from applying an AHL-null mutant (Schuhegger et al., 2006). These findings led to a subsequent study investigating whether AHLs were required to work in combination with each other, to trigger the immune response. It also questioned whether ISR could be activated indirectly by secondary metabolites produced during quorum sensing (QS). Two transgenic *Nicotiana tabacum* plants, one containing an AHL-producing gene and the other an AHL-degrading gene were used and treated with *Serratia marcescens* strain 90-166, known to produce at least two QS signals. When the AHL-producing plants were treated with *Serratia marcescens* strain 90-166 and subsequently infected with the bacterial pathogens, *Pectobacterium carotovorum* subsp. *carotovorum* and *Pseudomonas syringae* pv. *tabaci*, an increased resistance was observed. This was opposed to the AiiA (AHL-degrading) plants that illustrated a decreased level of ISR (Song and Ryu, 2013). A comprehensive review published in 2004, concluded that when considering ISR, an important factor to consider is the spatial

separation between the bacteria (also referred to as the inducing agent), and the pathogen challenging the plant (Ryu et al., 2004a).

### 1.3.4 Volatile Organic Compounds

Just over a decade ago, an interesting new mechanism for inducing plant growth was identified. In 2003 it was discovered that certain strains of commercially-used PGPR produce volatile organic compounds (VOCs) (Ryu et al., 2003). Both chemical and plant-growth data showed that the PGPR released a collection of volatile compounds that promoted growth in the model plant, *Arabidopsis thaliana*. After further investigation, the researchers identified two specific VOCs to be the main contributors in eliciting the growth effects. The compounds identified, namely acetoin and 2,3-butanediol, were found to be unique in the volatile blends produced by the two strains of PGPR. These strains were also the two that showed the most significant growth promotion amongst the strains being investigated (Ryu et al., 2003). Although this was the first time that acetoin and 2,3-butanediol had been identified in PGPR-released volatile blends, it was not the first time acetoin had been described. The compound 3-hydroxy-2-butanone, more commonly referred to as acetoin, was investigated in the suspension of cell cultures from crop plants, including carrots and maize. The study was able to identify and characterize three different enzymes responsible for acetoin synthesis (Forlani et al., 1999). A subsequent study described how low-molecular-weight plant volatile compounds (e.g. jasmonates and green leaf components) act as signalling molecule to different microorganisms propagating plant trophic levels (Farmer, 2001). A separate research group confirmed the findings, showing both growth promotion and reduced disease severity in treated *Arabidopsis* plants. The effects were observed when acetoin and 2,3-butanediol was exogenously applied to *Arabidopsis* plants, as well as when the plants were treated with the *Bacillus subtilis* strain (Rudrappa et al., 2010). Although subsequent studies based on these findings by Ryu et al., (2003) have confirmed the effects on plant growth and disease resistance, more research is required to fully understand the mechanisms at play.

What makes VOCs so interesting is their ability to not only enhance plant growth, but to simultaneously elicit an induced resistance in the plant, referred to as ISR (Loon et al., 1998). Apart from the growth enhancing effects shown by 2,3-butanediol and subsequently shown by acetoin, it was additionally shown that the compounds act as determinants for ISR (Ryu et al., 2004a). When *Arabidopsis* plants were treated with the two *Bacillus* spp. strains tested (*Bacillus subtilis* strain GB03 and *Bacillus amyloliquefaciens* strain IN937a), significantly reduced disease severity was observed against the plant pathogen known as *Erwinia*

*carotovora* subsp. *carotovora*. Two separate, subsequent studies further confirmed through biochemical analysis that 2,3-butanediol was the compound eliciting the response in the plant (Farag et al., 2006; Kwon et al., 2010).

A study undertaken in 2010, focussed on the changes that VOCs elicit on a protein level in treated *Arabidopsis thaliana* plants. The plants were exposed to the beneficial *Bacillus subtilis* GB03 PGPR strain, identified by Ryu et al., (2004). The ultimate goal of the study was to conclusively prove the beneficial effects VOCs have on plants. Studies done up to that point were of a molecular and phenotypic nature, but this study aimed to provide information on an enzymatic/protein level. A total of 95 differentially expressed proteins were identified through two-dimensional gel electrophoresis. From further analysis it could be concluded that the plants possessed an increased photosynthetic capacity, which in turn led to significantly higher root and shoot growth. The increase in photosynthetic activity was suggested to be the result of increased mineral uptake in the treated plants. The study also focused on resistance induction, identifying that several anti-oxidant proteins and ET biosynthesis-related genes were significantly upregulated. Several genes were investigated including ethylene (ET)-biosynthesis gene *SAM2*, ET-response gene, *ERF1*, JA response gene *PDF1.2*, and SA response gene *PR1*. A clear induction of the ET response genes were found, with the upregulation of the *ERF1* gene along with the JA response genes. These ET and JA signalling pathways have been suggested to be involved in cross-talk with each other, and it is thought that the induction of ET signalling is closely linked to induction of JA signalling (Bostock, 2005; Smith et al., 2009; Kwon et al., 2010). Interestingly, the SA marker gene, *PR1*, was also up-regulated, presenting the question whether the bacterial VOCs elicit a synergistic relationship between the SA and ET/JA-signalling pathways, which were previously reported to act antagonistically (Robert-Seilaniantz et al., 2007; Kwon et al., 2010). This cooperative nature between the pathways has been previously reported (Van Wees et al., 2008).

### 1.3.5 Acetoin and 2,3-butanediol biosynthesis

Acetoin is known to be a valuable industrial compound due to its broad usages. Both acetoin (also known as 3-hydroxy-2-butanone or acetyl methyl carbinol) and its analogue, 2,3-butanediol (2,3-BD) are widely applied in the food industry as additives to enhance fragrance and flavour (Celińska and Grajek, 2009). It is used during the production of cigarettes, cosmetics and detergents to form a product with both an appealing fragrance, with the option of an added flavouring composition. In agriculture the VOCs are used for pest control and to increase plant growth (Ji et al., 2011). Apart from the various applications for acetoin,

2,3-butanediol (2,3-BD) specifically has been used to produce synthetic rubber during World War II and is often used as an antifreeze agent (Celińska and Grajek, 2009). Both chemicals can be synthesised from renewable or excessive biomass and have therefore been classified as a bio-based platform chemicals, making the production of these compounds on a large scale a priority in industrial research and development (Ji et al., 2011). Currently acetoin is produced through a chemical synthesis process which creates a synthetic product less appealing to the consumer than the naturally-occurring compound despite the natural compound being more expensive. Research is therefore focussed on developing a large scale production system for natural acetoin with the help of biotechnology (Xiao and Lu, 2014). Synthetically-produced acetoin includes the use of intense chemical reactions, detrimental to the environment. This therefore creates the priority for development of a large scale bioreactor (Xiao et al. 2007). For industrial purposes a bacterial system was identified as the most ideal, due to it using a cheap biomass, in a sustainable manner. The system will exclude or at least limit the negative environmental impact that synthetic production has. Production will become more cost-effective and sustainable when using renewable biomass. Most research is thus focusing on the development of a bacterial system (Sun et al., 2012).

The production of acetoin occurs in various different organisms, including mammals (Otsuka et al., 1999) and plant cells (Forlani et al., 1999), although some of the plant and animal species only produce a small amount under very specific circumstances (Sun et al., 2012). Included in the biochemical pathways for acetoin (and 2,3-BD) are both the synthesis and/or break down of the compound. In general the pathway naturally reverts to the biosynthesis direction unless it is specifically lead towards the catabolism pathway (Xiao and Xu, 2007). For the bacterial acetoin biosynthesis pathway (Figure 1.3), three main enzymes are involved. Some other enzymes are also involved, but to a much lesser extent. The three key enzymes include 2-acetolactate synthase (ALS), 2-acetolactate decarboxylase (ALDC) and 2,3-butanediol dehydrogenase (BDH). These three enzymes are responsible for catalysing the conversion of pyruvate to acetoin and acetoin to 2,3-BD, respectively.

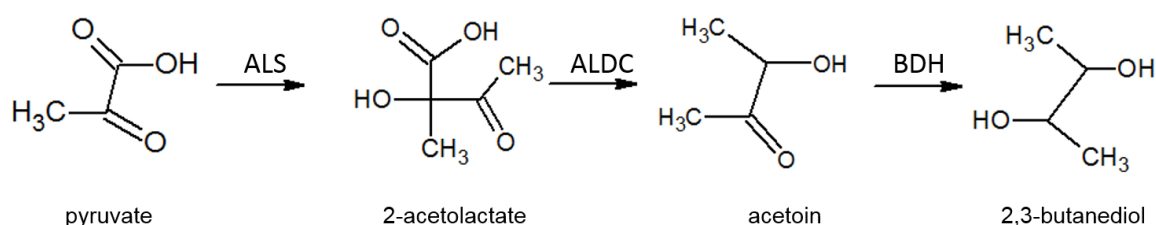


**Figure 1.3:** The acetoin and 2,3-butanediol biosynthesis pathway, present during bacterial fermentation.



Interestingly, the biological significance of 2,3-BD has yet to be determined, although some hypothesis exist. It is thought to aid in producing a neutral compound, preventing the acidification of intracellular environments (Booth, 1985). The production of 2,3-BD might counteract too high acidification during fermentation. This was supported when studies showed the induction of 2,3-BD through acid supplementation (Nakashimada et al., 2000). Unfortunately, most of the studies were done through the addition of acetic acid addition, which is also known to induce certain enzyme activity involved in 2,3-BD synthesis, leaving gaps in the research. A second possible metabolic function for the compound is to help regulate the NADH/NAD<sup>+</sup> ratio intracellularly, as is the case in other fermentation processes. Due to the carbon stored in the 2,3-BD, that can be recycle for energy during the stationary phase, the synthesis pathway is additionally regarded as an energy source (Xiao and Xu, 2007).

## **1.4 Project Rationale**

Traditional breeding of crops is no longer providing the required increase in crop yield. Research has therefore turned to biotechnological approaches to help achieve the necessary crop yields for the food demands of modern society (Iyer et al., 2000; Ashikari et al., 2014).

This project therefore aimed at enhancing plant growth in sugarcane. Two independent biotechnology approaches were employed for the purpose of increasing promoting plant growth. The first approach focused on optimizing a novel method for the construction of a suitable RNAi hairpin construct to silencing the *CKX* gene family in subsequent studies. The second part of the project focused on the introduction of the *ALDC* and *BDH1* genes into *Arabidopsis* and sugarcane. The effects of increased disease resistance was investigated as a proof of concept in the model plant, *Arabidopsis thaliana*, before further analysis of transgenic sugarcane occurred.

## **CHAPTER 2**

### **Construction of an RNAi vector for silencing *CKX* sugarcane genes**



## **2.1 Introduction**

The perennial grass, sugarcane, acts as an attractive source of biomass due to the high photosynthetic efficiency of the crop. It is cultivated in tropical, as well as subtropical areas for sugar production (Aitken et al., 2014). Sugarcane increased its importance by additionally becoming a potential source of ethanol, and is now classified as a potential biofuel crop (Kojima et al., 2009; Ashikari et al., 2014). Traditional breeding between different cultivars has resulted in complex aneu-polyploids, with chromosome numbers of up to 120 (Aitken et al., 2014). This autopolyploid genetics of sugarcane, along with the high heterozygosity that occurs in the commercially used cultivars, have greatly hindered further enhancement of plant traits. Due to this, enhancing beneficial traits through genetic engineering has become an attractive alternative.

### **2.1.1 The increase of sugarcane plant growth**

The ultimate aim of this study was to increase plant growth in sugarcane, with the goal of increasing the biomass yield of the crop. It was attempted to achieve this goal through the silencing of the cytokinin oxidase (*CKX*) gene family.

Cytokinins represent a class of plant phytohormones that play a vital role in plant development (Werner et al., 2001). The hormone is known to be involved in various developmental stages of plants and the specific roles of cytokinin includes the promotion of cell differentiation, seed germination, the delay of leaf senescence and the formation of shoot meristems, amongst others (Qin et al., 2011). Cytokinin levels are regulated by the cytokinin oxidase (*CKX*; EC 1.5.99.12) enzyme, which irreversibly inactivates the phytohormone (Houba-Hérin et al., 1999; Morris et al., 1999). Subsequent to the discovery of the enzyme it became evident that small families of the genes are present in plants. Several of these gene families have now been partially characterized in plant systems like the model plant *Arabidopsis* (Bilyeu et al., 2001) and various crops, including maize, rice, wheat and barley (Galuszka et al., 2004; Massonneau et al., 2004; Smehilová et al., 2009). The different genes that form a part of this gene family encode for proteins that differ in terms of their biochemical properties, with special focus on substrate affinity (Galuszka et al., 2004).

Recently, a positive result was obtained one of the *CKX* genes was silenced in the crop species barley and wheat (Zalewski et al., 2010). Stable RNA interference-based technology allowed for a reduced expression and activity of both the *HvCKX1* and *HvCKX2* in two

separate studies (Zalewski et al., 2010; Zalewski et al., 2012). A significant amount of reduced enzyme activity was observed in the T<sub>1</sub> generation plants, for both studies. Interestingly, it was observed that a reduction in enzyme activity of 34% resulted in increased productivity. The increased productivity was measured in terms of grain yield and a higher number of seeds. Additionally an increase of approximately 7.5 % in plant height was observed, along with an increased number of spikes (Zalewski et al., 2012; Zalewski et al., 2014).

### **2.1.2 RNA-interference based silencing**

The aim of the first section of the study focussed on creating a silencing construct (hpRNAi vector), which can in future be used to produce transgenic sugarcane lines with reduced CKX enzyme activity. For the construction of the silencing cassette, establishment of a novel method which had not previously been utilized in the IPB. The particular, novel method involves isothermal *in vitro* recombination, a system now referred to as IR-hpRNAi construction. Due to laborious, complicated and often expensive nature of existing methodologies like the Gateway® cloning technologies, the new technique was attempted to establish a less time-consuming method. The construction of an hpRNAi vector is often complicated and laborious due to the several time-consuming cloning steps (Jiang et al., 2013). For plant species where the genome has not yet been sequenced and only expressed sequence tags available, as for sugarcane, the GATEWAY® cloning system, designed by Invitrogen, is one of the few available, established construction methods (Oa et al., 2009; Jiang et al., 2013). Although it is more rapid than the traditional cloning methods, it still consists of a delicate two-step cloning system. The system is also quite expensive, amounting to a total of R1500 for a complete cloning into the final expression vector (pricing calculated when the cloning kit is purchased from Invitrogen, supplied by Thermo Scientific, Waltham, Massachusetts, USA). Additionally, the current available destination vector that would be employed for the GATEWAY® cloning, in this particular case, pHb7GW-I-WG-UBIL, is fit for monocot transformation, but is a very large vector (larger than 15000 bp), which in turn will hinder vector uptake during particle bombardment, the established method for sugarcane transformation at the IPB. Thus, it would be likely necessary to bombard with linearized minimal cassette fragments, not established for the IPB laboratory environment. Using the newly developed IR-hpRNAi construction method has several potential benefits above the existing alternatives, namely that it is in-expensive, with a single reaction amounting to R200 (calculated for use of the Gibson Assembly® Cloning Kit produced by NEB. United Kingdom). It allows the use of any transformation vector, eliminating any required modifications to the desired transformation vector. The method also includes a single cloning step, instead of multiple vectors and cloning steps as with alternative methods (Jiang et al., 2013). This

method was successfully employed by Jiang et al., (2013) for the silencing of the *Arabidopsis PDS3* gene. In this section, the optimization of the IR-hpRNAi construction is therefore described, including solving various problems during optimization.

## **2.2 METHODOLOGY**

### **2.2.1 Chemicals**

The primers that were designed with the web-based designing tool provided by NCBI ([www.ncbi.nlm.nih.gov/tools/primer-blast](http://www.ncbi.nlm.nih.gov/tools/primer-blast)) and used during this study, were all synthesised by and obtained from Inqaba Biotechnical Industries (Pty) Ltd, Pretoria. Unless otherwise specified, all the chemicals used were obtained from Sigma Aldrich Fluka (St. Louis, MO, USA), Merck (Wadeville, Gauteng, RSA) and Promega (Madison, WI, USA). The different enzymes for DNA manipulation were obtained from New England Biolabs® (NEB, United Kingdom).

### **2.2.2 Bacterial growth conditions**

#### *2.2.2.1 Luria Broth*

To grow liquid bacterial cultures of *Escherichia coli* DH5α cells, Luria Bertani (LB) medium containing 10 g/l tryptone, 5 g/l yeast extract and 10 g/l NaCl was inoculated with bacteria. A solid medium, LB agar (LBA) was created through the addition of 1.5% bacteriological agar, prior to autoclaving the medium. After the media was autoclaved (121°C, 1.2 kPa for 20 min) and had cooled to approximately 60°C, the required antibiotics for selection of cells carrying plasmid DNA were added to a final standard concentration.

#### *2.2.2.2 Bacterial transformation*

The standard heat-shock method described by Sambrook and Russell (2001) was used for plasmid DNA transformations into heat-shock competent *E. coli* DH5α cells. Plasmid DNA (50 to 100 ng/μl) was added to 50 μl of cell aliquots and incubated on ice for 30 min, after which the cells were heat-shocked in 42°C heat-baths for 45 s. After the heat-shock, the cells were immediately placed back on ice for 5 min, while 350 μl of LB medium was added to the transformed cells. The samples were then incubated at 37°C for 1-2 hours, with agitation (250 rpm) to allow for cell growth. Approximately 100 μl of the transformation culture was plated out onto LBA plates, (containing the appropriate antibiotic for selection) before incubating overnight at 37°C, allowing colony growth.

### 2.2.2.3 DNA isolations

To purify DNA fragments, including amplified DNA, linearized plasmid and restricted fragments, the Wizard® SV Gel and PCR Clean-Up System (Promega, Madison, WI, USA) was used, according to the manufacturer's specifications. For plasmid DNA isolation, the Wizard® Plus SV Minipreps DNA Purification System (Madison, WI, USA) was employed also according to the manufacturer's specifications.

## 2.2.3 Isolating partial CKX sequences from sugarcane

In order to obtain CKX sequence data from sugarcane, primers were designed based upon the available *Sorghum bicolor* and *A. thaliana* gene sequences. Two predicted cDNA sequences, SbCKX9 (XM\_002439661) and SbCKX3.1 (XM\_002454958) and two *A. thaliana* sequences that are known to be active, AtCKX2 (NM\_127508) and AtCKX4 (NM\_179139) were obtained from the Phytozome V9.1 database. Both the *S. bicolor* and *A. thaliana* sequences acted as template for the design of four different primer sets, each located in a different gene domain (Table 2.1).

### 2.2.3.1 Total RNA extraction and cDNA synthesis

Total RNA was isolated from sugarcane NCo310 plantlets. Young leaves were harvested and flash frozen in liquid nitrogen prior to extraction. Leaf samples were ground to a fine powder with a pre-chilled, autoclaved mortar and pestle. Approximately 200 mg of ground tissue was used during the RNA isolation. Total RNA was isolated according to the manufacturer's specifications provided with the RNeasy Mini Kit (Qiagen, Hilden, Germany). The RNA quality was assessed by incubating 5 µl of the total RNA extracted, with 10 µl of 2-mercaptoethanol for 15 min at 37°C and separation on a 1.5% (m/v) agarose gel containing 2.5 µl/ 50 ml of PRONOSAFE nucleic acid stain (Laboratorius CONDA, Italy) and visualised under UV light. DNase I was added to a total of 1 µg of RNA, according to the manufacturer's specifications included in the RNase-free DNase I enzyme kit (Thermo Scientific, Waltham, Massachusetts, USA). The DNase-treated sample was then used to synthesize complementary DNA (cDNA), with the Maxima H Minus First Strand cDNA Synthesis kit (Thermo Scientific, Waltham, Massachusetts, USA). The cDNA samples were aliquoted and stored at -80°C.

### 2.3.3.2 PCR amplification of partial CKX sequences

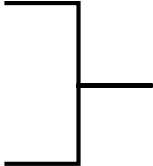
Using the different primer pairs described in Table 2.1, partial CKX fragments were amplified from the sugarcane cDNA. For amplification, the GoTaq™ DNA Polymerase kit (Promega,

Madison, WI, USA) was applied according to the manufacturer's specifications. The general programme followed for each PCR event was as described in Table 2.2.

**Table 2.1:** Primer pairs for the amplification of the partial sugarcane *CKX* gene fragments. Primers were designed based on the known sorghum or *A. thaliana* *CKX* genes and designed in such a way to either include the cytokinin binding domain (CTKD) and the flavin adenine dinucleotide (FAD)-binding domain, or to exclude the cytokinin binding domain (CTKD), that is universally present in *CKX* genes

PRIMER	SEQUENCE	AMPLICON SIZE	AREA	Tm
AtCKX2_Fwd	5'-TGCTTAAGAAGACGGCGG A-3'	1106 bp	Includes both the FAD and CTKD binding domain	60 °C
AtCKX2_Rev	5'-TCAAAAGATGTCTTGCCCTGGA-3'			
AtCKX4_Fwd	5'-ATAAAGGCTCAACCAGCCC-3'	1226 bp	Includes both the FAD and CTKD binding domain	60 °C
AtCKX4_Rev	5'-TGGTCCAAAATGTTTAACCCAATCT-3'			
Sb03_Fwd	5'-GAAACCTTCACCGAGGAC-3'	733 bp	Only amplifies the CTKD binding domain	60 °C
Sb03_Rev	5'-TCCGTTCAAATGTCTCCCAC-3'			
Sb09_Fwd	5'-GACGACATGCCACTACG-3'	1263 bp	Includes both the FAD and CTKD binding domain	60 °C
Sb09_Rev	5'-AAATGTCTCCCACCTTGCCT-3'			
SbCTKD_Fwd	5'-TTGCAGAGGATCAGGAGATG-3'	716 bp	Only amplifies the CTKD binding domain	60 °C
SbCTKD_Rev	5'-AATGTCTCCCACCTTGCCT-3'			
Sb09Full_Fwd	5'-ATGAAACCATCAGTTCTGCAGTAC-3'	1569 bp	Amplifies from the CTKX9 start codon	60 °C
Sbo09Full_Rev	5'-CGCCAATGGGTCATAGG-3'			

**Table 2.2:** General PCR conditions used during *CKX* gene fragment isolations

STEP	TEMPERATURE (°C)	TIME (min)	
Initial denaturation	95	3	
Denaturation	95	0.5	
Annealing*	*	1	
Extension	72	1	
Final extension	72	7	
Hold	4	Hold	

\*Specific annealing temperatures for each primer pair are listed in Table 2.1

Subsequent to successful amplification, the fragments were isolated from a 1.5% (m/v) agarose gel with the Wizard® SV Gel and PCR Clean-Up System (Promega, Madison, WI, USA), according to the manufacturer's specifications. Isolated fragments were cloned into the pGEM®-T Easy Vector System, as described by the manufacturer (Promega, Madison, WI, USA). The resulting clones were sent for sequencing at the Central Analytical Facility in Stellenbosch, for further phylogenetic analysis and hairpin construction.

#### 2.2.4 Phylogenetic analysis2.2.4.1 Sequence Collection

A BLAST search was done on the NCBI database ([www.ncbi.nlm.nih.gov](http://www.ncbi.nlm.nih.gov)) with the full length *AtCKX2* sequence, to identify all the available *CKX* sequences. Different coding *CKX* sequences were obtained, representing a variety of monocotyledon, dicotyledon and lower plant species. *Sorghum bicolor* *CKX* sequences were obtained from the Phytozome V9.1 database, as were the sequences for the lower plant species *Physcomitrella patens* and *Selaginella moelendorffii*. A total of 57 coding sequences were obtained (Annexure A).

#### 2.2.4.2 Drawing a dendrogram with MrBayes

Using the 57 CKX gene coding sequences collected, a multiple sequence alignment of *Physcomitrella*, *Selaginella*, *Arabidopsis thaliana*, tomato, potato, sorghum, maize, barley, rice and wheat, was performed with the help of ClustalW, in BioEdit. Thereafter, phylogenetic analyses was done with the MrBayes programme, version 3.2 (Ronquist and Huelsenbeck, 2003), which utilizes the Markov chain Monte Carlo (MCMC) methods. For this to be possible, a Nexus file containing the full multiple sequence alignment was generated with Tracer (version 6.1). Within the Nexus file commands were included for partitioning of data. Partitioning allowed for different rate and model of substitution based codon positions. Thus partitioning the nucleotides in position 1, 2 and 3. The nst=mixed command was included to average each partition over model space. Among-site variation was taken into account with a gamma rate correction. The full run of the MCMC chain was run for  $1 \times 10^7$  generations. Sampling occurred every  $1 \times 10^4$  generations. Sampling size was estimated at greater than 200, and all runs were converged on the same posterior. The run was ended and a summary of the tree was generated. The dendrogram was edited with the help of FigTree v1.4.2.

### 2.2.5 Hairpin RNA-interference (hpRNAi) cassette construction

#### 2.2.5.1 Chosen template sequence for sense and antisense fragments

The area included in the hairpin fragments (sense and antisense), was chosen based upon the phylogenetic analysis described above. From the dendrogram (Figure 2.2) it was determined that the SugarcaneCTKD acts as worthy candidate. Within this sequence an area of conservation was identified, which then subsequently acted as template for the hairpin design (Figure 2.3).

#### 2.2.5.2 Cloning SugarcaneCTKD into pJET

The chosen area of sequence, present within the SugarcaneCTKD sequence, was amplified with hairpin specific primers (Table 2.3). The fragment was amplified with the Q5® High-Fidelity DNA Polymerase (NEB, United Kingdom), according to the manufacturer's specifications. The PCR thermocycles were programmed as described in Table 2.4. The fragment was purified with the Wizard® SV Gel and PCR Clean-Up System (Promega, Madison, WI, USA). After purification, the fragment was cloned with the CloneJET™ PCR Cloning Kit (Thermo Scientific, Waltham, Massachusetts, USA), into the pJET1.2 blunt cloning vector according to the manufacturer's specifications.



**Table 2.3:** Primer sequences, as designed for sense and antisense hpRNAi amplification. The design includes overlapping, complementary vector or intron sequence (indicated lower case letters) attached to the gene specific sequence (indicated in uppercase). The optimized annealing temperatures determined for each primer pair are also provided

PRIMER	SEQUENCE	T <sub>m</sub>
CTKD8pUBISense_Fwd	5'- ctgttggttggtgcggccgcTCCTGCAGACATGTATACA -3'	59 °C
CTKD8Sense_Rev	5'- ctgagcagcatcacacttacATTTTCAGCAGAGAGGACCTT-3'	
CTKD8pUBIAnti_Fwd	5'-cctgcagaagtaacggtaccTCCTGCAGACATGTATACA-3'	58 °C
CTKD8Anti_Rev	5'- gtaagtgtgatgctgctcagATTTTCAGCAGAGAGGACCTT-3'	
NEBSense_Fwd	5'- ccctgttggttggtgcGCGGCCGCTCCTGCAGAC -3'	57 °C
NEBSense_Rev	5'-gtgtgatgctgctcagATTTTCAGCAGAGAGGACCTTCGATTACATAGAG -3'	
NEBanti_Fwd	5'- tgctgaaatctgagcagcatcacacttacATTTTCAGCAGAGAGGACC -3'	58 °C
NEBanti_Rev	5'- gcagaagtaacggtacggtaccTCCTGCAGACATGTATAC -3'	

### 2.2.5.3 Sense and antisense primer design

Two specific primer pairs were designed (Table 2.3). Both pairs were designed according to the specifications of Jiang et al., (2013), containing a gene-specific sequence (19 to 20 bp in size) and an overlapping sequence (20 bp in size), for the amplification of the sense and antisense strands, respectively (Table 2.3). The overlapping sequences, added to both the forward primers, were carefully designed to be complementary to the plant transformation vector being used, in this case pUBI510+. To create a synthetic intron in the hairpin, the reverse primers contain overlapping, complementary sequence. When assembled during the isothermal *in vitro* assembly reaction, these complementary regions anneals to create the required spacer in the hairpin. The sequence chosen was an exact copy of the synthetic intron used in the original study (Jiang et al., 2013). The gene-specific sequence was obtained from the identified area within the SugarcaneCTKD sequence, as described above. For the purposes of this study, and to prevent any future confusion, the primer sets were further

referred to as the GIBSON primers (CTKD8pUBISense and CTKD8pUBIAnti in Table 2.3). A second primer set was designed with the help of the New England Biolabs web tool (accessed at [www.neb.com](http://www.neb.com), September 2015). Specific overlapping sequence was automatically generated through the website. Although highly similar to the GIBSON primer sets, the overlapping sequences generated were somewhat longer (Table 2.3). The primer pairs designed in this manner were referred to as the NEB primers for the purposes of this study, as to prevent any future confusion with the GIBSON primers designed.

#### *2.2.5.4 PCR amplification of sense and antisense fragments*

Firstly, a gradient PCR was performed to optimize both the designed GIBSON primer pairs. The sense and antisense fragments were amplified with the GIBSON primer pairs (CTKD8pUBISense\_Fwd, CTKD8Sense\_Rev, CTKD8pUBIAnti\_Fwd and CTKD8Anti\_Rev, Table 2.3). A PCR reaction mix was set up according to the manufacturer's specifications, using 1 U of Takara™ Ex Taq™ Polymerase (CHEMICON International Inc., United States) in 50 µl mix. *pJET::SugarcaneCTKD* plasmid DNA acting as template, was added to a final concentration of 50 ng. The PCR was subsequently performed according to the manufacturer's specifications with an annealing temperature of 58°C, and the resulting PCR product was isolated subsequent to visualization on a 1.5 % agarose gel (as described in previous sections). This procedure was repeated for each of the primer sets, until a sense and antisense fragment could be obtained for both the GIBSON primers and the NEB primers using the *pJET::SugarcaneCTKD* plasmid as template.

#### *2.2.5.5 Plasmid linearization*

For the cloning, a linearized transformation vector (pUBI510+), containing an ubiquitin promoter and CamV terminator site, Annexure B) was required. For unique restriction sites, a combination of *KpnI* and *NotI* was used in a double digest reaction. The digestion mix was made up to a total of 10 µl with nuclease free water, containing 2 µl of each enzyme in 4 µl of 2.1 reaction buffer (NEB, United Kingdom), and approximately 1 µg of plasmid DNA. The reaction was incubated at 37°C overnight, and separated on a 1.5% (m/v) agarose gel. The linearized fragment was then subsequently purified from the agarose gel with the Wizard® SV Gel and PCR Clean-Up System (Promega, Madison, WI, USA), according to the manufacturer's specifications.

**Table 2.4:** General PCR conditions for the use of Q5® High-Fidelity DNA Polymerase

STEP	TEMPERATURE (°C)	TIME	
Initial denaturation	98	1 min	
Denaturation	98	10 sec	
Annealing	*	30 sec	
Extension	72	30 sec	
Final extension	72	7 min	
Hold	4	Hold	

\*Annealing temperatures are adjusted for the specific primer pair in use

#### 2.2.5.6 Isothermal in vitro recombination reaction setup

The 5x ISO reaction buffer used in the reaction was prepared as described by Gibson (2011). To make up the reaction buffer, the required chemicals were combined as described in Table 2.5. An isothermal recombination enzyme-reagent master mixture (IR buffer) was subsequently prepared. The required volumes of the 5x ISO buffer, T5 exonuclease (10 U/μl), Phusion polymerase (2 U/μl), *Taq* Ligase (40 U/μl) and water were added to a final volume of 1 ml according to the specification of both Jiang et al., 2013 and Gibson (2011). All the required enzymes were obtained from NEB (United Kingdom).

Approximately 75 ng (in total, for each) of the sense and antisense fragments amplified, containing the target sequence along with the required overlapping regions, were added to 5 μl of the 2x IR mixture. For the amplification of the sense and antisense fragments, the PCR was conducted with the GIBSON primer sets. The *KpnI* and *NotI* linearized pUBI510+ vector was added to a final concentration of 30 ng. Finally the reaction mix was adjusted to a total of 10 μl with nuclease free water. The mixture was incubated at 50°C for 30 min. A total of 1 μl was transformed into *Escherichia coli* DH5α competent cells. Colonies that were present after an overnight incubation period at 37°C, were tested with a colony PCR with the plasmid forward (UBI-exp), and plasmid reverse (CAMV-R) primers (Table 2.5). During troubleshooting

sessions, different concentrations of purified antisense and sense fragments were added to the mixture (the two respective DNA segments were added in equimolar amounts), with linearized vector, to optimize the reaction parameters. Concentrations added varied between 25 – 150 ng of purified DNA fragments and linearized vector.

**Table 2.5:** pUBI510+ sugarcane transformation vector specific primers

PRIMER	SEQUENCE	ANNEALING
UBI-exp	5'- ATACGCTATTTATTTGCTTGG-3'	53°C
CaMV-R	5'-AGGGTTTCTTATATGCTCAAC-3'	

After the incubation was completed, a transformation into chemical competent cells was done. The remainder of the samples (between 5 and 9 µl) were analysed on a 2% agarose gel (containing 2.5 µl per 50 µl PRONOSAFE nucleic acid staining from Laboratorius CONDA, Italy) and visualised under UV light. This was done to deduce whether the assembly was successful.

#### *2.2.5.6 Troubleshooting: Adjustments made to the IR mixture*

As part of the troubleshooting procedure, the 2x IR mixture components were adjusted from the specifications made in Jiang et al. (2013), to the specifications of Gibson (2011). A 100 µl master mix of the enzyme 2x IR mix was made up as specified in Table 2.6. Aliquots of 20 µl were then made and were frozen away at -20°C until needed. An enzyme mix aliquot was specified to remain functional for up to one year if frozen away.

#### *2.2.5.7 Assembly with the Gibson Assembly® Cloning Kit*

For the assembly of an hpRNAi cassette with the help of the Gibson Assembly® Cloning Kit (NEB, United Kingdom), a reaction mix was set up according to the manufacturer's specifications.

**Table 2.6:** All the different chemicals, with the respective concentrations that were combined to create the Gibson Assembly One-Step 5x ISO Buffer

CHEMICAL	STOCK SOLUTION	VOLUME REQUIRED
Tris-HCl, pH 7.5	1 M	3 ml
MgCl <sub>2</sub>	2 M	150 µl
dGTP	100 mM	60 µl
dATP	100 mM	60 µl
dCTP	100 mM	60 µl
dTTP	100 mM	60 µl
DTT	1 M	300 µl
PEG-8000	-	1.5 g
NAD <sup>+</sup>	100 mM	300 µl
dH <sub>2</sub> O	-	2 ml
TOTAL VOLUME		6 ml

\*500 µl aliquots of the ISO buffer was stored at -20°C

**Table 2.7:** The different components required for a 2x IR reaction buffer according to Gibson (2011)**For 100 µl of 2x IR reaction mix**

27 µl	5x ISO Buffer
5.4 µl	T5 Exonuclease (0.1 U/ µl)
1.7 µl	Phusion polymerase (2 U/ µl)
13.4 µl	<i>Taq</i> Ligase (40 U/ µl)
52.5 µl	Nuclease free water

## **2.3 RESULTS**

### **2.3.1 Isolation of partial sugarcane CKX coding sequences**

To amplify and isolate partial coding sequence for sugarcane *CKX* genes, gene sequences from the closest known relative to sugarcane were used as template for primer design. A search of the Phytozome V9.1 database delivered two independent *Sorghum bicolor* *CKX* coding sequences. The first sequence, *Sorghum bicolor* cytokinin dehydrogenase 3 (*SbCKX3.1*, XM\_002454958) was 1734 bp long. The second sequence, *Sorghum bicolor* cytokinin dehydrogenase 9 (*SbCKX9*, XM\_002439661) was 1569 bp in size. Both were putative sequences in the database, not yet fully characterized. Additionally, two of the characterized *Arabidopsis thaliana* cytokinin dehydrogenase coding sequences, which were used to design separate primer sets, were found in the Phytozome V9.1 database. The sequences included that of the cytokinin dehydrogenase 2 (*AtCKX2*, NM\_127508), which was 1667 bp in size, and a second, cytokinin dehydrogenase 4 (*AtCKX4*, NM\_179139), which was slightly larger with 1951 bp, from *Arabidopsis thaliana*.

With the help of standard PCR methods, the different primer sets were used to amplify partial sugarcane *CKX* genes from freshly made first-strand cDNA. Although the designed *Arabidopsis* primers did not yield any successful amplification from the sugarcane cDNA, multiple bands could be obtained when amplifying with the sorghum based primer pairs. This result can be explained by the fact that sorghum is the closest known relative to sugarcane, where *Arabidopsis* is much further removed from sugarcane evolutionary. Four different fragments of the expected sizes, were subsequently cloned into pGEM®-T Easy vectors and sequenced (Figure 2.1).

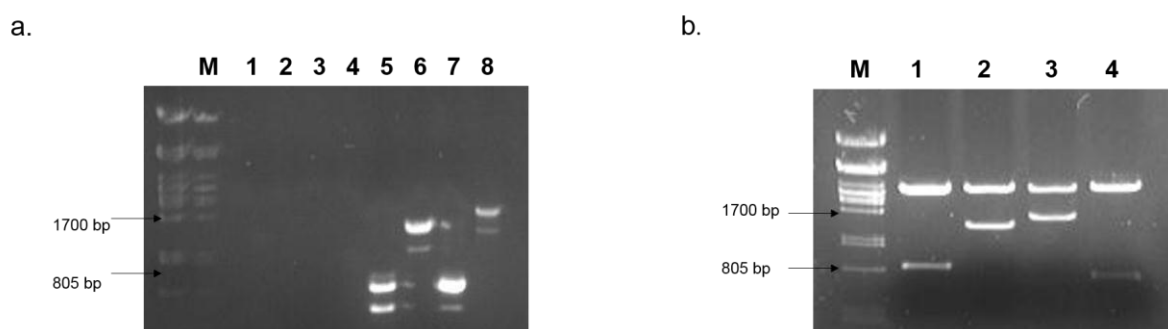


**Figure 2.1:** A visual representation of the 4 sugarcane partial *CKX* gene fragments through amplification with the sorghum-based primers. a) The unsuccessful amplification with *Arabidopsis*-based *CKX* primers (lanes 1-4) and the multiple bands that were successfully amplified with the sorghum-based primer sets (lanes 5-8), from sugarcane cDNA and b) the four respective fragments cloned into pGEM®-T Easy cloning vectors to allow for sequencing. A Lambda *Pst*I-marker was included in each, represented by M.

## 2.3.2 Phylogenetic analysis

### 2.3.2.1 The *CKX* dendrogram

For further analysis of the partial sugarcane *CKX* sequences obtained, a multiple sequence alignment was conducted. The alignment included 57 independent cytokinin dehydrogenase (*CKX*) coding sequences from 11 different species. The alignment was curated for phylogenetic analysis. Once it was ready, the multiple sequence alignment was used to draw a phylogenetic tree, also referred to as a dendrogram (Figure 2.2), rooted with the two different *Physcomitrella patens*, as well as the two *Selaginella selaginoides* *CKX* sequences included in the alignment (Figure 2.2, highlighted in yellow). The tree included two of the partial sugarcane sequences, designated Sugarcane03 and SugarcaneCTKD for the purposes of this study, (names were based upon the primer pair used to amplify the relevant fragment with).

From the resulting dendrogram (Figure 2.2), the partial sugarcane sequences tend to group with other monocot plants. The SugarcaneCTKD sequence was present on the same branch as the barley *CKX* 2 (*HvCKX2*) and *CKX* 3 (*HvCKX3*) (Figure 2, highlighted in red). The Sugarcane03 sequence was on the same branch as the well characterized maize *CKX* 2 (*ZmCKX2*). All of the partial sequences obtained were highly related to the *Sorghum bicolor* *CKX* gene representing the primer pair used to amplify the original fragments. The probability score between the SugarcaneCTKD and the sorghum *CKX9* exhibits a probability score of 1.

During assembly of a phylogenetic tree, the probability score for each branching event was calculated and indicated on the resulting dendrogram. A score of 1 is considered as a confident score, but anything above 0.95 is considered to be credible. For the Sugarcane03 sequence, the probability is slightly lower but still high at 0.94, just 0.01 short of a credible 0.95 value. The *AtCKX2* and *AtCKX4* (Figure 2, highlighted in blue), both known to encode for active proteins, clustered in the same clade as the sugarcane sequences. It is important to note that two of the branches separating these genes were of a low probability score, namely 0.86 and 0.58. Both scores are below 0.95, allowing a lower degree of confidence to these specific branching patterns. Therefore the relationship between the *Arabidopsis CKX* sequences and the isolated sugarcane sequences could change if more information became available, or the parameters included in the phylogenetic analysis were refined. However, due to the perfect probability score between the *HvCKX2* gene sequence and the isolated SugarcaneCTKD sequence, it was decided proceed with the SugarcaneCTKD sequence during RNAi vector construction.



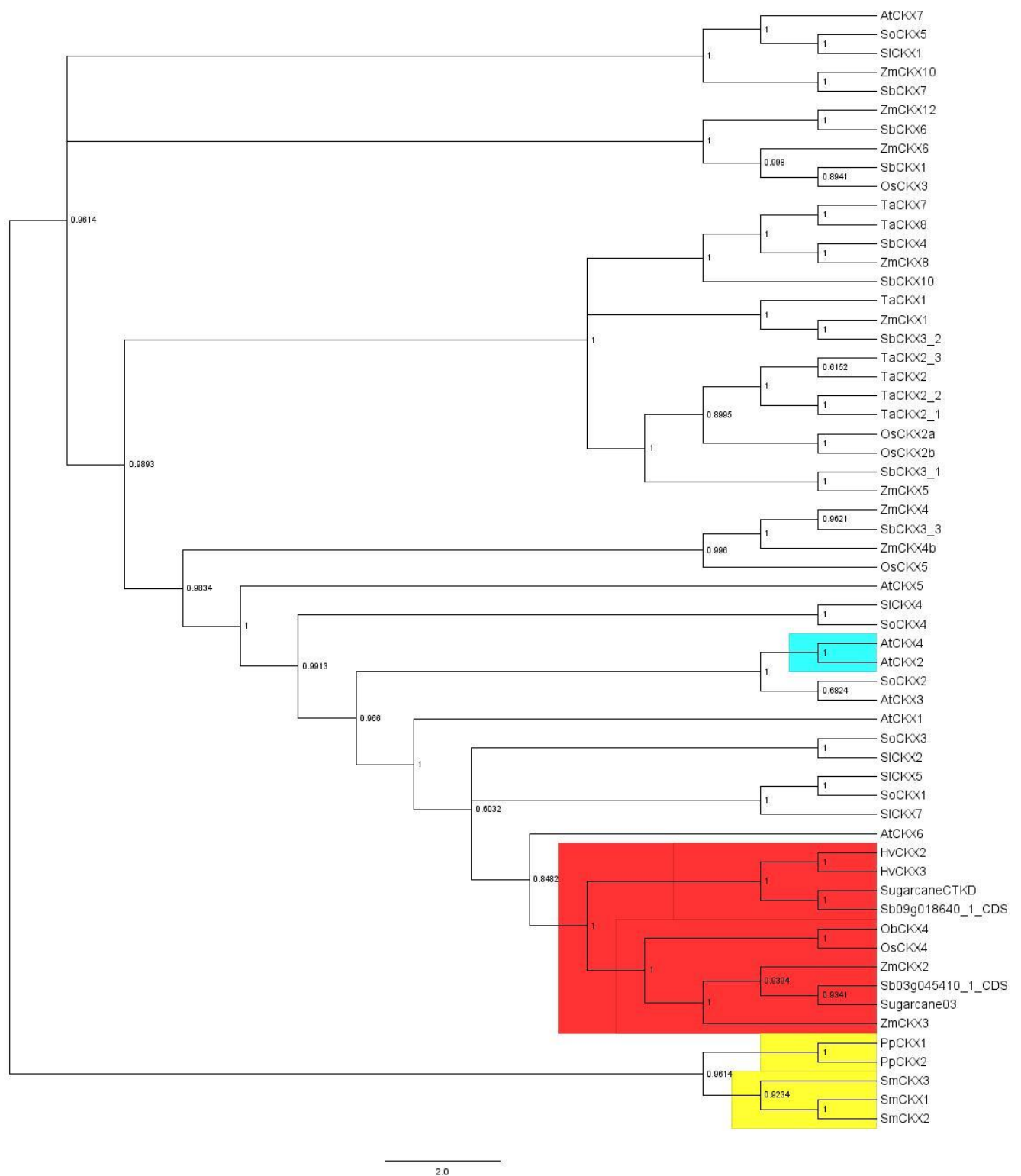


**Figure 2.2:** A phylogenetic tree representing 57 coding sequences of plant cytokinin dehydrogenases (CKXs), from 11 different plant species. The tree was constructed with the Bayesian MCMC program, MrBayes (Ronquist et al., 2012) and rooted with *Physcomitrella patens* and *Selaginella moelendorffii* sequences, which are highlighted in yellow. Red highlighting indicates the sugarcane sequence positions. The characterized *Arabidopsis* sequences, known to be active, are highlighted in blue.

### 2.3.3 RNAi assembly attempts

#### 2.3.3.1 Gene specific area chosen to act as template for hairpin design

Using the dendrogram data, it was decided to utilize the SugarcaneCTKD sequence fragment as template for the hpRNAi construct. From the SugarcaneCTKD sequence an area of fairly high conservation to the other plant CKX gene sequences, specifically within the cytokinin binding domain, was identified and isolated (Figure 2.3). The area of high conservation acted as template for the further design and creation of the hairpin cassette.

```

5'- TCTCCACCTTGCCTCAAAGTGGGCCTTCCACTCCTGTTAGTGTAGTTGGGCAGATATTGCTTCACCTAATA
CCTGCCTTGCCAGAGAATTCTATTATCTGGTTGTTGAGGTTCAATGCATGTTGATGGCGTGGGGGCTGATGAA
GATGGCACTGAGGATAGGAATCCMCTAGGTAGAAAATTCTCATCTGGTGTGACTACTGATGTTCTATTGTCC
CATCTGAATTTGTTTACTGGGTAGAGCAATATGGGACCACTGTTGCTGTCTTCGGGATTTCCCAAAGATCTCCC
TTGCAAATGTGTGGATCGAACTTTTGAACCATGAGATTTAGCCATGGGKGTGGGACCTCCACATCCCCTTAGC
TCTCAGTTTCACCTCAGAGGAGTGCACCTATCCAGGAATCGATGTAGGTAACATCTGTGTGGAATAGGGATGG
AGGCATATGTCTAAGTTGATACAGTAGGTTATTGACC TCTGCAGACATGTATACA CSTATTTGACCACTCTCAA
ATTGATTTGATTTGATTTGATATTAGTCACAAGTCGTAACATATTCAAGGGTATGTGAGCTAGCTGCTCACCTGT
TCCATGTTGTCTGCCTCCTCAGGGTTGTAGTTCTTGGTCATCTCGAGGCAGAAGATCACTCTTCATCTGATTCGAA
CTGGCTTGTCACACTGGATCCTGTGGGCTAAACGATGATCTCCAGTTGTTGAGGATTCCTGTCTGTTGATGATG
ACGAAGCCCTCTATGTAATCG AAGGTCCTCTCTGCTGAAAT AAG CATCTCCTGATCCTCTGCAA -3'

```

**Figure 2.3:** The newly isolated SugarcaneCTKD sequence included in RNAi vector design. The identified area of fairly high conservation is highlighted in green that acted as template for further hairpin cassette design and the subsequent areas identified for the forward primer (highlighted in purple) and reverse primer (highlighted in red).

#### 2.3.3.2 PCR amplification of sense and antisense fragments

For the RNAi assembly, both the sense and antisense fragments containing the relevant overhangs were required. The two sets of specific overhang primer pairs (GIBSON and NEB primer pairs) was used to isolate these fragments. Both primers pairs were optimized with gradient PCR's, after which they were applied to amplify the sense and antisense fragments, respectively (Figure 2.4).

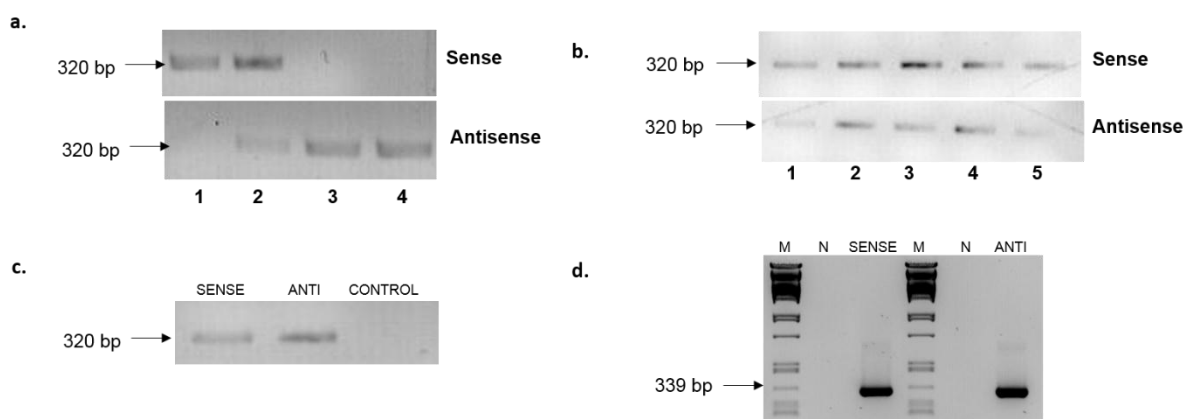


**Figure 2.4:** PCR amplification of the sense and anti-sense gene specific fragments used for creating the hpRNAi construct. a) The GIBSON sense and antisense primer pairs gradient PCR, representing temperature points 60°C (1), 59°C (2), 58°C (3) and 56.6°C (4); b) the NEB sense and antisense primer pairs gradient PCR for temperature points 60°C (1), 59°C (2), 58°C (3) 57.2°C (4) and 56°C. The subsequent amplification of the sense and antisense gene fragments, respectively, and negative water control (N) with the c) NEB primer pairs and the d) GIBSON primer pairs.

#### 2.3.3.3 Isothermal *in vitro* recombination – Attempt 1

For the first attempt at a full isothermal *in vitro* recombination, the conditions described in Jiang et al. (2013) were applied as outlined in section 2.2.5.6. The assembled DNA reaction was transformed into bacteria and PCR analysed with the plasmid specific primers binding in the promoter and terminator region of the vector (Figure 2.5). Two bands were visible, close in size. The second, slightly larger band seems to be in the range of 450 bp. These bands were larger than the expected 200 bp, for an empty vector. They were too small, however, for the full hairpin cassette, which should be 666 bp in size. Plasmid DNA was isolated from colony 1, 6 and 7, after which it was sequenced. The sequencing results confirmed that the plasmid was empty.

#### 2.3.3.4 Isothermal *in vitro* recombination – Attempt 2

Due to the unsuccessful assembly attempt, a control reaction was set up to test whether any assembly occurred during the reaction. The experiment was based upon an example shown in Jiang et al. (2013), with slight modifications. Five separate reactions were set up containing 75 ng of each sense and antisense fragment DNA (amplified with GIBSON primer sets). The five reactions mixes were incubated for a different time period, namely 0, 10, 20, 30 and 40 min, at 50°C. No linearized vector was added to this control experiment, to favour assembly of the sense and antisense fragments. As seen in Figure 2.6, no expected 666 bp band

(representing the full hairpin cassette) was present, although the unassembled sense and antisense fragments are present as bands at the approximate size of 339 bp.

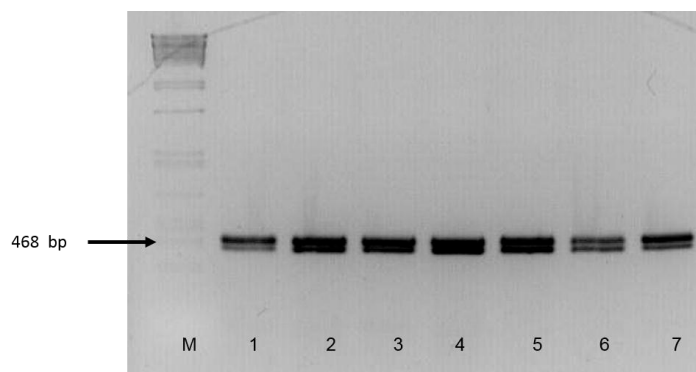


**Figure 2.5:** The colony PCR conducted on 7 colonies produced after the first cloning attempt of the hairpin cassette. When compared with the *Pst*I lambda marker (M), a band at the 468 bp mark was visible. The gel therefor indicated a negative result, with bands larger than the expected size of 150 bp when the plasmid is empty, but smaller than when the plasmid contained the full 666 bp hairpin fragment.

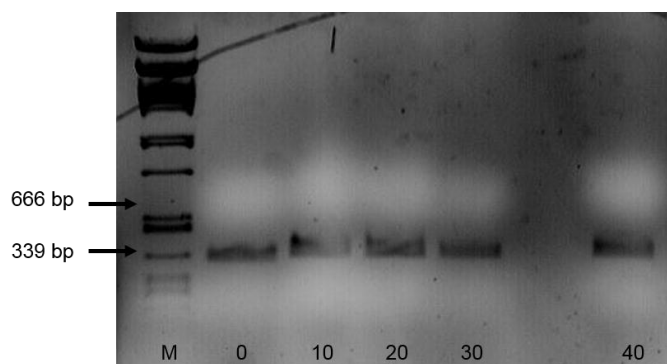


**Figure 2.6:** Gel electrophoresis of assembly attempt with sense and antisense fragments for different time intervals. Lanes represents five different 2x IR reaction mixes, containing only the sense and antisense fragments (both ~330 bp in size), which were incubated for 0, 10, 20, 30 and 40 min at 50°C. The required 666 bp assembled fragment was not seen when compared with the *Pst*I lambda marker (M).

### 2.3.3.5 Isothermal *in vitro* recombination – Attempt 3

A fresh 2x IR buffer was made up and the reaction mix was made up to the specifications of Gibson (2011), using the different enzyme concentrations (Table 2.8), as specified for an original Gibson Assembly set up. For this experiment, seven different reaction mixtures were set up. The seven reactions differed only in the amount of DNA added to each freshly made up 2x IR reaction buffer (Table 2.8). Once incubation was complete, 2 – 4 µl of each reaction mixture was used for transformation, while the rest was visualised on a 2 % (m/v) agarose gel (Figure 2.7). Apart from the sense and antisense fragments present at approximately 339 bp, a larger band of about 666 bp was expected. This would indicate that assembly did occur during the reaction. From Figure 2.7, no formation of a full hairpin cassette was present at the approximate size of 666 bp. The only bands visible were the linearized pUBI510+ band at 5400 bp, and the respective sense and antisense fragments. This supported the conclusion that the reaction was unsuccessful, as no colonies were present from the transformation after an overnight incubation of the plates at 37°C.

**Table 2.8:** The different DNA concentrations added for Attempt 3 at an isothermal *in vitro* recombination and assembly of an hpRNAi construct

Reaction	Amount of DNA for sense and antisense fragment (ng)	Amount of linearized pUBI510+ vector (ng)
Negative control	No DNA added to the 2x IR Mix	
1.	70	25
2.	140	25
3.	70	50
4.	100	50
5.	100	25
6.	140	0

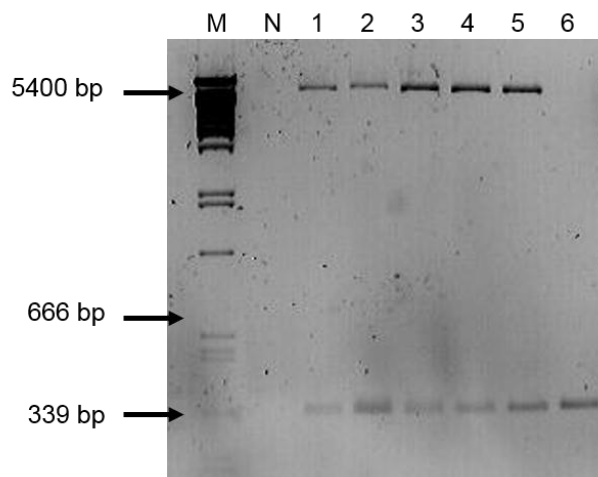


**Figure 2.7:** A visual analysis of the isothermal *in vitro* recombination - attempt 3, where differing DNA concentration combinations (as described in Table 2.6) were tested. A *Pst*I lambda marker (M) was included as well as a negative control (N), consisting of the 2x IR mix and no added DNA. A larger band at 666 bp was expected to be present. The linearized vector is present at approximately 5400 bp.

#### 2.3.3.6 Isothermal *in vitro* recombination – Attempt 4

At this point it was concluded that the 2x IR reaction mix was not effective enough to allow for assembly. A Gibson Assembly® Cloning Kit (NEB, United Kingdom) was acquired, which included a premixed 2x Gibson Assembly Master Mix containing all the required components. In combination with the kit, two new sets of primers were designed through the web-based tool available on the NEB website ([www.neb.com](http://www.neb.com)). Once the appropriate sense and antisense fragments, consisting of both a gene specific and overlapping area, was amplified, a fourth attempt was conducted with the provided master mix. The reaction was transformed into the provided NEB 5-alpha competent *E. coli* cells and 12 colonies were obtained. What was left of the reaction was visualised on a 2 % (m/v) agarose gel (Figure 2.8). Due to the possibility of the hairpin cassette folding during PCR amplification, the colonies were rather confirmed to contain the hairpin fragment through restriction digest (Figure 2.9a & b). Initially, plasmid DNA was purified from three of the colonies and subsequently digested with *Eco*RI and *Hind*III, as well as with *Bam*HI in a separate digestion. Based on Figure 2.9a & b, the first two colonies were empty. The third colony showed a unique digestion pattern, unlike what was expected for an empty vector, or even vector that contained the cassette. For the *Bam*HI digestion (Figure 2.9b), the plasmid remained undigested. It was therefore concluded that the third colony might possibly contain the cassette and that some form of assembly did occur. Purified plasmid DNA was sent for sequencing with the plasmid specific primers (Table 2.5).

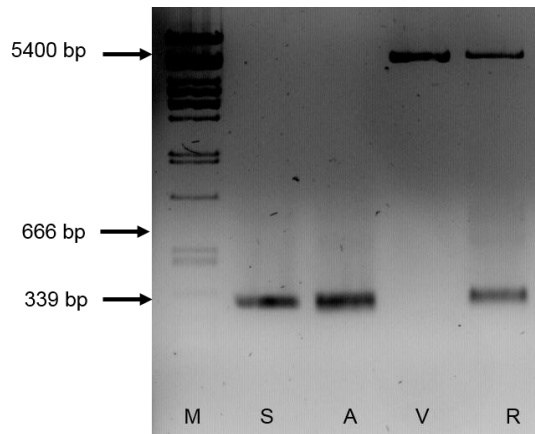


**Figure 2.8:** Analysis of the assembly reaction conducted with the Gibson Assembly Kit. Lanes indicate a sample of the sense (S) and antisense (A) fragments ~330bp in size, linearized vector (V) of 5400 pb in size and the reaction mix containing all three components (R). No band was present at the expected size of 666 bp when compared to the *PstI* lambda marker (M), indicating an unsuccessful reaction.

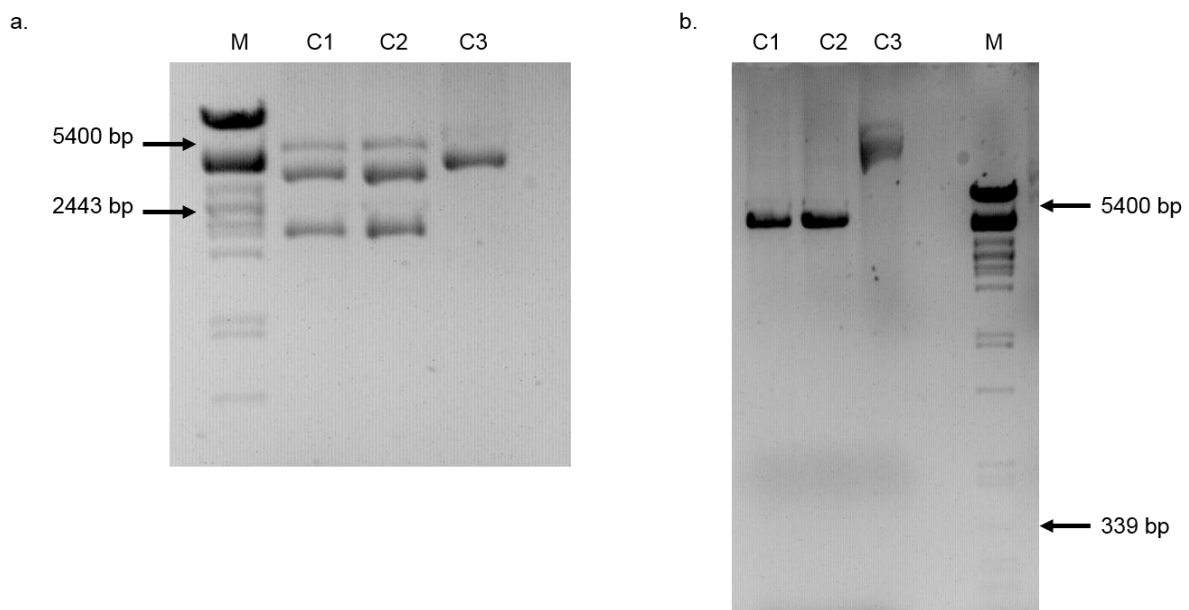


**Figure 2.9:** Analysis of isolated plasmid DNA from three separate colonies generated by the Gibson assemble kit digested with a.) *EcoRI* and *HindIII* and b.) *BamHI*. The first two colonies (C1 and C2) appeared to be empty. The third colony (C3) showed an odd, unexpected banding pattern, possibly indicating uncut plasmid DNA. A *PstI* lambda marker (M) was included in both gel photos.



Due to the inconclusive results from colony 3, it was decided to also do diagnostic tests on plasmid DNA from the remaining 9 colonies. Plasmid DNA was digested with *Bam*HI (Figure 2.10), because the fragments are known to contain two separate cutting sites, apart from the sites present in the vector. An empty pUBI510+ plasmid sample was also digested to act as control. If digested with *Bam*HI, the empty vector should linearize with no other fragments forming. A hairpin containing vector would produce two additional small fragments, no larger than 300 bp, due to the restriction sites present within the hairpin. When compared to the restriction pattern formed by the empty plasmid control, plasmids 1, 2, 8 and 9 did not contain an insert. The linearized vector is clearly visible, but no smaller fragments were visible on the gel. Plasmids 3, 5, 6 and 7 indicated undigested plasmid. Plasmid 4 showed a unique banding pattern (although not the desired pattern) and was sent for sequencing, which confirmed it to be an empty plasmid (Figure 2.10).

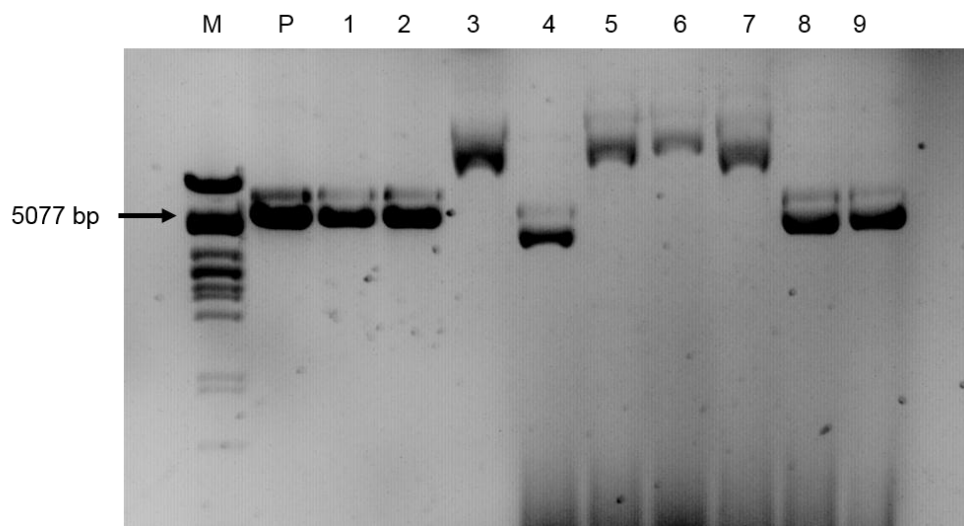


**Figure 2.10:** *Bam*HI restriction on the remaining nine colonies from attempt 3. From the 12 colonies obtained post transformation, plasmid DNA was isolated from the remaining nine colonies and restricted with *Bam*HI, which cuts twice in the hpRNAi cassette and once in the vector. Unfortunately no conclusion could be made from these digestions as the banding patterns were irregular, and none of the expected band sizes were present when compared to the *Pst*I lambda marker (M).

#### 2.3.3.7 Isothermal *in vitro* recombination – Attempt 5

For troubleshooting purposes the aim of this fourth attempt was to try and determine whether the reaction failed due to the reaction master mix being faulty or due to fault with the DNA fragments. The isothermal reaction was thus repeated (as for the third attempt) with freshly isolated sense and antisense fragment DNA as well as freshly linearized vector DNA. The



experiment additionally included a positive control. This control reaction was set up using the positive control DNA provided in the Gibson Assembly® Cloning Kit (NEB, United Kingdom), in combination with the manually made 2x IR reaction mix (thus NOT the provided mix in the kit). This was done to determine whether the DNA fragments and linearized vector was the limiting factor during the assembly. The fifth attempt therefore included three separate reactions summarized in Table 2.9. As seen in Figure 2.11, the positive control successfully produced colonies post transformation and overnight incubation at 37°C. When 2 µl of the reaction was transformed, a lesser amount of colonies were obtained (Figure 2.11a) than when 4 µl of the total reaction was used (Figure 2.11b) for subsequent transformation. For the normal assembly using the kit provided reaction mix, as well as the manually made reaction mix (Reaction 1 & 2), no colonies were present post transformation and overnight incubation. The results indicated that the DNA might be the limiting factor, and not the 2x IR enzyme mix.

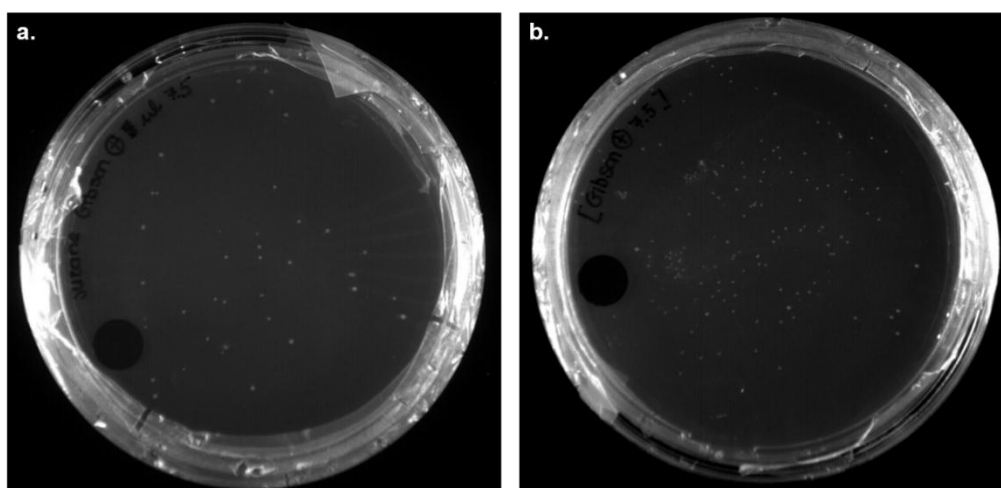


**Figure 2.11:** Transformation of the positive control, included in attempt 4. Using the positive DNA provided by the Gibson Assembly® Cloning Kit assembled with a manually made 2x IR mix, plates post transformation with a.) 2 µl and b.) 4 µl showed colony formation.

**Table 2.9:** Attempt 4 experimental set up

REACTION	DNA INCLUDED	ENZYME MIX USED
Positive control	Positive control provided in kit	Manually made 2x IR reaction mix
Reaction 1	Sense, antisense and linearized vector	Manually made 2x IR reaction mix
Reaction 2	Sense, antisense and linearized vector	Kit provided 2x IR reaction mix

#### 2.3.3.8 Isothermal in vitro recombination – Attempt 6

As a final attempt, sense and antisense fragments were amplified with the originally designed GIBSON primer sets. Approximately 160 ng of total DNA was added to the master mix of the Gibson Assembly Cloning kit, along with 80 ng of linearized *pUBI510+* vector DNA. After the reaction was incubated for an hour at 50°C, 2 µl of the reaction mixture was transformed into the provided NEB 5-alpha competent *E. coli* cells and the remaining reaction mix was visualised on a 1,5% agarose gel photo. Figure 2.12 shows the reaction where the sense and antisense fragments are present close to 339 bp, as well as a faint assembled band closer to 650 bp, as expected.

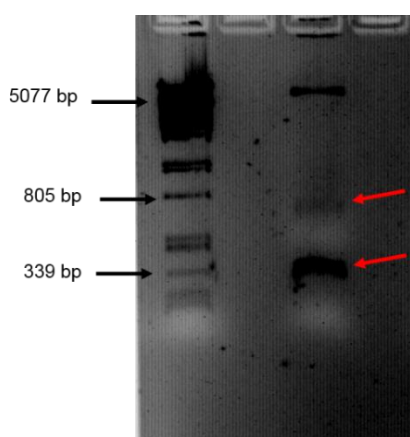


**Figure 2.12:** A visualisation of the successful Gibson Assembly reaction (attempt 6) on a 2% agarose gel. A faint band of approximately 650 bp (indicated with a red arrow) and a high intensity band representing the sense and antisense fragments of approximately 339 bp (indicated with a second red arrow) was present on the gel picture, indicating assembly was occurring.

The transformation reaction was plated out onto selection plates and three, respective colonies grew overnight. Plasmid DNA was extracted from subsequently made liquid cultures and an initial overnight digestion was done on each of the three colonies with *XhoI* (Figure 2.13). The enzyme has a single cutting site present in the vector, as well as two in the hairpin fragment. Although the smaller expected fragment of approximately 200 bp was not visible on the gel, the banding pattern of plasmid A and C (Figure 2.13) seemed to indicate a positive result. Two bands of ~1600 bp were expected along with the vector backbone of ~3000 bp. At least one band was present for plasmids A and C, with the possibility of the two bands lying on top of each other. It was clear that, when compared with the control empty vector, the third plasmid isolated (B), represented an empty vector.

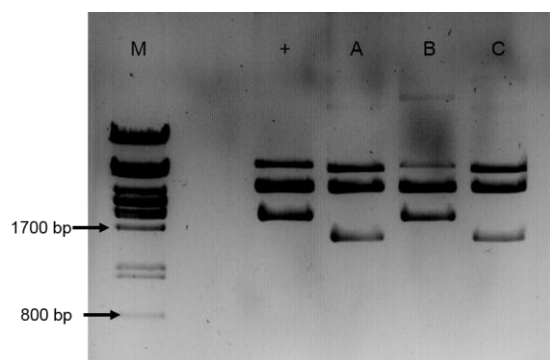


**Figure 2.13:** A visual representation of the *XhoI* digestion to confirming A and C as positive clones. The *XhoI* digest of control empty plasmid (+), and isolated plasmids A, B and C are shown. Colonies A and C showed the desired ~1600 bp size band, together with the smaller than 4700 bp but larger than 2800 bp vector backbone, as desired.

Prompted by this result, further diagnostics were performed in the form of additional digestions and PCR analysis. Additional overnight digestions were performed with *BamHI*, which has two cutting sites present in the hpRNAi cassette, apart from a single site present in the pUBI510+ vector. This should produce two small fragments, less than 250 bp in size and the vector backbone, if the hairpin fragment was present. From Figure 2.13, a linearized backbone of vector is present, but no smaller band can be located for colony B. This is comparable with the empty plasmid control, which shows a similar pattern, as well as with the previous digestion analysis with *XhoI* (Figure 2.13). DNA from colonies A and C, however, showed undigested plasmid present. Additionally, a double digest was performed with *KpnI* and *NotI*, corresponding with the sites originally used to linearize the pUBI510+ vector. Once again, colony B showed a consistent result of being empty, but colony A and C remained undigested (Figure 2.14). It has been suggested that this might be due to the sites being lost during the

recombination reaction, where the exonuclease digestion and *Taq* polymerase may alter the digestion sites in the multiple cloning site and hairpin fragment.

Therefore PCR analysis was also done with plasmid specific primers. The primers used, bind in the ubiquitin promoter area and the CamV terminator area of the pUBI510+ vector. The PCR analysis confirmed that vector B was empty, but plasmid DNA from A showed amplification of a band larger than 514 bp, which is indicated on the *Pst*I Lambda marker (Figure 2.15). This showed that the hpRNAi cassette was most likely present within the vector, since the expected band is supposed to be 666 bp in size. In a subsequent PCR, the same 650 bp band was present for vector DNA from C (Figure 2.15). Finally the integrity of the hpRNAi vector construct will be confirmed with sequence analysis currently being attempted by Inqaba Biotechnologies (Pretoria, South Africa). To avoid folding of the hairpin during the sequencing reaction, a likely problem when sequencing hairpin constructs, approaches such as buffer changes/additions will be utilised by the sequencing company. As an alternative, an additional primer pair will be designed to allow for PCR analysis of the potential positive clones. The pair will include a forward primer which anneals within the intron area of the hairpin fragment, and a reverse primer which anneals in the CaMV terminator area of the pUBI510+ vector.

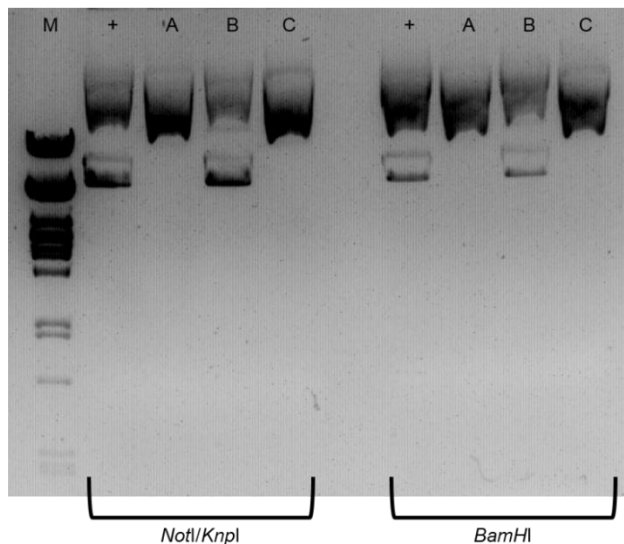


**Figure 2.14:** Insert confirmation of possible positive RNAi vector clones, with restriction digest. The first digestion was conducted with *KpnI/NotI*, and in the second *BamHI* was used. It confirmed that colony B was an empty plasmid when compared to the empty plasmid control (+). Plasmid samples, A and C remained undigested. As size indicator the *Pst*I lambda marker (M), was included.

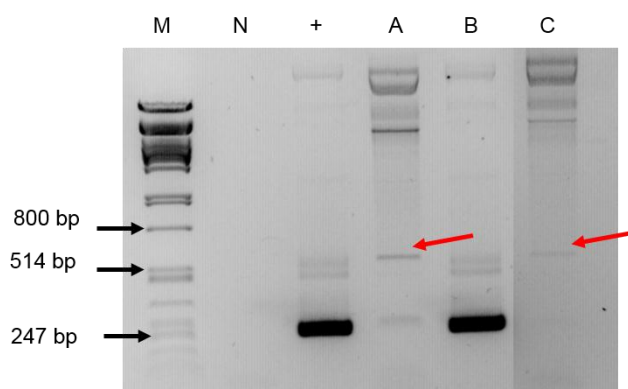


**Figure 2.15:** PCR confirmation of potentially positive RNAi hairpin constructs, A and C. A plasmid specific forward and reverse primer pair was able to amplify an amplicon larger than 514 bp for both plasmids A and C. Plasmid B appears to be empty when compared to the empty vector (+) control.

## **2.4 DISCUSSION**

### **2.4.1 Gene silencing in sugarcane**

As a progression towards the successful silencing of the cytokinin oxidase/dehydrogenase (*CKX*) gene family present in sugarcane, two separate silencing cassettes containing a suitable hairpin construct, were created. Two different methodologies were employed for the creation of the cassettes: The first cassette was created with a novel method based on the Gibson Assembly™ cloning technology. The second cassette was created with the established GATEWAY® vector cloning system as precautionary measure (Annexure C).

#### *2.4.1.1 Stable RNA interference-based technologies*

Over the past two decades researchers have specifically focused on gene silencing techniques, as it holds the advantage of the suppression of multiple genes (Ingelbrecht et al., 1999; Jiang et al., 2013). For sugarcane in particular, it holds an additional advantage. Sugarcane is very effective in silencing an alien gene, causing transgenic methods of introducing transgenes to be an ineffective strategy (Osabe et al., 2009). The silencing, or down-regulation, of endogenous sugarcane genes acts as a valuable alternative (Osabe *et al.*, 2009). A recent study showed great success by using RNA-interference based methods to stably suppress transcript levels for caffeic acid O-methyltransferase (*COMT*) (Jung et al., 2013) The study reported a decrease in *COMT* transcript levels of between 80 and 91%, resulting in transgenic sugarcane lines with reduced lignin levels of 6-12% (Jung et al., 2013). The transgenic sugarcane lines requires less 3-4 hydrolysis for the release the fermentable

sugars used in bioethanol production, making the breakthrough extremely valuable (Jung *et al.*, 2013). In a separate study the Pyrophosphate:fructose 6-phosphate 1-phosphotransferase (*PFP*) activity was reduced up to 70% in sugarcane lines that constitutively expressed an antisense form of the endogenous sugarcane *PFP*- $\beta$  gene (Groenewald and Botha, 2008). With the help of stable RNA interference (RNAi), gene expression can easily be manipulated for quality traits in crop, shifting the focus from single gene manipulation to multiple gene manipulation. The strategy involves the construction of a hairpin gene construct, contained in an RNAi vector, transformation of the plant and analysis of the resulting phenotype (Saurabh *et al.*, 2014).

Gene silencing can occur on two respective levels: transcriptional or post-transcriptional. Both are due to the naturally occurring defence organisms have developed against viral infection. The phenomena is especially prevalent in plants. The introduction of an exogenous gene (a transgene) suppresses the expression of an endogenous, homologous gene. During transcriptional silencing the promoter of the involved gene/s is affected, but with post-transcriptional silencing the expressed RNA is degraded with the help of DICER and the RISC complex (Osabe *et al.*, 2009; Jung *et al.*, 2013).

RNAi triggered by hairpin RNA involves various cloning steps and vector construction is both complicated, laborious and in certain cases a costly affair. Various attempts have been made to simplify the process, including the development of the GATEWAY<sup>®</sup> Cloning System (Jiang *et al.*, 2013). The GATEWAY<sup>®</sup> Cloning System produced by Invitrogen, utilizes a two-step recombination process, where both an entry vector, and subsequently used destination vector is required. The entry is used to clone the fragment of interest into and create donor vector. The fragment can then subsequently be cloned into a suitable expression vector, utilizing the recombination sites present in the donor vector. The system allows for a site-specific recombination reaction (Oa *et al.*, 2009). Site specific recombination is mediated by an enzyme mix containing Integrase, Integration Host factor and Excisionase allow for the recombination between the entry clone containing attL sites, flanking the gene of interest and the destination vector with complimentary attR sites (Karimi *et al.*, 2007). The system provides the advantage that once the fragment is successfully cloned into the donor vector, a simple reaction is required for subsequent cloning into the desired expression vector. The reaction excludes traditional restriction enzyme/ligase cloning. Another advantage is that the technology is well-established due to its popularity amongst researchers. A large variety of both donor and expression vectors are available (Karimi *et al.*, 2007). It does however require a two-step cloning that can be tricky and time-consuming (Jiang *et al.*, 2013). For this particular study, the expression (destination) vector available for monocot transformation, was the 15416

bp pHb7GW-I-WG-UBIL vector. The pUBI510 transformation vector is almost a third of the destination vector's size with only 5404 bp. Recent studies have indicated that simpler transformation cassettes (containing only a promoter, a gene of interest and a terminator, as the case with vector pUBI510 vector) that are more efficient for biolistic based transformation (Joyce et al., 2014). Alternatively, the hairpin fragment can be removed from the vector and bombarded as a linearized fragment. Bombardment with fragment DNA has, however, been already successfully optimized for various wheat varieties including both spring and winter bread wheat (Pastori et al., 2001). It suggests that it is also possible to optimize the biolistic-mediated transformation protocol for sugarcane with linearized fragment DNA, albeit not ideal. Considering that the hairpin fragment known to fold on itself during PCR amplification, linearized fragment will have to be obtained through restriction digest. Therefore another important factor to consider is whether the pHb7GW-I-WG-UBIL vector has any restriction sites available for cutting out the hairpin fragment. The vector contains 27 unique restriction sites (Annexure D), but only 14 sites between the left and right borders.

Alternative to GATEWAY® cloning, another ligation independent cloning method was developed by Hauge et al. (2009). The method uses uracil DNA glycosylase (UDG) for hairpin RNA preparation. The method requires, however, various complex steps where the sense and antisense strands are tagged with specific single stranded tails. The single stranded tails attached are unique, complementary strands that allow for ligation in a set orientation. The advantage is that fragments have a more than 90% chance of being in the correct orientation. The tagging process includes several PCR steps. The second PCR event requires the use of Splice Overlap Extension (SOE)-PCR (Jones and Barnard, 2005). Also, the single-stranded tags required are unique to each experiment, resulting in a great deal of optimization to obtain the perfect conditions under which ligation occurs (Hauge et al., 2009).

The direct amplification of intron-containing RNA construct (DA-ihpRNA), a method developed by Xioa et al. (2006), is unsuitable for making hairpin constructs from intron-less genes or genes that only have expressed sequence tags (EST's), as the case for sugarcane. Sugarcane has a complicated genetic makeup, due to centuries of cross-breeding. Modern cultivars are highly heterozygous, with reports of up to 10 alleles at each locus (Osabe et al., 2009). The genetic complexity of the crop has delayed the development of a comprehensive genetic map, or the sequencing of the whole genome (Aitken et al., 2014). Sugarcane *CKX* gene sequences were therefore obtained in this study through the manual isolation and cloning of partial genes, as no sequence was available at the time. This rendered the DA-ihpRNA method unusable for the purpose of this study.



More recently the Gibson Assembly<sup>®</sup> method was developed (Ellis et al., 2011; Gibson, 2011), where DNA fragments with overlapping ends are chewed back at the 3' end, by the DNA exonuclease. This then causes the formation of complimentary single-stranded overhangs. DNA polymerase acts to fill in the gaps, once the fragments have been annealed and DNA ligase seals the nick. The potential use of Gibson Assembly<sup>®</sup> in the construction of a hairpin containing RNAi vector, was identified by Jiang et al., (2013). The specific research group further manipulated Gibson Assembly<sup>®</sup> to facilitate the construction of a hairpin RNA construct which in turn was used to successfully silence the *Arabidopsis PDS3* gene. The parameters involved in the one-step *in vitro* recombination system developed, including primer design, was optimized. When the method was assessed, an average 60% cloning efficiency was achieved. The study also confirmed that both a native and an exogenous intron can effectively be used in the hairpin RNAi construct. Several benefits for this novel cloning system was identified, including cost-effectiveness and efficiency. A second benefit is in the reduced cloning steps, where only a single reaction is required for complete assembled. The method has also been shown to reduce PCR faults in the inverted gene sequence, which may occur during traditional methods. This is due to the complimentary parts of the same DNA fragment annealing to each other (Jiang et al., 2013). The last, and probably the most attractive benefit of the method, was included in the fact that for this method any available transformation vector could be employed. This allowed for the use of the pUBI510+ sugarcane transformation vector, the traditional vector employed for sugarcane transformation. Therefore, due to the various benefits provided by the novel method and the promising results obtained by Jiang et al., (2013), it was decided to apply the newly developed isothermal *in vitro* recombination system (IR-hpRNAi) in this study. However, a large amount of method optimization was required due to the novelty of the method, especially for this particular research environment.

An important component in creating an hp-RNAi construct is the design of the self-complementary sequence used to form the hairpin fragment. To increase efficiency, a spacer/intron is inserted between the two complementary sequences (Wesley et al., 2001). To design an effective hairpin construct for silencing of the endogenous *CKX* sugarcane gene family, a homologous area within the gene family needed to be identified. For this, phylogenetic analysis was conducted on 57 different *CKX* gene sequences. A combination of monocotyledonous and dicotyledonous was included in the analysis. Sequences from *Physcomitrella patens* and *Selaginella moellendorffii* were included, for rooting the tree. Once a phylogenetic tree was obtained the most suitable of the amplified partial sugarcane *CKX* fragments could be identified. Of the two that was obtained, the second sequence (SugarcaneCTKD) was identified to be more suitable, as it was closely related to the *HvCKX2* and *HvCKX3* genes. In a previous study conducted by Zalewski et al., (2012), it was shown



that when the *HvCKX2* was silenced, a decrease of 34 % in the CKX enzyme activity was observed. As the SugarcaneCTKD showed close relation to the *HvCKX2* sequence, it was chosen as the sequence to be used in RNAi-construct creation. From the multiple sequence aligned used to draw the phylogenetic tree, a conservative nucleic acid segment could be identified. This area of conservation was hypothesised to be a segment which could possibly lead to the silencing of multiple CKX genes within sugarcane. The approach used for identification of a conserved gene area was based upon the methodology described in Zhou et al., (2014), where a multiple sequence alignment was utilized to identify a suitable gene area within different *Sorghum mosaic virus* (SrMV) strains. The resulting hpRNAi construct was used to produce transgenic sugarcane lines exhibiting an 87.5% resistance against SrMV (Zhou et al., 2014).

For optimization of the IR-hpRNAi recombination method, different assembly incubation times were tested, along with the optimal primer design, and required amounts of each enzyme (*Taq* ligase, Phusion polymerase and T5 Exonuclease) and template (including the sense, antisense and linearized pUBI510+ vector) for successful assembly. From initial unsuccessful attempts, it was clear that using shorter overlapping regions (10-20 nt in total) for primer design, was more favourable. The NEB-designed primer pair included overlapping regions that were much longer than the original GIBSON primer pair, which was based upon the suggestions made by Jiang et al., (2013). Successful assembly occurred when the sense and antisense fragments contained the shorter overlapping overhangs and were added to the kit provided reaction mix. This supports the findings of Jiang et al., (2013), who concluded that when overhang sequences between 20 and 30 bp were used, a maximum cloning rate of 75.7% could be achieved. It was also concluded from this result that an incubation period of 30 min at 50°C, as specified by the Gibson Assembly® Cloning Kit (NEB, United Kingdom), was sufficient for the assembly reaction to occur. Although it was previously shown that assembly started to occur after as little as a 2 min of incubation and optimum assembly only occurred after 40 min (Jiang et al., 2013). The results shown here (Figure 2.13), indicated a much fainter assembly band than what was obtained by Jiang et al., 2013, after 30 min. This might indicate, that depending on the DNA used, the incubation time required could differ and that optimization is required for each individual hairpin design. For enhanced assembly, it is suggested to test a longer incubation time of up to 60 min, depending on the size of the fragments being assembled. A longer incubation time could increase the amount of positive clones obtained, but if too long a period of incubation is included, it might lead to unspecific or unwanted assembly reactions.

A second challenge and limitation during the project was confirmation of a positive RNAi vector. Initial attempts to confirm a positive clone with PCR amplification was unsuccessful due to complementary fragments folding on themselves, inhibiting the amplification process. It was found that the optimum method for confirmation of a positive clone was through restriction digest. In the case of PCR amplification, the possibility of PCR failure remains due to the complementary inverted segments of the hairpin that tend to self-anneal during the reaction (Xiao et al., 2006; Oa et al., 2009; Jiang et al., 2013). For future confirmation of positive clones, it is suggested that an internal primer which anneals to the intron section of the hairpin fragment be designed. This intron-based primer could then be combined with a primer binding in the terminator area of the pUBI510+ transformation vector or alternatively with a promoter primer binding to the Ubiquitin promoter in the vector. These primer combinations will allow for colony PCR screening of potential positive clones and will also allow for sequencing of the RNAi hairpin vectors as a final confirmation method.

Once the required method optimization was complete, an hpRNAi construct was confirmed through restriction digest and PCR amplification. An additional silencing construct was successfully created with the GATEWAY® cloning system as precautionary measure (Annexure C). The GATEWAY® construct, created with the pHb7GW-I-WG-UBIL vector as destination vector, was confirmed with restriction digest (Figure C3). After initial delays in optimization of the IR-hpRNAi method, GATEWAY® cloning was done in case the original method chosen was unsuccessful.

Future works will include the complete sequencing of the hpRNAi *pUBI:CKX* cassette as final confirmation, before it can be utilized for sugarcane transformation through particle bombardment. After the transformation event and subsequent confirmation of sugarcane transgenic lines, the expression levels of the *CKX* genes will be investigated with sqRT-PCR analysis. It is hoped that a decrease in transcription levels and/or enzyme activity will be present in the transgenic lines as shown by Zalewski et al., (2010 and 2012). The aim is to correlate the decreased CKX enzyme activity with increased plant growth.

## **2.5 CONCLUSIONS**

The newly developed isothermal *in vitro* recombination reaction (IR-hpRNAi) has been introduced into the Institute for Plant Biotechnology. The method has been optimized for immediate application and a first hairpin-containing RNA-interference based transformation vector has been produced. Particular care was required for primer design, as the overlapping regions added at the 5'- and 3' ends of the primers play a pivotal role in the success of the process. Designed primers include a forward primer in the hairpin intron area, and a complementary vector terminator-based reverse primer for subsequent screening with PCR and sequencing purposes. The first produced construct will now allow testing *CKX* gene silencing.

## **2.5 ANNEXURES**

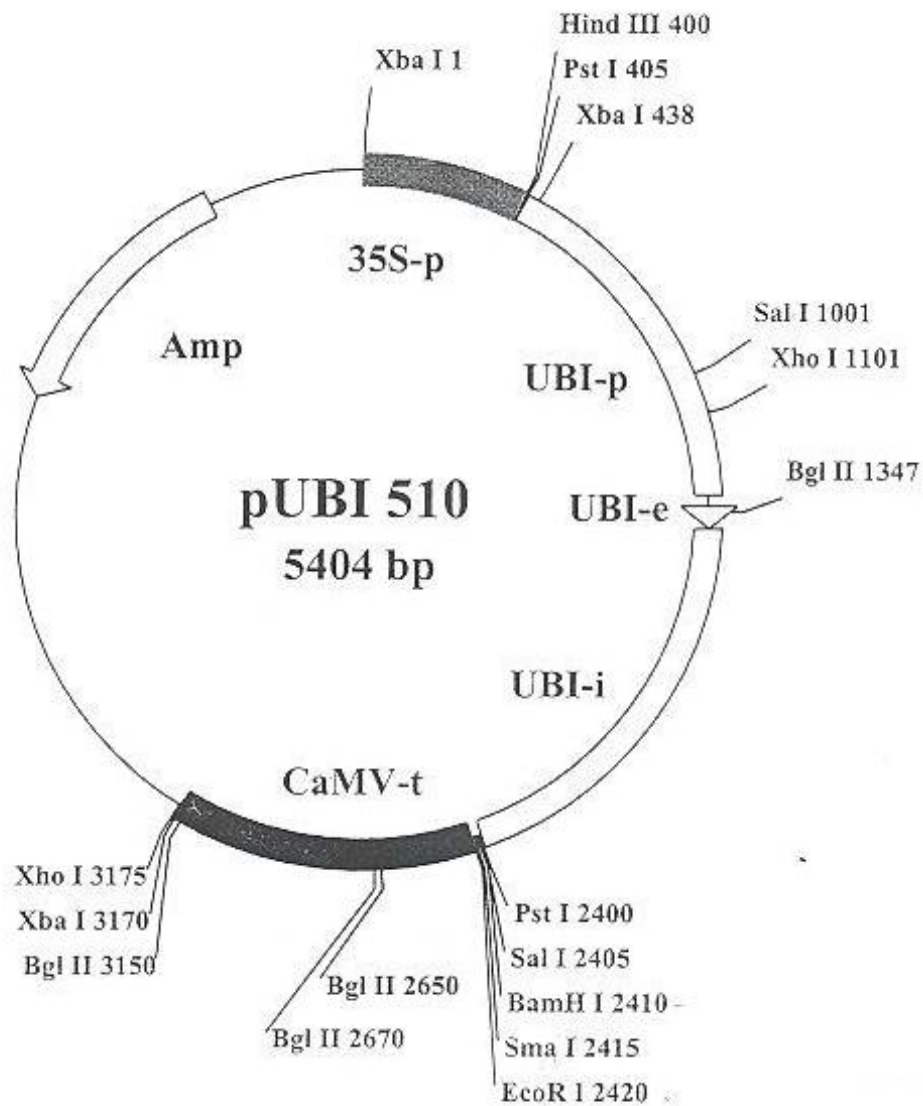
### **Annexure A**

*The cytokinin oxidase/dehydrogenase sequences used in phylogenetic analysis*

<b>Gene</b>	<b>Organism</b>	<b>Accession</b>	<b>Size (bp)</b>
AtCKX1	<i>Arabidopsis thaliana</i>	NM_129714	1964
AtCKX2	<i>Arabidopsis thaliana</i>	NM_127508	1667
AtCKX3	<i>Arabidopsis thaliana</i>	NM_125079	1595
AtCKX4	<i>Arabidopsis thaliana</i>	NM_179139	1951
AtCKX5	<i>Arabidopsis thaliana</i>	NM_106199	2711
AtCKX6	<i>Arabidopsis thaliana</i>	NM_116209	2007
AtCKX7	<i>Arabidopsis thaliana</i>	NM_180532	1848
TaCKX1	<i>Triticum aestivum</i>	JN128583	1572
TaCKX2	<i>Triticum aestivum</i>	JN128584	1854
TaCKX2.2	<i>Triticum aestivum</i>	GU084177	1813
TaCKX2.1	<i>Triticum aestivum</i>	FJ648070	1909
TaCKX2.3	<i>Triticum aestivum</i>	JF293079.1	1876
TaCKX7	<i>Triticum aestivum</i>	JN128588	1601
TaCKX8	<i>Triticum aestivum</i>	JN128589.1	1602
TaCKX9	<i>Triticum aestivum</i>	JN128590.1	788
TaCKX11	<i>Triticum aestivum</i>	JN128592.1	735
HvCKX2	<i>Hordeum vulgare</i>	AF540382.1	1857
HvCKX3	<i>Hordeum vulgare</i>	AY209184	1866
ZmCKX1	<i>Zea mays</i>	NM_001112121.1	1776
ZmCKX2	<i>Zea mays</i>	NM_001112056.1	2264
ZmCKX3	<i>Zea mays</i>	AJ606944	2146
ZmCKX4	<i>Zea mays</i>	GU160398	1641
ZmCKX4b	<i>Zea mays</i>	GU160399	1607
ZmCKX5	<i>Zea mays</i>	GU160400	1753
ZmCKX6	<i>Zea mays</i>	GU160401	1638
ZmCKX8	<i>Zea mays</i>	GU160402	1623
ZmCKX10	<i>Zea mays</i>	FJ269181.1	1578
ZmCKX12	<i>Zea mays</i>	GU160403	1602
OsCKX1	<i>Oryza sativa</i>	NM_001048787	1799

OsCKX2	<i>Oryza sativa</i>	AK243684	2148
OsCKX2	<i>Oryza sativa</i>	AB205193	1698
OsCKX3	<i>Oryza sativa</i>	AK103272	2191
OsCKX4	<i>Oryza sativa</i>	AK121317	2328
OsCKX5	<i>Oryza sativa</i>	AK101022	1930
OsCKX9	<i>Oryza sativa</i>	NM_001061906.2	1566
SbCKX1	<i>Sorghum bicolor</i>	XM_002467017	1587
SbCKX3.1	<i>Sorghum bicolor</i>	XM_002454958	1734
SbCKX3.2	<i>Sorghum bicolor</i>	XM_002454988.1	1909
SbCKX3.3	<i>Sorghum bicolor</i>	XM_002458537.1	1647
SbCKX4	<i>Sorghum bicolor</i>	XM_002453499	1614
SbCKX6	<i>Sorghum bicolor</i>	XM_002446759	1593
SbCKX7	<i>Sorghum bicolor</i>	XM_002445565.1	1563
SbCKX9	<i>Sorghum bicolor</i>	XM_002439661	1569
SbCKX10	<i>Sorghum bicolor</i>	XM_002438558.1	1650
ObCKX4	<i>Oryza brachyantha</i>	XM_006645247	1717
PpCKX1	<i>Physcomitrella patens subsp. patens (Moss)</i>	XM_001777458	2333
PpCKX2	<i>Physcomitrella patens subsp. patens (Moss)</i>	XM_001776874	1569
SmCKX1	<i>Selaginella moellendorffii (Spikemoss)</i>	XM_002977568.1	1503
SmCKX2	<i>Selaginella moellendorffii (Spikemoss)</i>	XM_002975161.1	1595
SmCKX3	<i>Selaginella moellendorffii (Spikemoss)</i>	XM_002988079.1	1620
SICKX1	<i>Solanum lycopersicum</i>	NC_015445.2	1560
SICKX2	<i>Solanum lycopersicum</i>	NM_001257980	1602
SICKX4	<i>Solanum lycopersicum</i>	NM_001279322.1.	1575
SICKX5	<i>Solanum lycopersicum</i>	NM_001257978.1	1632
SICKX7	<i>Solanum lycopersicum</i>	NM_001257979	1614
SoCKX1	<i>Solanum tuberosum (Potato)</i>	NM_001288101	1921
SoCKX2	<i>Solanum tuberosum (Potato)</i>	NM_001288472.1	1871
SoCKX3	<i>Solanum tuberosum (Potato)</i>	NM_001288077	1602
SoCKX4	<i>Solanum tuberosum (Potato)</i>	NM_001288028.1	1581
SoCKX5	<i>Solanum tuberosum (Potato)</i>	NM_001288192	1770

---

**Annexure B***pUBI510 vector map*

## Annexure C

### *Backup GATEWAY® cloning*

A second hairpin cassette was cloned, as a backup, with the established GATEWAY® method. The fragment was amplified from the *pJET::SugarcaneCTKD* construct using the GATEHP\_FWD (5'-CAC CTC CTC CAC ACA TGT ATA CA-3') and GATEHP\_REV (5'-ATT TCA GCA GAG AGG ACC T-3') primer pair. For PCR amplification the Q5® High-Fidelity DNA Polymerase (NEB, United Kingdom) was used according to the manufacturer's specifications and thermal cycles programmed as described in Table 2.3.

Once isolated (Figure C1), the fragment was directionally cloned into the donor vector with the Invitrogen pENTR™ Directional TOPO® Cloning Kit (K2400-20, Thermo Scientific, Waltham, Massachusetts, USA) and confirmed by restriction enzyme digest (Figure C2). With the help of the **GATEWAY®** LR Clonase™ Enzyme Mix (11791-019, Thermo Scientific, Waltham, Massachusetts, USA), the fragment was transferred into the 15,416 bp entry vector, pHb7GW-I-WG-UBIL vector and confirmed by restriction enzyme digest (Figure C3).

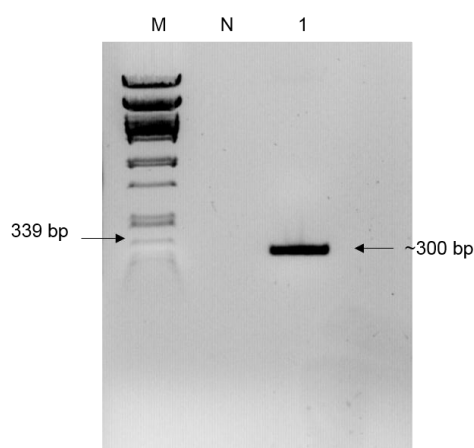


**Figure C1:** CTKD fragment, 300 bp in size, as amplified for cloning into the pENTR/D-TOPO vector.

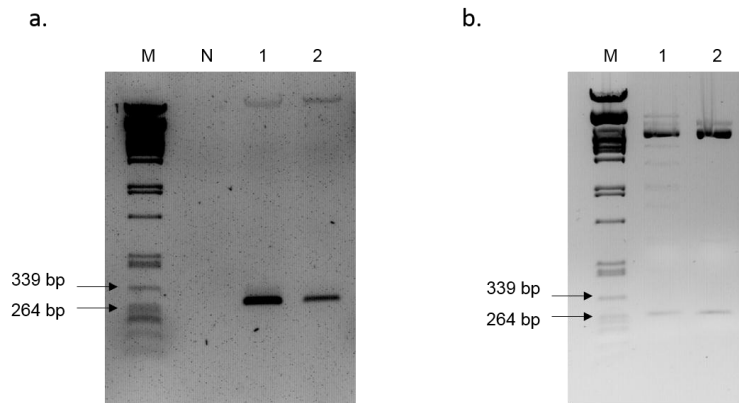


**Figure C2:** Insert confirmation for the pENTR/D-TOPO, with a.) PCR amplification and b.) restriction enzyme digest with *AvaI* cutting in the fragment and *EcoRV* cutting in the plasmid. A band slightly smaller than 300 bp was present indicating the *CKX*-gene fragment. The *PstI* lambda marker was included in both gel pictures as M.

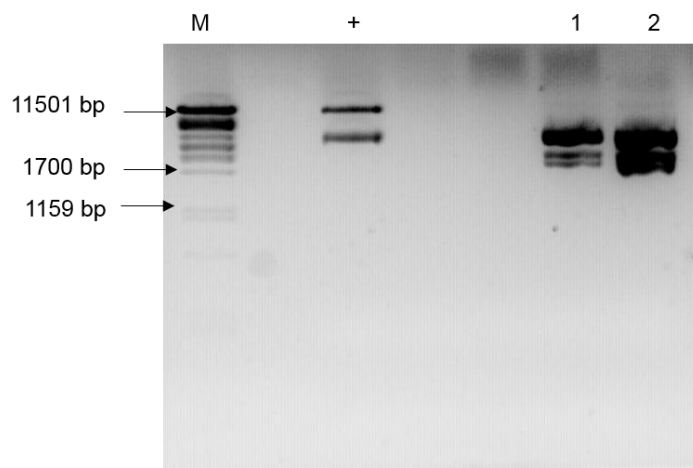
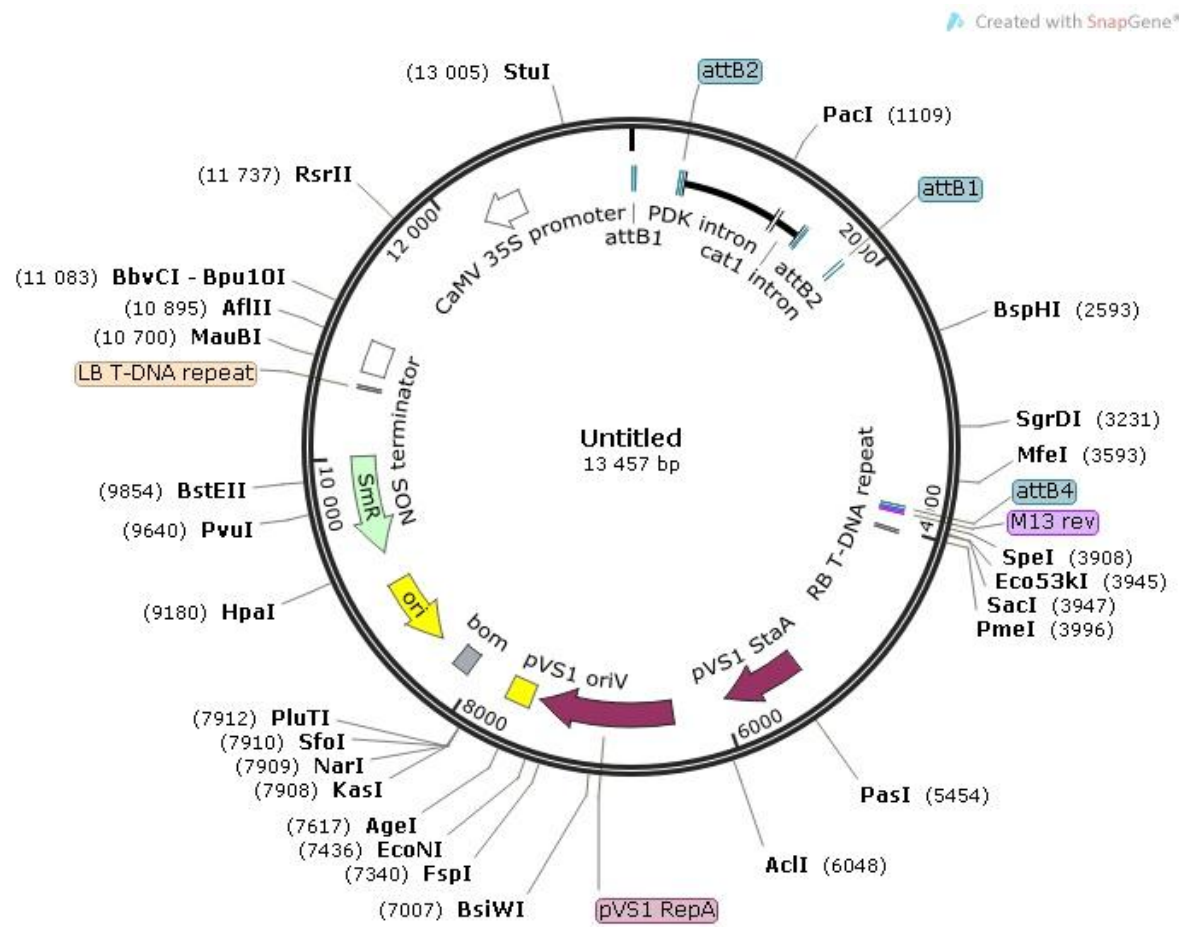


**Figure C3:** Insert confirmation for the Destination vector. A restriction enzyme digest was performed with *XhoI* (which cuts both in the vector and the fragment) on the empty vector (+) and isolated plasmid DNA from colony 1 (1) and 2 (2). Two bands, ~1600 bp and 1500 bp in size, were present between the 1700 bp and 1159 bp markers (M), along with a faint band indicating the vector backbone at 11000 bp.



## Annexure D

*GATEWAY Destination vector with unique cutting sites indicated (as created by Snapgene)*



## **CHAPTER 3**

### **Enhancing plant resistance with VOCs**

### **3.1 INTRODUCTION**

Plants exude a significant amount of nutrients into the surrounding soil through their roots. This in turn attracts various organisms, including insects, bacteria and fungi (Choudhary and Johri, 2009; Nehra and Choudhary, 2015). The area immediately surrounding plant roots is specifically referred to as the rhizosphere. This is a complex ecosystem with various root to root or root to microbe interactions. Certain interactions between plant and microbes are mutually beneficial. A group of beneficial bacteria, known as plant growth-promoting rhizobacteria (PGPR), is an example of this symbiotic relationship. PGPR are able to enhance plant growth (Ryu et al., 2005; Kwon et al., 2010) and PGPR are able to increase disease resistance and enhance the efficiency of fertilizers (Choudhary and Johri, 2009). A recent study has provided also some evidence that a type of signalling mechanism is involved in the release of volatile organic compounds (VOCs) by PGPR (Ryu et al., 2003).

Previous research has identified a role of low-molecular-weight plant volatiles (e.g. terpenes or jasmonates) as potential signalling molecules on a trophic level, with the emission of volatiles by bacteria as a communication mechanism rather unexplored. Certain PGPR strains used in agriculture release blends of volatile components. Through the release of these compounds, plant growth is promoted (Ryu et al., 2003). Compounds released in the blends, responsible for these beneficial effects, were then identified, namely acetoin and 2,3-butanediol. Further research then identified increased disease resistance after plant treatment with VOCs (Ryu et al., 2004a). The *ALDC* gene, responsible for acetoin production, and the *BDH1* gene, responsible for 2,3-butanediol production, have been also isolated. Coding sequences of these genes were used to produce transgenic *Arabidopsis thaliana* plants for producing VOCs (Dempers 2014). Obtained transgenic plants had better growth but better disease resistance was not investigated.

In this chapter, the disease resistance of transgenic *Arabidopsis* lines containing the *ALDC* and *BDH1* genes was therefore investigated. This investigation was conducted in correlation of the ultimate aim to increase plant growth. Transgenic lines were exposed to *Botrytis cinerea* infection and special attention was given to lesion development and the Induced Systemic Response (ISR) in the infected plants, in comparison to wild type Col-0 plants. Additionally, the *ALDC* and *BDH1* genes were cloned into a suitable sugarcane transformation vector (pUBI510), for subsequent sugarcane transformation through particle bombardment. The ultimate aim is to produce transgenic sugarcane lines which show an increase in plant growth and/or disease resistance. Increased disease resistance will also allow increased plant growth when growth inhibitions enforced by pathogens are avoided.

## **3.2 MATERIALS AND METHODS**

### **3.2.1 Bacterial growth conditions and transformations**

Refer to section 2.2.2 “Bacterial growth conditions”.

### **3.2.2 Plant growth conditions**

The seeds from respective *Arabidopsis thaliana* lines used in this study were surface sterilized with the optimized vapour sterilization method, using chlorine gas, as described by Clough and Bent (1998). Once the seeds were surface-decontaminated, they were plated out onto half-strength Murashige and Skoog (MS) medium (Murashige and Skoog, 1962), supplemented with 1% (m/v) sucrose and adjusted to a pH of 5.8 with KOH, before adding 9 g/L Phyto-agar and autoclaving (121°C, 1.2 kPa for 20 min) the media. Surface-sterilised seeds were plated out by re-suspending them in 0.05% agarose (40 µl of seeds per 1 ml of agarose) and spreading the seed-agarose suspension with a 1 ml pipette onto the plates. Approximately 3 to 4 ml of agarose-seed suspension is enough to cover one Cellstar® 100 x 20 mm cell culture dish. Plates were left to dry in the laminar flow cabinet until the seeds stabilized onto the plates. The seeds were thereafter stratified in the dark for 3 days at 4°C before the plates were placed in the growth room (16:8 h light:dark photoperiod under cool white fluorescent tubes, OSRAM L 58V/640, 50 µmol photons/m<sup>2</sup>/s<sup>-1</sup> at 22°C day and 15°C night temperatures). Two weeks post-germination, plants were transferred to pots containing peat discs (Jiffy-7® bags, Jiffy Products Int.) as soil medium and placed in a short day length growth room (10h:14h light:dark photoperiod) with a 22°C day temperature and a 15°C night temperature.

### **3.2.3 *Agrobacterium*-mediated plant transformation**

Wild type (WT) *A. thaliana* plants were transformed using a modified *Agrobacterium*-mediated floral dipping method (Zhang et al., 2006). Both the pCambia2300::*FNR:ALDC* and pCambia1300::*FNR:BDH1* plasmids previously constructed by D. Dempers from this research group (Dempers, 2014), were used in the transformation (Annexures A and B). For each of the two plasmids, the glycerol stock culture, which was stored at -80°C, was used to inoculate 200 ml liquid broth, supplemented with kanamycin to a final concentration of 50 µg/L. These

cultures were then incubated at 28°C in the dark, with shaking at 240 rpm, and grown to an OD<sub>600nm</sub> of between 1.5 and 2.0. Once the appropriate OD<sub>600nm</sub> was reached, the culture was centrifuged for 10 min at 4000 xg at room temperature. The supernatant was removed and the cell pellet gently re-suspended in a fresh 5% (m/v) sucrose solution. Before the suspension was used for dipping, a final concentration of 0.02% (v/v) Silwett-L77 (LEHLE Seeds, Round Rock, TX, USA) was added and the solution was mixed well. Flowering plants, grown on peat discs, were then inverted and dipped in the *Agrobacterium* cell suspension. The flowers were kept in the suspension for no more than 10 s at a time, with gentle agitation. To ensure that shorter auxiliary buds were not missed, the rosette was also included when dipping the plant. The plant was then removed from the suspension and excess liquid allowed to drain off. Dipped plants were covered with plastic bags to ensure high humidity conditions and laid on their sides in the dark for 24 h. The plants were then placed back in the growth chamber and allowed to grow under normal conditions. The dipping process was repeated after 1 week to increase the probability of a successful transformation. The plants were then allowed to grow for another month, until the siliques turned brown, at which point watering of the plants was suspended and the inflorescences bagged to collect the seed. Once plants had completely dried out, seeds were harvested and stored at 4°C until use.

### 3.2.4 *In vitro* screening for primary *Arabidopsis* transformants

Surface decontaminated seeds were plated out on selection plates containing half-strength MS media supplemented with carbenicillin (100 mg/l), to kill any remaining *Agrobacterium* contamination, and selection antibiotics, kanamycin (50 mg/l) and hygromycin (25 mg/l) respectively, for the *ALDC* and *BDH1* gene constructs. Approximately 14 d post-germination, putative transformants could be clearly distinguished by their extensively developed root systems and the development of bright green true leaves (indicated with a red circle, Figure 3.1) compared with non-transformants, which failed to develop on the selective media. Once the true leaves and roots had developed, the putative transformants were transferred to fresh plates, containing no selective agents. One week later, the seedlings were transferred to Jiffy-7® peat discs and placed in a covered plastic tray to maintain a high humidity environment for 3 days. The hardened off seedlings were grown in the short day length growth room until they were old enough to bolt. The conditions were then adjusted to a long day length (16h:8h, light:dark photoperiod at 22°C day and 15°C night temperatures) to induce bolting and allow for seed collection.



**Figure 3.1:** An example of the *in vitro* screening for *Arabidopsis* transformants. Positive plantlets (indicated with a red circle) showed well-established root systems after two weeks (post-germination) and showed a bright green colour. Non-transgenic plantlets did not develop past the two-leaf stage and no root system developed, as indicated with the yellow circle.

### 3.2.5 Genotyping putative transformants

#### 3.2.5.1 Genomic DNA extraction

To confirm the presence of the *ALDC* and *BDH1* genes in putative transformants, the extraction method described by Edwards et al. (1991) was employed. After sampling leaf material from the putative *Arabidopsis* transformants, the frozen leaf samples were ground to a fine powder using liquid nitrogen. Grinding the material was performed in the original microfuge tube, using a disposable plastic pestle. Once the material was fully ground, 400  $\mu$ l of extraction buffer (200 mM Tris-HCl pH 7.5; 250 mM NaCl; 25 mM EDTA; 0.5% sodium dodecyl sulphate [SDS]) was added to the samples which were immediately vortexed, until completely thawed in the buffer. The samples were then centrifuged for 1 min at maximum speed in a desktop centrifuge. The supernatant (approximately 300  $\mu$ l) was transferred to a fresh microfuge tube, to which a 1:1 volume of isopropanol was added. The samples were left at room temperature (25°C) for 5 min. Once the DNA had precipitated, the samples were centrifuged for 5 min at maximum speed in the microfuge to pellet the DNA. After centrifugation, the supernatant was removed and the pellet left to dry for 30 min. When the

pellet was completely dry, 100 µl of 1x TE buffer (1 M Tris-HCl, pH 7.5 and 0.5 M EDTA, pH 8.0) was applied to suspend the pellet. Samples were stored at -20°C.

#### 3.2.5.2 Gene insert confirmation

For the PCR, 1 µg of the isolated genomic *Arabidopsis* DNA was used as template. To amplify the *ALDC* and *BDH1* genes, the GoTaq™ DNA Polymerase kit (Promega, Madison, WI, USA) was applied, in combination with the gene specific primers designed (Table 3.1) for each respective gene. Slight modifications were made to the manufacturer's protocol by adding 2.5 µl of each primer stock solution (10 µM). The PCR thermal cycles were as described in Table 2.2. These PCR conditions were repeated for the *BDH1* primer pair, with a different annealing step of 60°C for 1 min. PCR products were subsequently separated on a 1.5% (m/v) agarose gel containing 2.5 µl PRONOSAFE nucleic acid staining (Laboratorius CONDA, Italy) per 50 ml gel and visualized under UV light.

### 3.2.6 Expression analysis

#### 3.2.6.1 Total RNA extraction and cDNA synthesis

In order to isolate total RNA from *Arabidopsis* leaf samples the RNeasy Mini Kit (Qiagen, Hilden, Germany) was utilized according to the manufacturer's instructions. To assess RNA quality post extraction, 5 µl RNA aliquots were incubated with 10 µl of 2-mercaptoethanol at 37°C for 15 min. An additional 5 µl of RNA running dye (6x) (Thermo Scientific, Waltham, Massachusetts, USA) was added to the samples post incubation and the samples were then separated on a 1.5% (m/v) agarose gel. Contaminating genomic DNA was removed using the RNase-free DNase I (Thermo Scientific, Waltham, Massachusetts, USA) following the manufacturer's specifications. The Maxima H Minus First Strand cDNA Synthesis kit (Thermo Scientific, Waltham, Massachusetts, USA) was then applied to synthesize cDNA from a total of 1 µg of DNase-treated RNA. The cDNA samples were aliquoted and stored at -80°C until required.

#### 3.2.6.2 Semi-quantitative PCR

Semi-quantitative analysis of transgene expression was used to assess both the levels of *ALDC* and *BDH1* gene expression in putative *Arabidopsis* transformants. For this purpose, the GoTaq™ DNA Polymerase kit (Promega, Madison, WI, USA) was used to set up the PCR event with the same thermal cycle conditions as described for the genotyping of putative transgenics, with the exception of 25 instead of 30 cycles used for amplification. A reaction

was also set up with primer for the constitutively expressed housekeeping gene *actin2* (*ACT2*, AT3G18780) from *A. thaliana* (Table 3.1).

**Table 3.1:** Gene specific primers for genotyping of potential transgenic plants

PRIMER NAME	PRIMER SEQUENCE	PRODUCT SIZE	T <sub>m</sub>
*ALDCFwd_BAMHI	5'-TTGGATCCATGACCACCGCTGTCACCGCC-3'	1177 bp	66°C
*ALDCRev_ECORI	5'-TAGAATTCTTAGTGAGAAGTGGGGACTCCC-3'		
BDH1_Fwd	5'-ATAGGTACCATGACCACCGCTG-3'	1375 bp	62°C
BDH1_Rev	5'-GAGCTCTTACTTCATTTACCGTG-3'		
ACT2_Fwd	5'-ATGGCTGAGGCTGATGATAT-3'	500 bp	58°C
ACT2_Rev	5'-CCATCACCAGAATCCAGCAC-3'		
UbiProm_FWD	5'-AAT TTGATATCCTGCAGTGCAGCGTG-3'	Depends on insert size	53°C
CAMV-REV	5'-AGG GTT TCT TAT ATG CTC AAC-3'		

\*The ALDC primer pair was used both for cloning and in subsequent genotyping

### 3.2.7 Infection protocol of *Arabidopsis thaliana* with *Botrytis cinerea*

For this study, three transgenic lines, A3 (*ALDC*), B8 (*BDH1*) and AB2 (*ALDC+BDH1*), generated by Dempers, (2014), were utilised due to delays in the generation of transgenic lines. Seed stocks from newly generated double transgenic lines did not germinate sufficiently and plantlets that did develop showed inhibited growth due to the selection on two antibiotics (hygromycin and kanamycin). Plants of the transgenic *Arabidopsis* lines A3, B8 and AB2 were leaf-drop inoculated with *B. cinerea* based on the method of Muckenschnabel et al., (2002), with minor modifications. Briefly, fungal spores from different spore isolates, initially isolated from infected peach orchards, were harvested 10 to 14 days after sub-plating onto potato dextrose agar (PDA, Sigma Aldrich, St. Louis, MO, USA), with the pH adjusted to 3.5 with 10% (v/v) tartaric acid. Prior to infection, spores were harvested and suspended in 15 ml inoculum medium (MS medium supplemented with 1% [m/v] sucrose and 5 µl Tween80), and filtered through sterilized cheese cloth squares. After filtering, a spore count was carried out using a haemocytometer. For all the infection experiments in this study, suspensions of  $1 \times 10^5$



conidia.ml<sup>-1</sup> were used. The spore suspension was kept in the dark for 24 h at 20°C, to allow for initial germ tube formation. The following day, the suspension was used to inoculate five alternate leaves from 6-week-old *Arabidopsis* plants with 5 µl droplets. Infected plants were then transferred to transparent plastic propagator boxes, which were then sealed to maintain 100% humidity. The boxes were placed under cool white fluorescent light (OSRAM L58W/640, Germany 50 µmol/photons/m<sup>2</sup>/s<sup>-1</sup>) and long day length (16h:8h, light:dark photoperiod at 22°C day and 15°C night temperatures). Inoculated plants were evaluated at 1, 2, 3, 5 and 7 days post inoculation (dpi) for qualitative evaluation of the infection data. Infected leaves were harvested at 0 h, 24 h and 48 h post inoculation for semi-quantitative PCR analysis of gene expression.

### 3.2.8 VOC Exposure experiments

#### 3.2.8.1 Effects of acetoin and 2,3-butanediol on plant disease resistance

An infection trial was designed to test the direct effect of acetoin and 2,3-butanediol on plant disease resistance. Wild type *A. thaliana* Col-0 plants were exposed to synthetic acetoin (Sigma Aldrich, St. Louis, Missouri, USA) and 2,3-butanediol (Sigma Aldrich, St. Louis, Missouri, USA), and subsequently infected with *Botrytis cinerea*. The trial was designed to test gene expression at three different time points, namely 0 h (T<sub>0</sub>), 24 h (T<sub>24</sub>) and 48 h (T<sub>48</sub>) post-infection. Each time point included 3 biological repeats. Plants were incubated alongside 1 ml of a 10 mM volatile solution (either acetoin or 2,3-butanediol). The 10 mM aliquots were made up in distilled water, with a 1 ml aliquot of dH<sub>2</sub>O acting as a negative control. Five alternate, juvenile leaves were inoculated with 5 µl of spore suspension (previously described), 24 h post-incubation (hpi) with the different volatiles. A separate set of plants were also mock-inoculated with suspension media containing no *B. cinerea* spores to act as a second negative control. During inoculation of plants with the pathogen, the volatile solutions were replaced with fresh 1 ml aliquots. Sampling occurred at the designated time points, by removing the five inoculated leaves, pooling all the leaves per replicate into one 2 ml microfuge tube. The leaves were flash frozen in liquid nitrogen and stored at -80°C, until RNA could be extracted. To monitor disease development between the different volatile treatments, an average disease development percentage was calculated for each biological repeat. The number of leaves showing disease development (leaves with a lesion developing on them, regardless of size) for each time point was counted and divided by the total number of leaves originally inoculated. This number was then multiplied by a 100 to obtain a percentage value which was then used to determine whether the volatile treatment increased disease resistance. For an additional

photographic representation (qualitative analysis) of disease development, a sixth leaf was inoculated on each plant and marked. The specific marked leaf was then subsequently detached at each time point and photographed. For each plant, care was taken to be consistent in specifically removing the sixth leaf inoculated in order to maintain objectivity.

### 3.2.8.2 Effect of acetoin and 2,3-butanediol on *B. cinerea*

*Botrytis cinerea* cultures were sub-plated onto fresh potato dextrose agar (PDA) (Sigma Aldrich, St. Louis, MO, USA) and incubated at 25°C in the dark for 10 to 14 d. A small plug, 0.5 cm in diameter, was then cut from the plates and transferred to the centre of a fresh PDA plate. The plug-containing plates were then incubated at the bottom of plastic propagator boxes, similar to those used in the plant infection trials. Alongside the plates, a vile containing 1 ml of a 10 mM solution of either acetoin or 2,3-butanediol was placed in the propagation box (Figure 3.2). The box was subsequently sealed and the fungus was allowed to grow for 36 h at 25°C in the dark, after which the colony size on each plate was measured (indicated in Figure 3.2 with a red circle). The experiment included 5 replicates for each volatile treatment. A control was included, where only 1 ml of distilled water and no volatile was added to the vile. The colony diameter for the 5 replicates and the control were documented in MS Excel and averaged with the appropriate function (sum of diameter/number of replicates). Averages plus/minus standard error were compared to the control treatment, to determine the effect of each volatile on fungal growth.

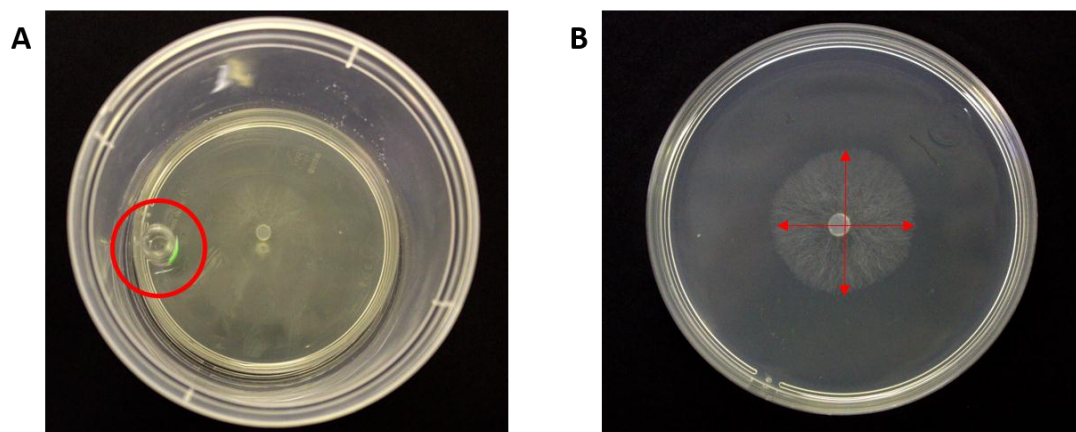


**Figure 3.2:** Assessment of the effects of volatile acetoin and 2,3-butanediol on *B. cinerea* growth directly. a) Fungal plates were incubated at the bottom of plastic propagator boxes, alongside a glass vile (circled in red) containing 1 ml of a 10 mM volatile solution (either acetoin or 2,3-butanediol) and incubated in the dark for 36 h, at room temperature. After 36 h b), the plates were removed from the boxes and the diameter of each colony was measured as indicated with red arrows.

### 3.2.9. Disease development assessments

#### 3.2.9.1 Lesion diameter evaluation and evaluation through a scoring system

Lesion size was measured at three separate time intervals. Measurements were made 1, 2, and 3 days post inoculation (dpi). Each of the five infected leaves on a specific plant was monitored and the developing lesion diameter was determined, as described in Ederli et al. (2015), Meng et al. (2013) and Govrin and Levine (2002), with slight modifications. The lesion diameters were logged in an Excel spreadsheet where the average lesion diameter per plant was calculated. The average plus/minus standard error was calculated for each of the three biological repeats present for each biological line. Lesion development was additionally estimated visually with the help of a predetermined scoring system (Figure 3.3), based upon the scoring methods described in Redmond et al. (1987) and Brauc et al. (2011), with modifications to include specific phenotypic responses observed during the study. Scoring commenced at 1, 2 and 3 dpi. All five inoculated leaves per biological repeat were scored and logged in an MS Excel spreadsheet where the data was subsequently analysed with a t-test, to determine significance.

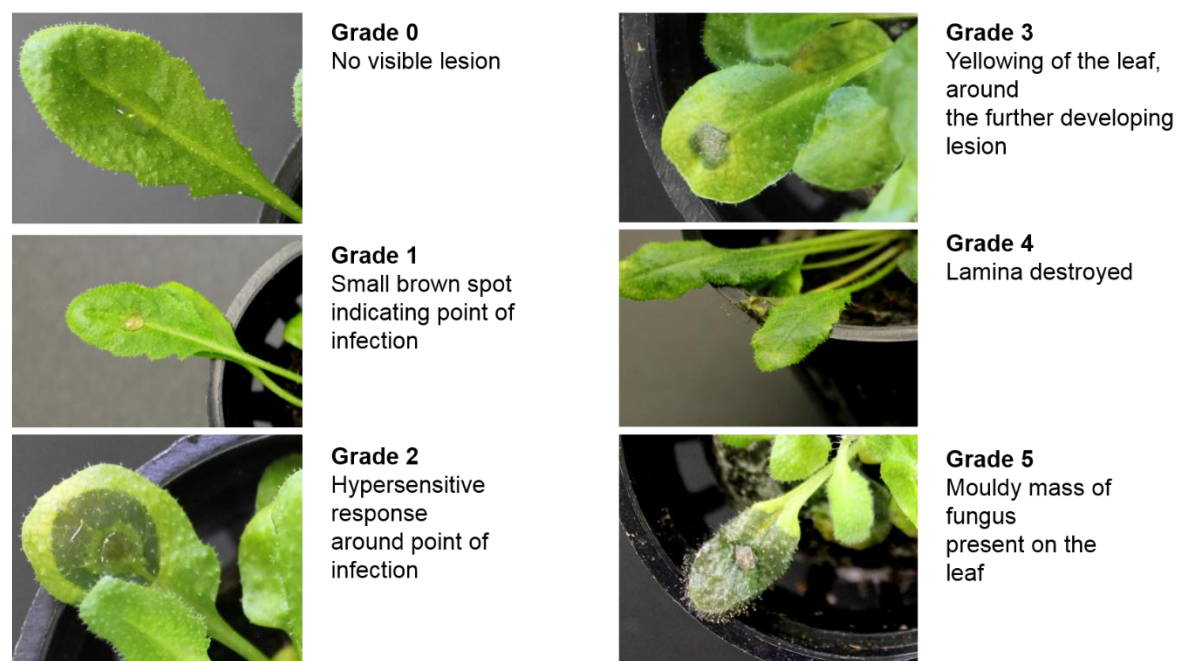


**Figure 3.3:** A visual representation of the predesigned lesion scoring system used during lesion evaluation. A lesion was given a score between 0-5, representing the different phenotypes observed, at 1, 2, and 3 dpi. For this particular scoring system, lesion size was not the determining factor.

### 3.2.10 Gene marker profile analysis

Eight published hallmark genes (Table 3.2) that are commonly used during immunological studies were selected. Those chosen for initial analysis included ethylene (ET)- and jasmonic (JA)-response genes. The *PR2* control gene that is known to be activated during systemic acquired resistance was also included. Total RNA was extracted from infected leaf material at time points  $T_0$ ,  $T_{24}$  and  $T_{48}$ . Thereafter, 1  $\mu$ l of cDNA was used in PCR reactions, which were carried out with the GoTaq™ DNA Polymerase kit, according to the manufacturer's specifications. The candidate genes were analysed for each time point using the PCR programme described in Table 2.2, except that the denaturing, annealing and extension steps were only repeated for 25 cycles. A reference reaction was also set up with primers for the constitutive marker gene *actin2* (*ACT2*, AT3G18780) from *A. thaliana*. This enabled normalization of the PCR results. The amplified PCR products were subsequently analysed with electrophoresis using a 1.5% (m/v) agarose gel.

**Table 3.2:** The specific primers that were designed to amplifying a 500 bp fragment during sqRT-PCR analysis of the *B. cinerea* infected *Arabidopsis* plants. The table contains eight hallmark genes, as well as the *ACT2* primers used for standardization.

GENE	LOCUS IDENTIFIER	PRIMER NAME	PRIMER SEQUENCE
<i>ACT2</i>	AT3G18780	ACT2_Fwd	5'-ATGGCTGAGGCTGATGATAT-3'
		ACT2_Rev	5'-CCATCACCAGAATCCAGCAC-3'
<i>JAR1</i>	AT2G46370.1	Primer Fwd:	5'-TGGTACGGATTGATTCCCG-3'
		Primer Rev:	5'-TGAGAGTCTCTTTGCAGCCG-3'
<i>PR2</i>	AT3G57260.1	Primer Fwd:	5'-CTTGAACGTCTCGCCTCCAG-3'
		Primer Rev:	5'-GATCCGCCCCCTGATTTCTC-3'
<i>NPR1</i>	AT1G64280.1	Primer Fwd:	5'-GCAATGTGAAGACCGCAACA-3'
		Primer Rev:	5'-CGTACCAGTGAGACGGTCAG-3'
<i>VSP2</i>	AT5G24770.1	Primer Fwd:	5'-TGGCACCTTGGTGTGAGAC-3'
		Primer Rev:	5'-TGACTTGTACACCACTTGCCT-3'
<i>MYB75</i>	AT1G56650.1	Primer Fwd:	5'-CAAAGGGCTGCGAAAAGGTG-3'
		Primer Rev:	5'-AAGTCCAAGGCATGGAGGATT-3'
<i>ERF1</i>	AT3G23240.1	Primer Fwd:	5'-ATTCTCCGGCTTCTCACCG-3'
		Primer Rev:	5'-TGGTCATTCTCCGTCTCATCG-3'
<i>MYC2</i>	AT1G32640.1	Primer Fwd:	5'-CGCCGGAGAATCAGATCACT-3'
		Primer Rev:	5'-ATCAACGCCGACATCAACCT-3'
<i>PDF1.3</i>	AT2G26010.1	Primer Fwd:	5'-TCTTCACACTACACACAAATACAT-3'
		Primer Rev:	5'-CGTACATAATTCTTTATTTT-3'

### 3.2.11 Preparation of sugarcane transformation constructs

#### 3.2.11.1 Cloning of the *ALDC* gene

Appropriate primers containing restriction sites for *EcoRI* and *BamHI* (Table 3.1) were designed for the amplification of the  $\alpha$ -acetolactate decarboxylase (*ALDC*, EC4.1.1.5) gene from *Aspergillus niger*, with a chloroplastic transit peptide from *Spinacia oleracea*, ferredoxin-NADP<sup>+</sup> reductase (*FNR*, EC 1.18.1.2), from the *pCAMBIA2300::FNR:ALDC* construct (Dempers, 2014) for cloning into the sugarcane transformation vector pUBI510. The chloroplast localization peptide is included in the vector design, because of  $\alpha$ -acetolactate (from which the acetoin and 2,3-butanediol is produced) being present in the chloroplast of plants. The *FNR:ALDC* gene was amplified with PCR using Q5<sup>®</sup> High-Fidelity DNA Polymerase (NEB, United Kingdom). The PCR conditions are described in Table 2.4.

The amplicon with a correct size (1177 bp) was separated by gel electrophoresis on a 1.5% agarose gel, before purifying the fragment with the Wizard<sup>®</sup> SV Gel and PCR Clean-Up System. The pUBI510 sugarcane transformation vector (Chapter 2: Annexure B) was linearized with *EcoRI* and *BamHI* restriction enzymes to allow for directional cloning. Subsequent to restriction, the linearized vector was purified with the Wizard<sup>®</sup> SV Gel and PCR Clean-Up System and the DNA concentration was determined on a NanoDrop ND 1000 (Thermo Scientific, Waltham, Massachusetts, USA). The *FNR:ALDC* fragment was digested (with *EcoRI* and *BamHI*) and purified in a similar fashion as described for the vector, then ligated into pUBI510 and transformed into 50  $\mu$ l of competent *E. coli* DH5 $\alpha$  cells prepared according to (Sambrook and MacCallum, 2013). The transformed cells were then plated onto LBA plates containing 50  $\mu$ g/ml ampicillin and incubated overnight at 37°C. Colony PCR was used to confirm gene insertion with *ALDC* gene-specific primers (Table 3.1). For this colony PCR, the GoTaq<sup>™</sup> DNA Polymerase kit was used according to the manufacturers' instructions. Thermal cycle conditions were as described in Table 2. The denaturing, annealing and extension steps were repeated for 34 cycles. For gel electrophoresis, 5  $\mu$ l of the PCR amplification products were separated on a 1.5% (m/v) agarose gel. Once a positive colony was identified, the colony was grown overnight at 37°C, with agitation (250 rpm) in 15 ml LB containing 50  $\mu$ g/ml ampicillin. Plasmid DNA was isolated from the liquid culture using the Wizard<sup>®</sup> Plus SV Miniprep DNA Purification System.

#### 3.2.11.2 Cloning of the *BDH1* gene and orientation confirmation

The 2,3-butanediol dehydrogenase (*BDH1*, NC\_001133.9) gene, fused to the *FNR* transit peptide, was amplified by PCR with Q5<sup>®</sup> High-Fidelity DNA Polymerase (NEB), from the *pCAMBIA1300::FNR:BDH1* plasmid (Dempers, 2014). Thermal cycle conditions were set to



the conditions described in Table 2.4. The denaturing, annealing and extension steps were repeated for 34 cycles. The *FNR:BDH1* fragment was cloned into the *Sma*I site of *pUBI510*, which had been previously linearized by digestion with *Sma*I at 37°C for 1 h. The ligation reaction was transformed into *E. coli* DH5α competent cells (as described above). Colony PCR was performed on putative transformed colonies using the GoTaq™ DNA Polymerase kit and plasmid DNA was isolated as previously described. Before proceeding, gene orientation in the *pUBI510::FNR:BDH1* construct was confirmed with PCR applying different primer combinations. The first combination included the gene specific forward primer and the plasmid-specific CAMV reverse primer. The second combination was the plasmid specific UbiProm forward primer, paired with the gene specific reverse primer. As a positive control, the original *pCAMBIA1300::FNR:BDH1* was used along with the *BDH1* gene specific primers. All the primer sequences and combinations used are listed in Table 3.1.

Once plasmid DNA was isolated from liquid cultures, the DNA concentration was determined with a NanoDrop ND 1000 (Thermo Scientific, Waltham, Massachusetts, USA). Samples (100 ng DNA/μl) were sent for sequencing at the Central Analytical Facility, Stellenbosch University. The plasmid-specific primers UbiProm Forward (5'-AAT TTGATATCCTGCAGTGCAGCGTG-3') and CAMV Reverse (5'-AGG GTT TCT TAT ATG CTC AAC-3') were used for sequencing.

### 3.2.12 Microprojectile Bombardment of Sugarcane Callus

#### 3.2.12.1 Callus culturing conditions

The sugarcane hybrid NCo310 acted as a source of embryogenic callus. The callus was grown continuously in the dark at 26°C. To initially induce callus development, mature stalks from sugarcane plants were harvested on the Welgevallen Experimental Farm, Stellenbosch University, Stellenbosch. After thorough surface-sterilization and complete removal of all leaf and old stalk tissue, the remaining meristematic leaf tissue was cut into 2 mm thick discs. The discs were then transferred to MSC<sub>3</sub> callus induction medium. Newly formed callus clumps were sub-cultured onto fresh media every two weeks. The MSC<sub>3</sub> callus induction media used, contained 20 g/L sucrose, 0.5 g/L casein and 0.03 g/L 2,4-dichlorophenoxyacetic acid (2,4-D). The media was solidified with 2.2 g/L gelrite (Sigma Aldrich, St. Louis, MO, USA), which was added after the pH was adjusted to 6 with KOH. The medium was autoclaved (121°C, 1.2 kPa for 20 min) prior to use.

### 3.2.12.2 Preparation of target tissue

Four hours prior to the bombardment event, small clumps of embryogenic, nodular calli were transferred to MSC<sub>3</sub>Osm medium (MSC<sub>3</sub> medium containing additional 0.2 M sorbitol and 0.2 M mannitol). The callus clumps were arranged in close proximity to each other, covering a diameter of 2-3 cm.

### 3.2.12.3 Microprojectile preparation

For bombardment, 5 mg of tungsten (Bio-Rad, Hercules, CA, United States), 0.7 micron per particle, were weighed and surface sterilized with chemical grade absolute ethanol. The tungsten was then subsequently washed with sterilized, de-ionized water. The wash step was repeated up to four times to remove all ethanol. Once sterilized the tungsten was suspended in 50 µl of sterilized, de-ionized water. To this mix was added 4 mg of the selectable marker, pEmuKN plasmid DNA and 6 mg of transgene plasmid DNA (both the *pUBI510::FNR:ALDC* and the *pUBI510::FNR:BDH1*), as well as 50 µl CaCl<sub>2</sub> (2.5 M) and 20 µl (0.1 M) spermidine. The mixture was kept on ice throughout its preparation.

### 3.2.12.4 Bombardment

For the particle bombardment procedure, the petri dishes, containing the callus on osmotic medium, were placed 12 cm from the micro-carrier in a locally constructed micro projectile accelerator under vacuum. Once bombarded, callus was kept on osmotic medium for 3 hours post-bombardment, after which it was transferred to solid MSC<sub>3</sub> medium (4.4 g/l MS salts and vitamins). Three days post bombardment, the callus was placed on selection media (MSC<sub>3</sub> solid medium supplemented with 50 µg/ml geneticin [Sigma Aldrich, St. Louis, MO, USA]). The bombarded callus was kept on selection for eight weeks, in the dark at 26°C and sub-cultured every two weeks onto fresh selection media. After selection, putative transgenic callus was regenerated on MS solid medium containing no selective agent and placed under a 16h/8h day/night growth cycle under cool white fluorescent lights (OSRAM L 58W/640, Germany, 50 µmol photons/m<sup>2</sup>/s<sup>-1</sup>) at 24°C. For the next six weeks, the positive clones were allowed to regenerate shoots, whilst being transferred to fresh media every two weeks. For the development of roots, the regenerated shoots were transferred to small magenta boxes containing MS medium for up to eight weeks.



## **3.3 RESULTS**

### **3.3.1 Marker gene selection for sqRT-PCR analysis of ISR**

As an indication of the induced systemic response (ISR) in plants to pathogen attack, certain marker genes have been identified (AbuQamar et al., 2006; Kwon et al., 2010; Mathys et al., 2012). These genes are used for semi-quantitative real-time PCR (sqRT-PCR) and quantitative RT-PCR analysis to indicate the type of immune response that is being elicited in the plant, during infection. To narrow down which potential genes would act as suitable markers during this particular study, several different genes and their expression patterns, were evaluated for a period of 48 h during *Botrytis cinerea* infection of wild-type (WT) Col-0 *Arabidopsis thaliana* plants.

A strong down-regulation of the *PR2* gene was observed during sqRT-PCR analysis, in pathogen infected leaves (represented by I), after 24h compared, to  $T_0$  (time point 0). After 48 h a similar decrease in expression of the gene was then observed in the mock (M) and uninfected leaf (U) samples, compared to  $T_0$  (Figure 3.4a). The *PDF1.3* gene was strongly up-regulated after 24 h in infected leaves only, but decreased again to basal levels after 48 hpi. The *JAR1* gene showed a general down regulation from 24 to 48 hpi in all three leaf treatments. The expression analysis of *MYB75* showed an upregulation of the gene in infected leaves between 24 and 48 hpi (Figure 3.4a). When the expression of *MYC2* and *VSP2* (Figure 3.4b) was analysed, *MYC2* was up-regulated in both infected and uninfected leaves after 24 h, with a further increase in expression in uninfected leaves after 48h, when compared to the mock (M) leaves where expression remained constant from 24 to 48 hpi. In *VPS2*, noticeably low expressions levels of expression were found after 25 cycles. The low level of expression was insufficient to confidently observe an expression trend for *VSP2*, even when the experiment was repeated again. It was therefore decided to exclude *VSP2* in further analyses expression patterns. The expression of *NPR1* remained unchanged at 24 hpi, with a slight increase of expression at 48 hpi for the inoculated leaves when compared to  $T_0$ . The last potential marker gene analysed, was *ERF1* (Figure 3.4c). A distinct upregulation of this gene was visible in infected leaves (I) after 24 h, with a further increase in expression after 48 h. Although a similar trend was observed for all treatments, the expression levels of mock in mock infected and uninfected leaves were distinctly lower than those observed in the infected leaves.

It could therefore be summarized that most genes show an up-regulation during infection. Although the trends differed between some of the genes tested, only the VSP2 gene did not exhibit a clear expression pattern and it was therefore excluded from further experiments.

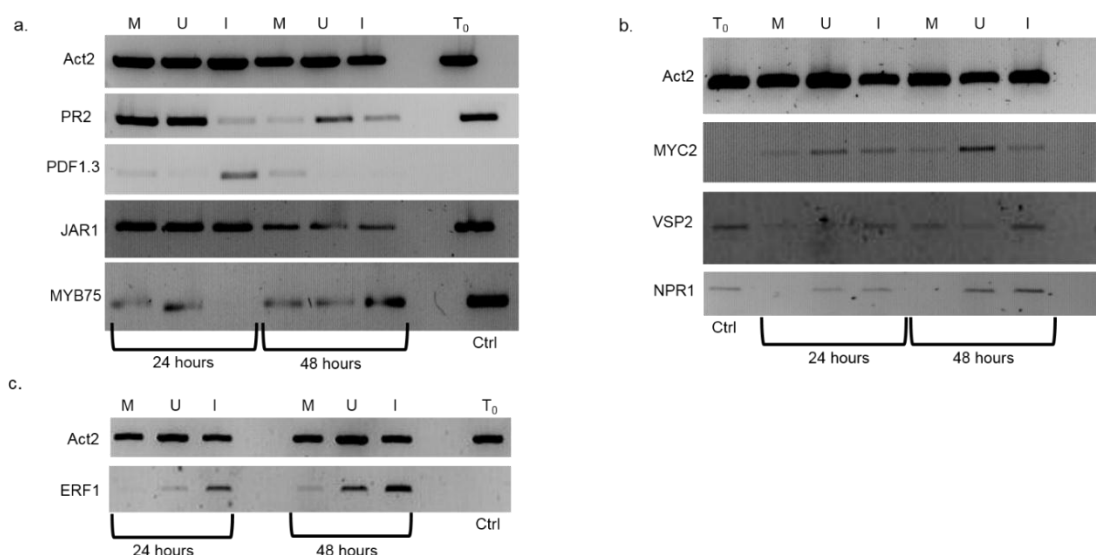


**Figure 3.4:** sqRT-PCR results illustrating gene response profiles. a) *PR2*, *PDF1.3*, *NPR1*, *MYB75* b) *MYC2*, *VSP2*, *NPR1* and c) *ERF1*. The constitutively expressed *Actin2* gene (*ACT2*) was used for standardization. The expression was monitored for 48 hpi (with 24 h intervals). Response was monitored for mock inoculated (M), un-inoculated (U) leaves from inoculated plants and inoculated (I) leaves from inoculated plants. A 0 hour (T<sub>0</sub>) control was included for each primer pair.

### 3.3.2 Confirmation of transgenic *Arabidopsis* lines

Seed obtained from transformed *Arabidopsis* lines were screened *in vitro*, on double selection with kanamycin and hygromycin, for the *pCAMBIA2300::FNR:ALDC* and *pCAMBIA1300::FNR:BDH1* plasmids. Plantlets that maintained resistance to the antibiotics were then genotyped to confirm *ALDC* and *BDH1* gene presence. Total RNA extractions were performed for confirmation of gene expression (Figure 3.5). Expression was confirmed for 3 separate lines, namely 3, 4, and 5.

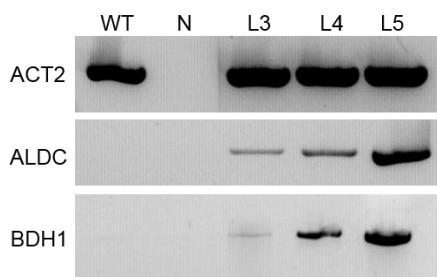


**Figure 3.5:** Confirmation of gene expression for the *ALDC* and *BDH1* genes in putative transgenic *A. thaliana* plants.

### 3.3.3 Trials with acetoin and 2,3-butanediol

For the experiment, synthetic acetoin (AC) and 2,3-butanediol (2,3-BD) were included in the plastic propagation boxes containing the *Arabidopsis* plants. Special attention was given during the investigation, to confirm whether the bacterial volatile organic compounds prime the plant prior to infection. Thus, the WT plants were incubated along with the VOCs, 24 hours prior to inoculation. At the point of inoculation, the AC and 2,3-BD stocks were replenished.

The water, AC and 2,3-BD treated plants were compared through a visual representation of disease development on detached leaves. A sixth, separate leaf was inoculated on each WT plants, which was subsequently detached during each sampling session (at time points 24 and 48 hpi) and photographed. In each case care was taken to be consistent in using the sixth leaf inoculated, to obtain objectivity. Lesion development seemed to be delayed in the AC treated plants, compared to the water and 2,3-BD leaf (Figure 3.6). A clear area of infection was present on both the water treated and 2,3-BD treated leaf, but not for the AC treated leaf.

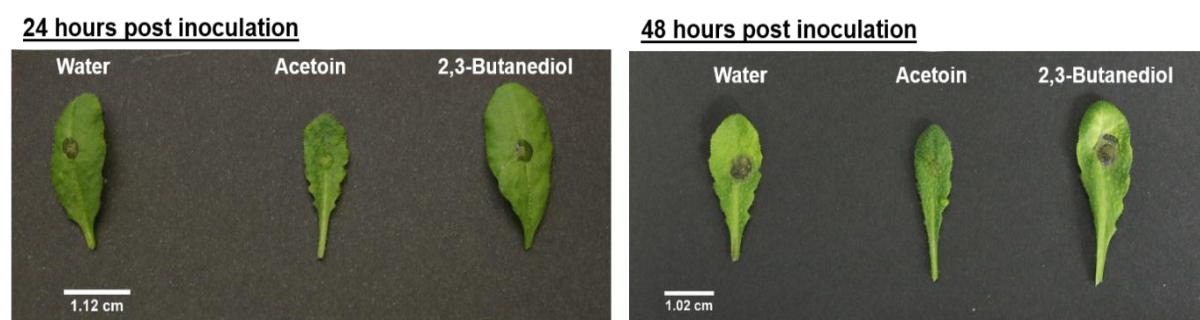


**Figure 3.6:** *Botrytis* infected *Arabidopsis* leaves from acetoin and 2,3-butanediol treated plants. Leaves represent the acetoin and 2,3-butanediol treated leaves, compared to water treated plants. Leaves from acetoin treated plants indicated slower lesion development at both 24 and 48 hpi.

Gene expression profiles from the chosen seven immune-related gene markers was compiled through sqRT-PCR. When considering the water control plants, the mock inoculated (M) leaves exhibited a constant expression level throughout the 48 h time period for all the different pairs, whilst the un-inoculated (U) and inoculated leaves (I) showed an up-regulation in expression 24-48 h post incubation (hpi) for all primer pairs tested, when compared to the water control (Figure 3.7). For the AC treated plants, up-regulation over 48 hours was observed for the M, U and I leaves in the *PDF1.3*, *PR2*, *JAR1*, *NPR1*, *MYC2* and *ERF1* genes (Figure 3.7). The *MYB75* gene exhibited up-regulation for the I leaves, but not for the M or U leaves. Plants treated with the 2,3-BD exhibited expression of the *PR2*, *MYC2* and *ERF1* genes at  $T_0$  (Figure 3.7). This initial expression was not observed for the *PR2*, *MYC2* and *ERF1* genes in the acetoin or water treated plants. Expression levels for the *PDF1.3* and *MYB75* genes in the U and I leaves at  $T_{48}$ , were also higher than in the U and I leaves of the acetoin and water treated plants, whilst expression levels in U and I leaves for *NPR1* and *JAR1* decreased compared to the other treatments at  $T_{24}$ .

The main observation that could be made from the different gene profiles, between the different treatments, was the presence of gene priming. Gene priming was less prevalent for the acetoin treated plants, but the 2,3-butanediol plants showed clear priming of the *PR2*, *MYC2* and *ERF1* genes.

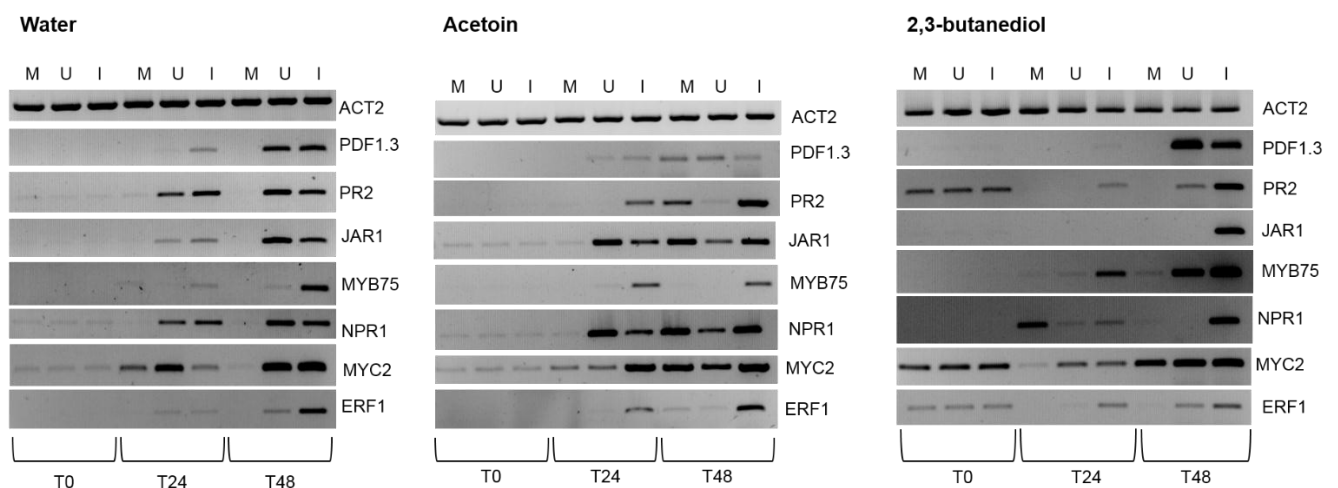


**Figure 3.7:** sqRT-PCR analysis on the water, acetoin and 2,3-butanediol treated *Arabidopsis* plants, 24 and 48 hours post inoculation with *B.cinerea*. Seven different gene profiles were combined to act as visual representation of the overall immune observed for each of the three treatments. The mock (M) inoculated, uninfected leaves (U) from inoculated plants and infected leaves (I) were included in analysis.

A last general observation was done of the overall level of lesion development for each of the separate treatments. The number of lesions present at each time point, was counted, in order to determine how many of the originally inoculated 5 leaves developed disease symptoms (lesions) and at what rate. From this an average level of infection was calculated (presented as a % of diseased leaves per plant), for each of the three biological repeats (Table 3.3). In general, the acetoin treated plants showed slower lesion development.

**Table 3.3:** A comparison of the average lesion development observed between the acetoin, 2,3-butanediol and water treated *A. thaliana* plants, in *B. cinerea* infected plants.

**24H TIME POINT**

Treatment	Plant	# of Infected leaves	Average (%)
Acetoin	1	2	47
	2	2	
	3	3	
2,3-Butanediol	1	3	73
	2	4	
	3	4	
Water	1	5	80
	2	4	
	3	3	

**Table 3.3:** A comparison of the average lesion development observed between the acetoin, 2,3-butanediol and water treated *A. thaliana* plants, in *B. cinerea* infected plants (continued)**48H TIME POINT**

Treatment	Plant	# of Infected leaves	Average (%)
Acetoin	1	3	80
	2	4	
	3	5	
2,3-Butanediol	1	5	100
	2	5	
	3	5	
Water	1	5	87
	2	3	
	3	5	

**3.3.3.1 Effects of the VOCs on *Botrytis cinerea* growth**

*B. cinerea* plates were incubated with water, synthetic AC (1 M) and synthetic 2,3-BD (1 M). Each treatment included five replicates. The diameter of each colony was measured and logged after 36 hours of incubation in the dark (at room temperature). The average colony size for AC treated *B. cinerea* was 33.5 mm. For 2,3-BD *B. cinerea* colonies it was 33.4 mm, and for the water treated colonies it was 33.6 mm. The small differences between treatments indicated that fungal growth was not affected by the AC and 2,3-BD.

**3.3.4 Phenotypic response of transgenic lines to *Botrytis cinerea* inoculation**

A photographic trial was done for comparison between the single transgenic A3 line, the single transgenic B8 line, the double transgenic AB2 line (Dempers, 2014) and wild-type plants. This would allow for an overall visual comparison of disease development. Each plant was drop-inoculated with fungal spore suspension on five alternate juvenile leaves. A mock inoculated

(with suspension media only) plant was included as a negative control. The disease development was then monitored for 7 days post inoculation (dpi). After 7 days, no notable difference could be observed between the different plants. The AB2 line displayed an interesting phenotype during infection, compared to the WT (Figure 3.8). A notable difference between infected AB2 leaves and infected WT leaves was that the AB2 leaves completely disintegrated, where the WT leaves created a fungal mass on the infected leaves. This phenomenon can be observed in close up images of the AB2 infected and WT leaves (Figure 3.10). It would therefore seem that some sort of unique immune-response was present in AB2 plants when challenged with *B. cinerea* infection.

For plants from the transgenic line A3, it was observed that leaves abscised below the point of infection, before the infection could spread and fungal spores develop (Figure 3.10). For the B8 line, infected leaves had completely deteriorated to a fungal mass at 7 dpi, similar to that of the WT leaves (Figure 3.10). In general the single transgenic line A3, and double transgenic line AB2 showed slightly better resistance to the fungal infection than observed for B8 and WT plants. Overall, the A3 plant exhibited the most interesting response to *B. cinerea* infection and results should be confirmed in different ALDC-containing transgenic lines to confirm the response.



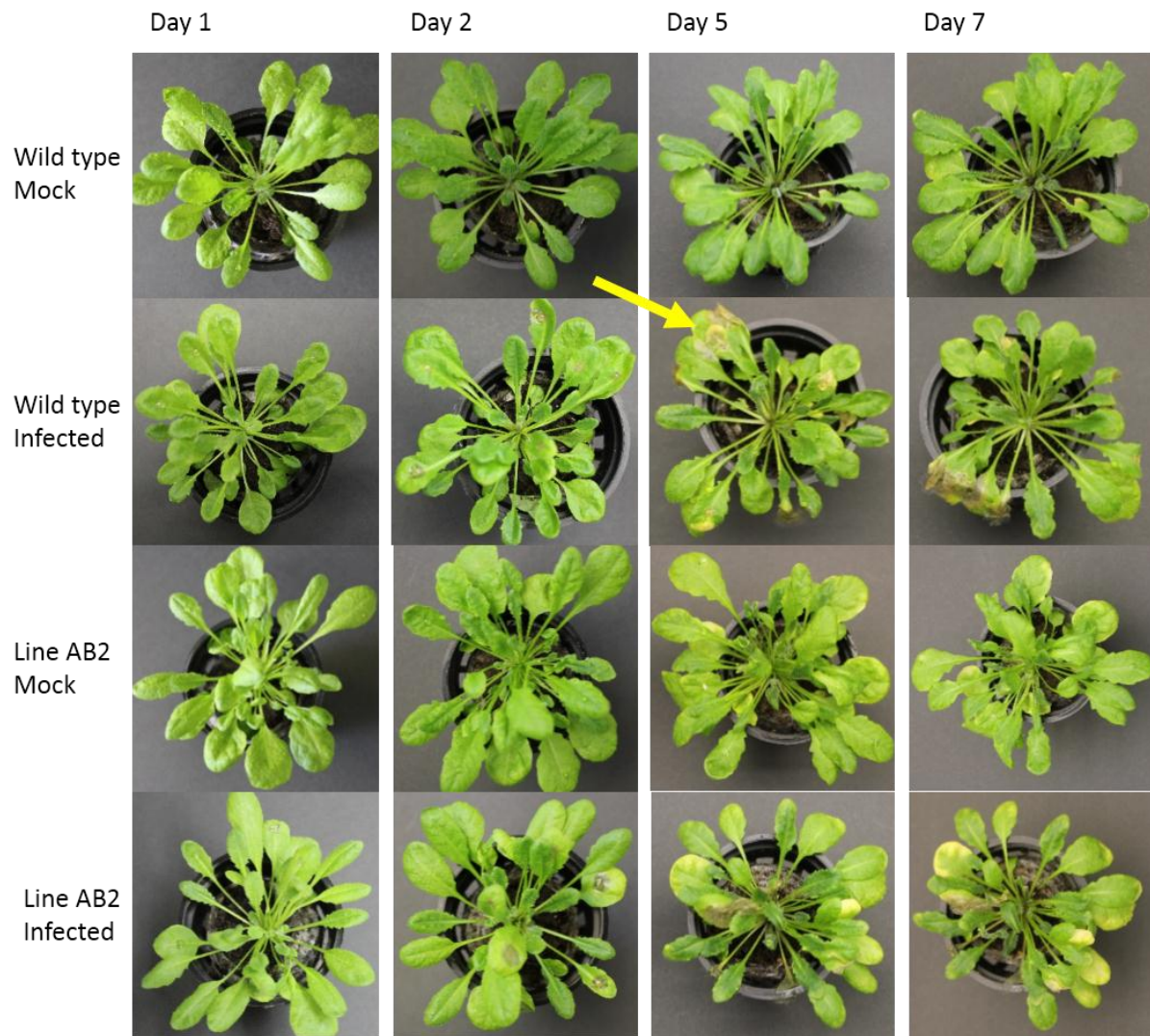


**Figure 3.8:** *B. cinerea* disease development of double transgenic *Arabidopsis* plants containing the *ALDC* and *BDH1* genes (Line AB2), as seen on Day 1, 2, 5 and 7 post inoculation. The scale bar (in white) was set to 2.1 cm. Infection indicated with an yellow arrow.



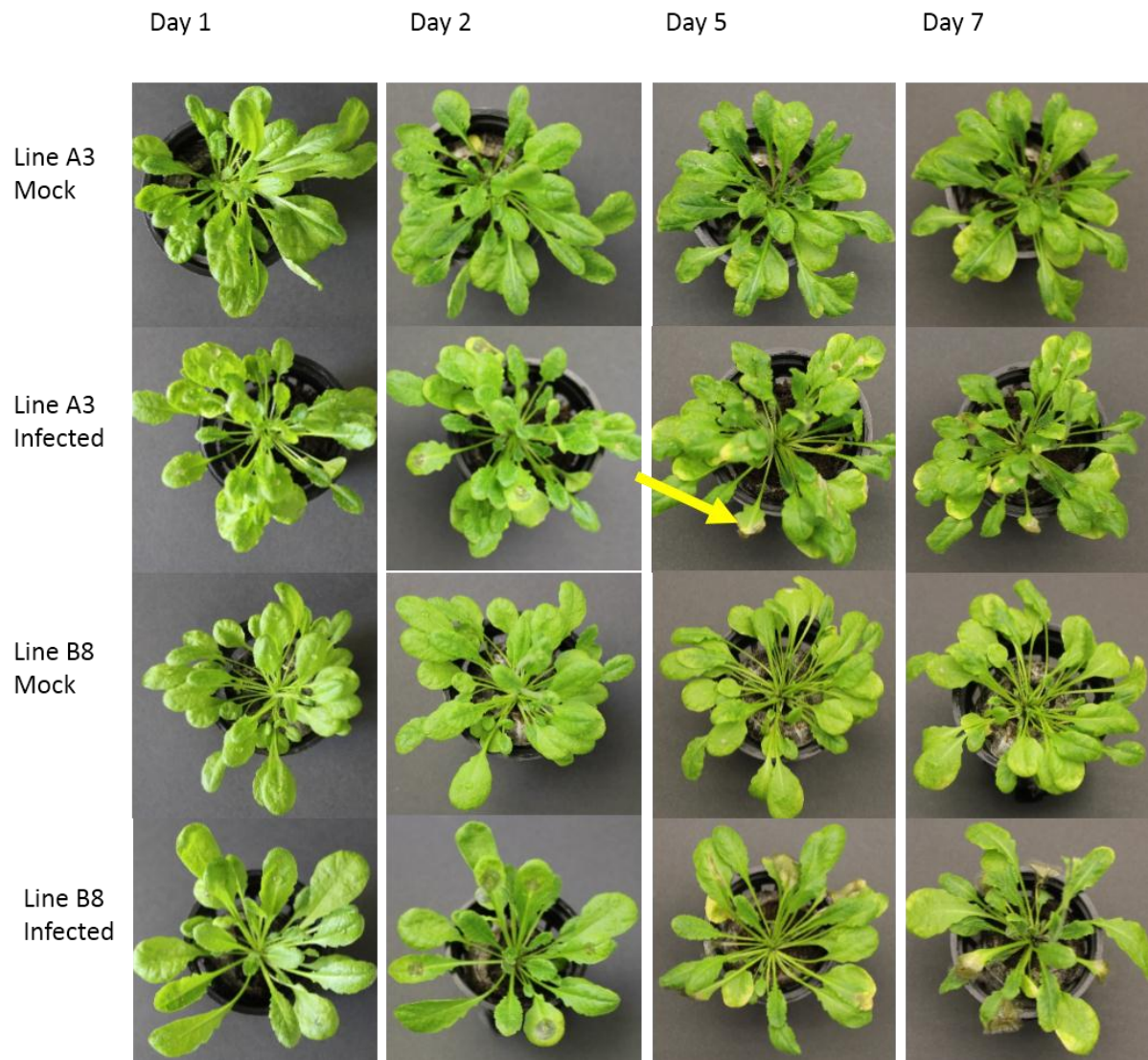


**Figure 3.9:** Disease development in the single expressing *ALDC*-line, A3 and the single expressing *BDH1*-line, B8 post infection with *B. cinerea*. The scale bar (in white) was set to 1.6 cm. Leaf cut off phenotype indicated with an yellow arrow.

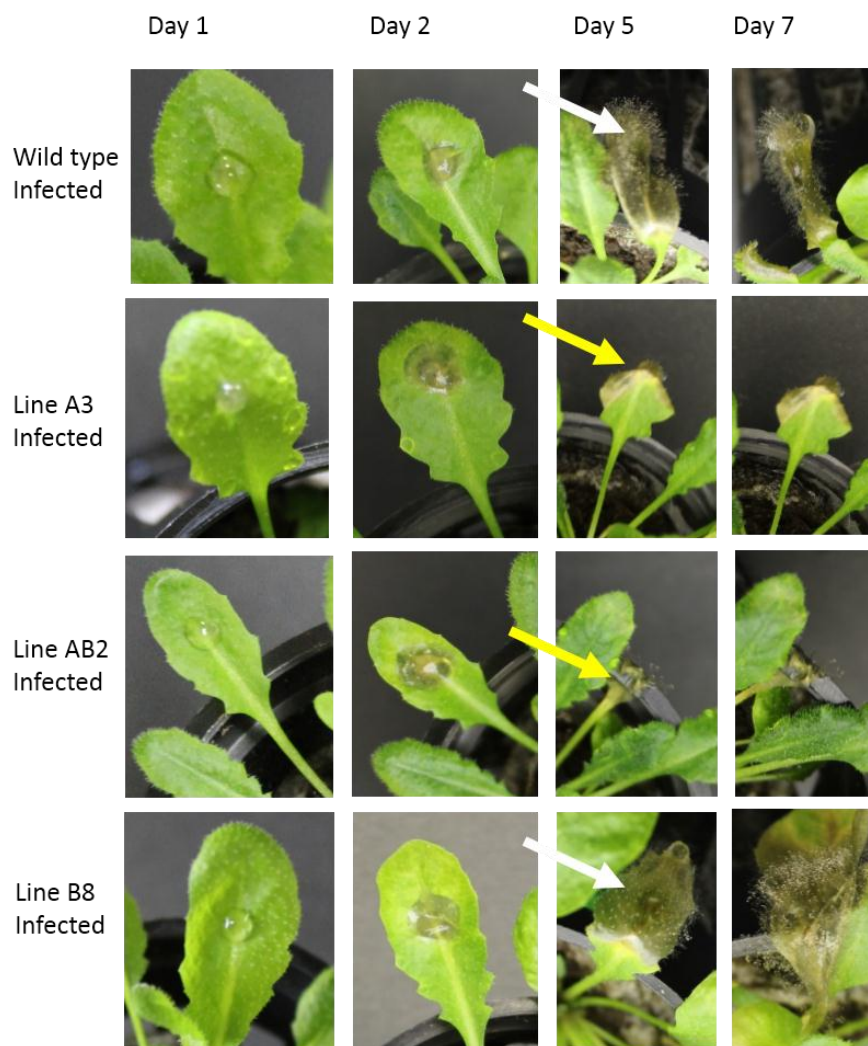


**Figure 3.10:** Close up example of *Arabidopsis* leaves with different diseased phenotypes post *B. cinerea* inoculation. For the single expressing A3- and double expressing AB2-line, a similar phenotype of leaf deterioration was observed (indicated with a yellow arrow). An expected disease phenotype was present in the single expressing B8-line, compared to the wild-type plants (indicated with a white arrow).

### 3.3.5 Disease development

To further understand the effect of infection on the various transgenic lines, a final experiment was conducted to assess the lesion development in inoculated plants for 3 days following inoculation. Again five alternate, juvenile *Arabidopsis* leaves were infected. Three plants as biological repeats were included for lines A3, B8, AB2 as well as the WT. A mock inoculated plant was also included as a negative control for each genotype. At each time point (namely  $T_0$ ,  $T_{24}$  and  $T_{48}$ ), the lesion diameter for each infected leaf was measured. An average diameter size was determined for each line on each specific day. The different lesion diameters for each line were assessed with a simple t-test to determine significance and subsequently plotted on a graph (Figure 3.11). The inoculated leaves were also allocated a score as described in Figure 3.3. Each of the three biological repeats, included for each line, was assessed with the scoring system. The different scores then allocated were statistically analysed with a t-test and plotted on a graph (Figure 3.11).

The average lesion size for line A3 and the WT was fairly similar over the course of the three days, with A3 exhibiting only a slight improvement to the WT at 3 dpi (Figure 3.15). The difference was found to be statistically insignificant after a p-value higher than 0.05 was obtained. The AB2 and the B8 lines had much larger lesions at 3 dpi, although statistically these were not different from the other treatments. The B8 and AB2 lines responded very similarly to infection, which was also evident from the lesion scoring over the course of three days (Figure 3.16). Differences were, however, statistically not significant (mention p value). Lesions were scored according to a specific lesion type, with a score of 5 being the worst, and 0 being no infection present. For this result, A3 exhibited the best results, scoring lower than the WT at 3 dpi, however, the A3 lines developed lesions the quickest of all the lines (Figure 3.15). Although these results provide an indication of increased disease resistance for line A3, future studies need to confirm these experiments for a sound conclusion of increased disease resistance in ALDC-expressing *A. thaliana* plants. It would be beneficial if more than one transgenic A line could be obtained for analysis, and if lesion development could be scored over a longer period than 3 dpi. Once again, none of this data is statistically significant, however, with no p-value smaller than 0.05 after the t-test was conducted.

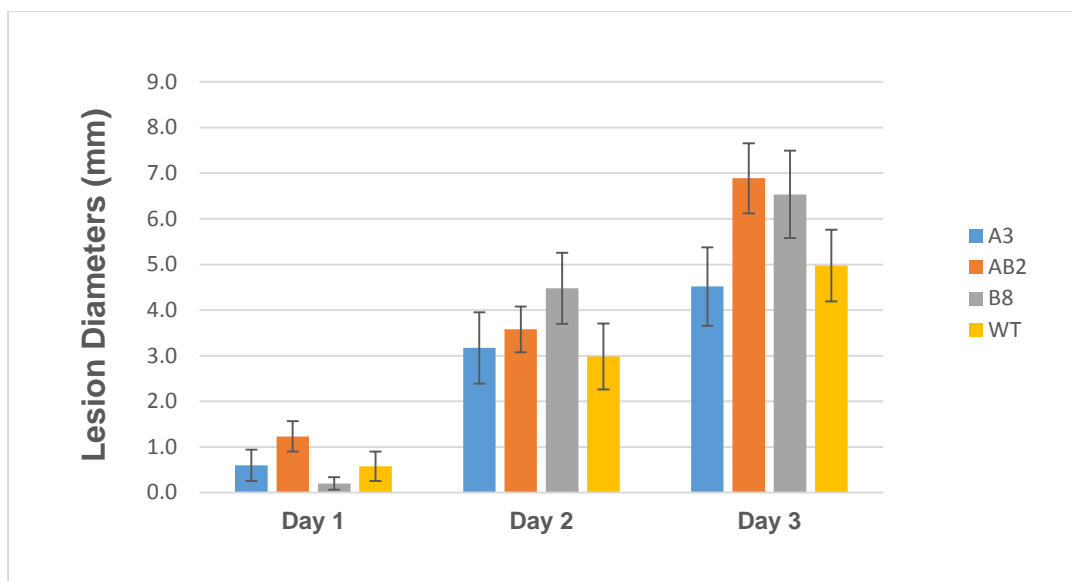


**Figure 3.11:** The lesion diameter for the AB2, A3, B8 and WT lines, 24 h (Day 1), 48 h (Day 2) and 72 h (Day 3) post inoculation with *B. cinerea*, is plotted. The average lesion size was larger for the B8 and AB2 lines than for the WT and A3 lines. The A3 line showed the smallest lesion diameter at 3 dpi, but the difference was not statistically significant when standard deviation was calculated for the five leaves inoculated on three respective plants.

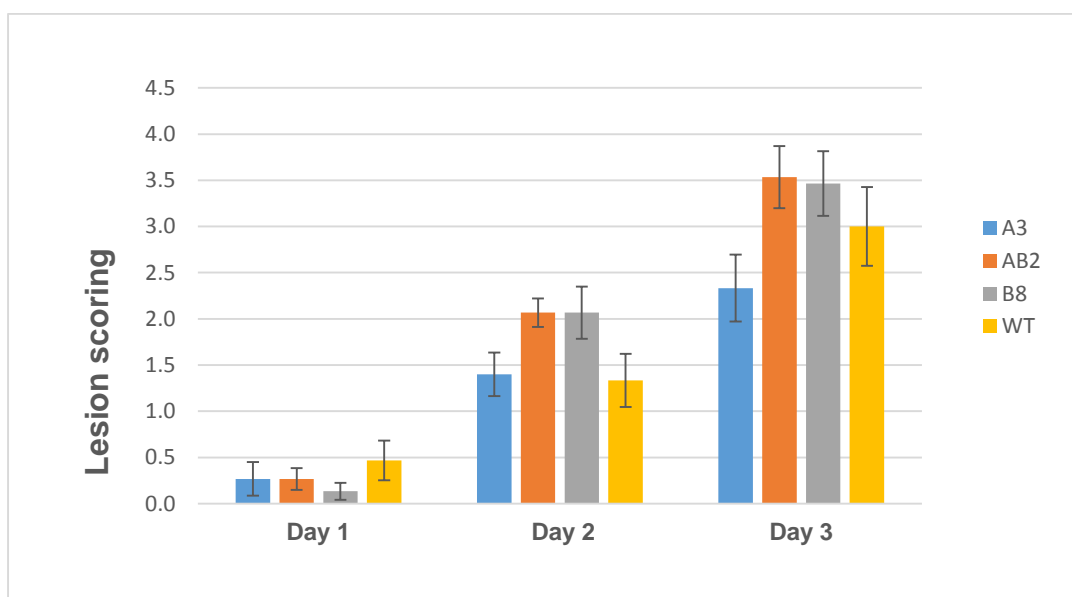


**Figure 3.12:** A score was awarded for the AB2, A3, B8 and WT lines, 24 h (Day 1), 48 h (Day 2) and 72 h (Day 3) post inoculation with *B. cinerea*. The average lesion score allocated was lowest for line A3 at 3 dpi. Line AB2 and B8 responded very poorly to infection, but the differences observed for all the lines were determined to be not statistically significant when standard deviation was calculated for the five leaves inoculated on three respective plants.

### 3.3.6 Gene infection profiling of *Botrytis cinerea* infected double transgenic AB2 lines

Compared to the WT, the *MYB75* gene expression was generally up-regulated in the double transgenic AB2 *Arabidopsis* line (Figure 3.13). At the  $T_{48}$  time point, the gene expression was observed to be lower than when compared to the WT. A high level of expression was observed in the WT inoculated leaves (I) for  $T_{48}$ . In contrast to this, a high level of expression was present in the un-inoculated (U) leaves of the AB2 line, but not in the inoculated leaves, at the same time point. A high level of expression was also present in the U leaves of the 2,3-butanediol (2,3-BD) treated plants (Figure 3.7).

Levels of *MYC2* expression was higher in AB2 at  $T_0$  than the WT, when considering the mock and the inoculated leaves. This higher level of expression is also present at  $T_{24}$  for both the mock and inoculated leaves. At  $T_{48}$  the uninoculated leaves show higher expression for AB2, compared to the WT. The gene evaluated in the inoculated leaves have a lower level of expression considering the AB2-line, when compared to WT at  $T_{48}$  (Figure 3.13). This does not correspond to the higher levels of expression present for *MYC2* when considering Figure 3.7. It does correspond with the *MYB75* expression profile, where the highest level of expression for AB2 is present at  $T_{48}$  in the U leaves (Figure 3.13). An extremely slight down-regulation of the *MYC2* gene is present over 48 hours in AB2 when compared to the WT, which exhibited a clear up-regulation in the inoculated leaves over 48 hpi. The AB2 down-regulation corresponds to what was observed for the *MYB75* gene, but for *MYB75*, the down-regulation is more prominent in the WT than in the AB2 line.

For *ERF1* clear upregulation is present in the AB2 line after 48 hpi, with a less intense band present for the uninoculated leaves. The uninoculated leaves for the WT showed an increase in *ERF1* expression after 48 hpi (Figure 3.13). This level of *ERF1* expression was not observed in the AB2 line uninoculated leaves. The highest level of expression was also present in the inoculated leaves for the acetoin and 2,3-BD treated plants, although the pattern for AB2 corresponds the best with the acetoin treated plants (Figure 3.7).

Expression of the *JAR1* gene is present at  $T_0$  for all three leaf types in the AB2 line, but not in the WT (Figure 3.13). This corresponds to low levels of expression at  $T_0$  for the acetoin treated plants. The expression is not present for the 2,3-BD treated or WT plants (Figure 3.7). Similar to *ERF1*, the *JAR1* gene is up-regulated over the 48 hours in the inoculated leaves in the AB2 line. The up-regulation is also present for the WT, but expression is not present at  $T_0$  and  $T_{24}$  as for the AB2 line. The mock inoculated (M) leaves exhibit no expression in the WT, but a strange up-regulation is present in the M leaves at  $T_{24}$ .



An up-regulation of *PR2* expression is observed in the inoculated leaves from the AB2 line (Figure 3.13). The highest level of expression is present 48 hpi. A different expression pattern is present for the WT, where a high level of expression is present in the inoculated leaves after 24 hpi, whereafter it decreases at 48 hpi. This is similar to what was observed for the acetoin treated plants (Figure 3.7). Neither the AB2 nor WT showed any expression for the mock leaves throughout the 48 h time period. Priming of the *NPR1* gene is present for the AB2 line at time 0, when comparing expression levels to the WT (Figure 3.13). This priming is present for all three leaf samples, due to higher *NPR1* expression when compared to then WT *NPR1* expression levels. Unfortunately no expression could be obtained at 25 cycles for the *PDF1.3* primer pair. This was not the case for the acetoin and 2,3-BD treated plants (Figure 3.7), although expression levels were low for the acetoin treated plants as well as during the original optimization of the primer pair (Figure 3.4).

### 3.3.7 Gene expression analysis of single transgenic *ALDC* plants

Due to the potential increase in resistance that the A3 plants exhibited (Figure 3.11 and 3.12), a trial was conducted to investigate the gene expression profile of A3 during infection. Expression analysis of infected A3 lines (Dempers, 2014) was conducted.

Four of the seven genes (*JAR1*, *MYB75*, *MYC2* and *PR2*), exhibited expression at  $T_0$ , which the WT plants did not. This expression was present for the mock inoculated (M), as well as the un-inoculated (U) and inoculated (I) leaves from *B. cinerea* infected plants (Figure 3.14). This basal level of expression was also present for *JAR1* and *MYB75* in the acetoin treated plants (Figure 3.7).

A broadly similar response was present for *PDF1.3* and *ERF1* for both the A3 and WT lines, with a general increase in expression present over the 48 h time period. The *PDF1.3* gene exhibited a slightly lower level of expression in the I leaves, compared to the WT (Figure 3.14). This slight decrease in expression was similar to the observed expression pattern for *PDF1.3* observed in the acetoin (AC) treated plants (Figure 3.7). Interestingly, the *NPR1* gene appeared to be up-regulated in the A3 line, compared to the WT, after 24 and 48 h (Figure 3.14). Once again, this was similar to what was observed in the AC treated plants (Figure 3.7).

Gene profiling of the *B. cinerea* infected single-expressing A3 line therefore indicated an up-regulation in ISR-related genes.

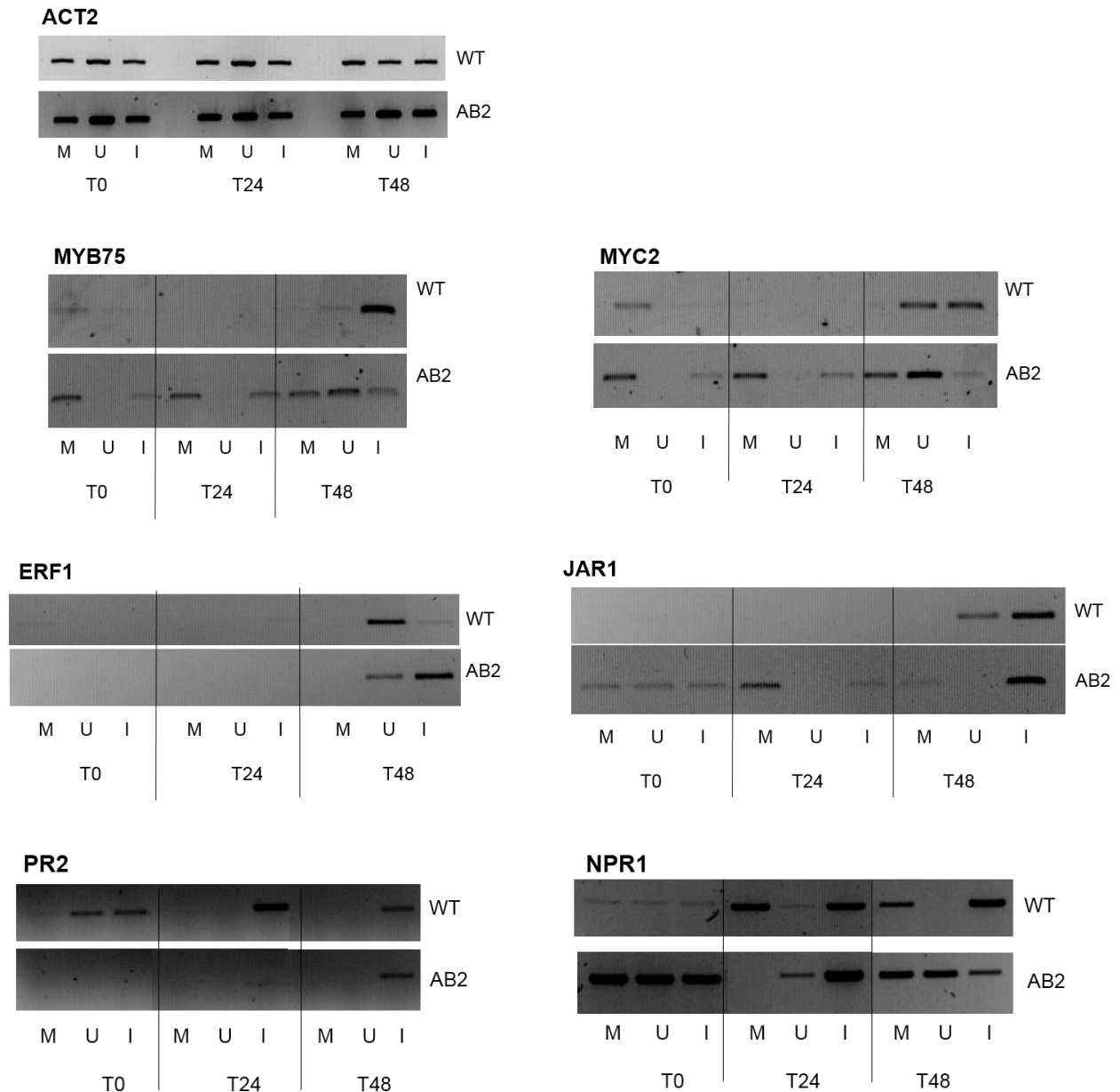


**Figure 3.13:** Semi-quantitative RT-PCR analysis of *B. cinerea* infected double expressing *ALDC* and *BDH1* AB2 line. Analysis was standardized with the *Actin2* (*ACT2*) gene, after which the expression profiles of seven genes, including *JAR1*, *PDF1.3*, *ERF1*, *NPR1*, *MYB75*, *MYC2* and *PR2*, were compiled. No expression profile could be obtained for *PDF1.3*.

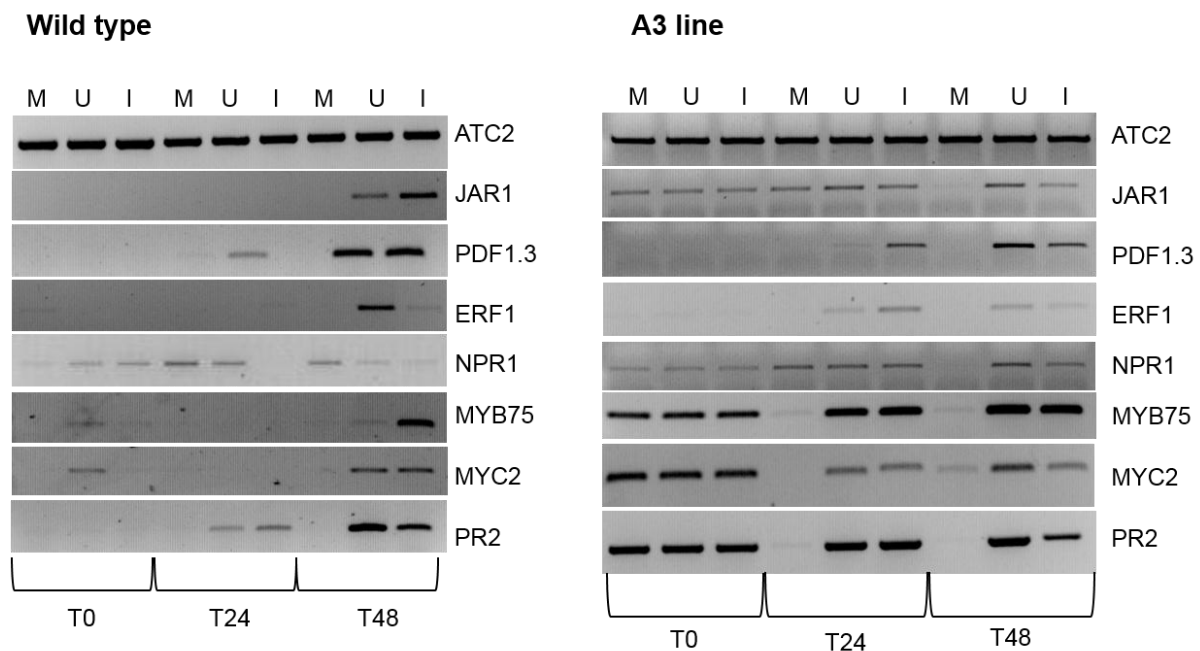


**Figure 3.14:** Semi-quantitative RT-PCR analysis of *B. cinerea* infected transgenic line A3 plants. Analysis was standardized with the *Actin2* (*ACT2*) gene, after which the expression profiles of seven genes, including *JAR1*, *PDF1.3*, *ERF1*, *NPR1*, *MYB75*, *MYC2* and *PR2*, were compiled.

### 3.3.8 Expression of *ALDC* and *BDH1* in sugarcane

#### 3.3.8.1 Isolation and cloning of *ALDC* and *BDH1*

Both the *ALDC* and *BDH1* genes were isolated by PCR amplification from the original pCambia cloning vectors shown in Annexures A and B (Dempers, 2014). The ferredoxin-NADP<sup>+</sup> reductase (*FNR*) transit peptide sequence attached to both genes was also included during the amplification (Figure 3.15a). The isolated genes were subsequently cloned into the pUBI510 sugarcane transformation vector. Subsequent sequencing confirmed the presence of both genes in the vector (Annexures C and D). The *pUBI::FNR:ALDC* and *pUBI::FNR:BDH1* vectors were co-bombarded, along with the selection plasmid pEmuKN into sugarcane embryogenic callus. Following eight weeks of *in vitro* selection on geneticin, several surviving callus clumps were identified (circled in red, Figure 3.15b). The surviving callus transferred to the light for plant-regeneration. Once plants are large enough, they will be genotyped and expression of the *ALDC* and *BDH1* genes will be confirmed. The plants will also be assessed phenotypically to confirm an increase in growth. Infection studies will be conducted to confirm an increase in disease resistance.



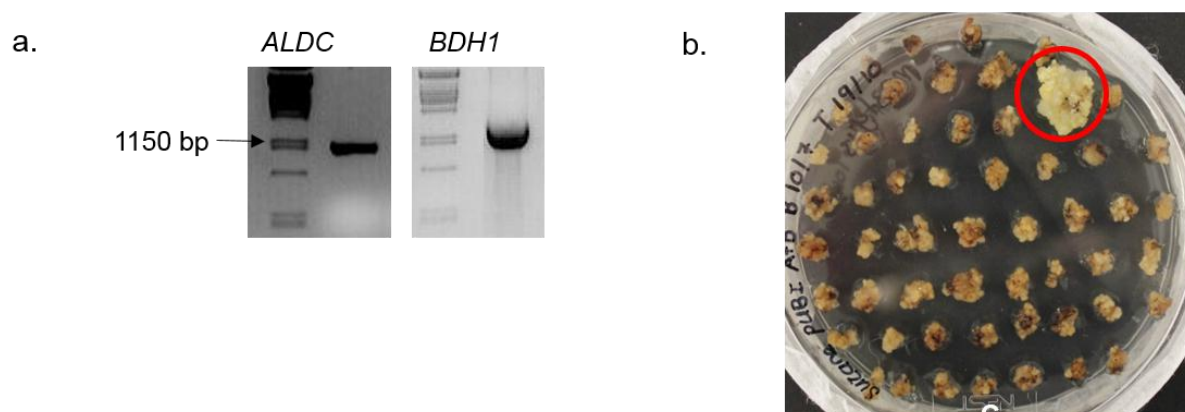


**Figure 3.15:** *pUBI::FNR:ALDC* and *pUBI::FNR:BDH1* positive transformants. Successful isolation of the a) *ALDC* (~1200 bp) and *BDH1* (~1300 bp) genes for subsequent cloning into pUBI510. Subsequent to transformation and 8 weeks on selection with genetic b) regenerating callus was identified and circled in red.

### **3.4 DISCUSSION**

The presence of beneficial microbes within the rhizosphere has been well studied, along with the beneficial effects they have on plant health (Pieterse et al., 2014b). Studies have characterized a certain group of these beneficial microbes as plant growth-promoting rhizobacteria (PGPR), which are known to increase plant pathogen resistance through the priming of plant defences (Loon et al., 1998; Mathys et al., 2012). The plant's enhanced defence is then capable of protecting it against a range of pathogens, as well as insect herbivores (Pieterse et al., 2014b). The plant defence response elicited by PGPR is referred to as induced systemic resistance (ISR) (Loon et al., 1998).

This study examined the ability of transgenic *A. thaliana* lines, overexpressing the *ALDC* and *BDH1* genes, to resist *B. cinerea* infection. Double transgenic lines containing both the *ALDC* (responsible for AC production) and *BDH1* (responsible for 2,3-BD production) genes, showed a decrease in resistance. This could possibly be explained by the hypothesis that the newly introduced chemical pathway (acetoin and 2,3-BD production) is now taking too much energy and attributing a disadvantage to the transgenic lines when challenged with *B. cinerea*. Interestingly, the results presented also indicated that transgenic line containing only the *ALDC* gene, A3, exhibited a possible increased resistance to infection. Quantitative measurements of lesion development indicated stunted disease development in A3 lines, but increased levels of disease occurrence in the AB2 lines. Qualitative data including photographic documentation supported these results. It was also shown via sqRT-PCR that the presence of AC and 2,3-BD primed certain immune-regulated genes.

#### *3.4.1 Selecting marker genes for sqRT-PCR analysis*

For the purposes of this study, a total of seven possible reference genes were finally identified. Genes that were included were *PDF1.3* (ET/JA-signalling), *PR2* (SA-signalling), *NPR1* (ISR hallmark), *JAR1*, *MYC2* (both JA-signalling), *ERF1* (ET-signalling) and *MYB75* (phenylpropanoid pathway).

Much research has been done to identify alternative hallmarks for ISR, after the discovery of its independence from pathogenesis-related proteins (Loon et al., 1998; Kwon et al., 2010; Mathys et al., 2012; Pieterse et al., 2014b). It is now understood that jasmonic acid (JA)- and ethylene (ET)-responsive genes play a vital role in mediating ISR. When proteome and transcriptome analysis was conducted prior and post pathogen infection, a clear correlation with JA/ET-response pathways was identified, although the specific regulatory pathway is not yet fully understood (Kwon et al., 2010). For this particular study, the ET-response gene, *ERF1* and the JA-response gene, *JAR1*, showed clear expression differences when transgenic lines

were compared with control WT plants. The information provided by the *ERF1* and *JAR1* genes during this study was valuable and attributed in constructed a hypothesis around the immune-response elicited when *ALDC* and *BDH1*-expressing transgenic lines were challenged with *B. cinerea*.

It was also decided to include the *PDF1.2*, *PR1* and *NPR1* genes results presented in previous studies regarding VOCs and ISR (Kwon et al., 2010; Rudrappa et al., 2010). When proteome analysis was conducted on *Arabidopsis* plantlets exposed to the VOCs AC and 2,3-BD, it was found that ET-response gene, *ERF1*, was up-regulated during exposure. Data presented in previous studies indicated the importance of ET-biosynthesis for the elicitation of ISR. During this particular study a similar up-regulation was observed over a time period of 48 hours post inoculation (hpi). Up-regulation of *PDF1.2*, *VSP1* and *PR1* genes was illustrated in the previously conducted proteome analysis, suggesting that the VOCs in particular prime the plant with up-regulation of ET- and JA-responsive genes (Kwon et al., 2010), thus, making these genes suitable hallmarks for studying ISR-priming and ISR-boosts. The priming of immune related genes, specifically linking to ISR, was present in this study, particularly when single expressing *ALDC* A3 lines were considered. A priming of SAR-related *PR2* was also present, suggesting that salicylic acid and the systemic acquired resistance was present at that point in the A3 plants. The *PDF1.2* and *PR1* genes acted as indicators of an immune response in a previously conducted study by Rudrappa et al., where the effects of pathogen challenge post VOC exposure was investigated (Rudrappa et al., 2010). Unfortunately the sqRT-PCR analysis in this study was optimized with the *Actin2* reference gene with a primer pair that amplifies a 500 bp band. The *PDF1.2* and *PR1* genes are both smaller than 500 bp in size, making them too small for this Master's study. The genes were used by Rudrappa et al., for Quantitative Reverse Transcriptase PCR (qRT-PCR) and optimized for a smaller 200 bp band (Rudrappa et al., 2010). This Master's study then chose the *PDF1.3* and *PR2* genes as an alternative. Thorough investigation of alternative marker genes showed that they are a part of the same gene families as *PDF1.2* and *PR1*, and are also suitable hallmarks for ISR (Mathys et al., 2012). The use of *PDF1.3* and *PR2* is not advised in future studies due to inconsistent patterns observed during our sqRT-PCR analysis. The lack of a conclusive result could, however, be due to a lack of technique mastery. For future studies the use of qRT-PCR analysis is advised for obtaining more conclusive results.

A fourth gene, *VSP2*, involved in the JA-pathway was included in this Master's study (Lee et al., 2012; Mathys et al., 2012). In correlation to this, the transcription factor *MYC2* was included, due to its function as both activator and repressor of distinct JA-responsive genes in *Arabidopsis* (Lorenzo et al., 2004). It is also known to be related to *VSP2* expression. The use

of *VSP2* was excluded after sqRT-PCR analysis due to inconsistent expression patterns between different experiments and low levels of expression, limiting the conclusions that could be made from this gene. Another JA-related gene, *JAR1*, was included as sixth choice due to the accumulating evidence of JA involvement in ISR response. The *JAR1* gene has been postulated to be involved in signal transduction leading to ISR initiation (Glazebrook, 2005). The results present in this Master's study illustrated a clear priming of the *JAR1* gene during acetoin treatment, indicating its involvement in the defence response against *B. cinerea* infection in the presence of the VOCs. The different immune responses, regulated by these three hormones (JA, SA and ethylene), were investigated in Arabidopsis plant in this study with the ultimate goal of modelling the interactions that occur between the hormones, during a pathogen challenge. Although not directly linked to ISR, *jar1*-mutants showed a decreased level of resistance against fungal pathogenic attack, including *B. cinerea* by Kunkel and Brooks (2002). The *JAR1* response, in combination with the *PDF1.3* and *VSP2/MYC2* genes therefore allowed for a conclusive coverage of JA-signalling and might aid in concluding the involvement of JA in ISR.

The *MYB75* gene was included in this study as an indication of ISR priming (up-regulation of ISR-related gene markers before pathogen challenge) and boosting (up-regulation of ISR-related gene markers during pathogen attack). The gene is specifically known to be upregulated during fungal pathogen attack, including *B. cinerea* and is linked to the phenylpropanoid pathway (Mathys et al., 2012). The *ERF1* gene was chosen as an indicator of ethylene involvement. Although some controversy exists around the role ET plays in plant defence, it was clearly shown in this study that when exposed to bacterial VOCs, ET-biosynthesis is induced and the up-regulation of *ERF1* was a strong indication of ET-response in the volatile-treated plants (Kwon et al., 2010; Mathys et al., 2012).

### 3.4.2 Gene response to fungal infections

To establish whether the eight chosen possible hallmark genes would be suitable candidates to analyse the ISR in this study, an initial *B. cinerea* infection trial was conducted on 6-week-old wild-type (WT) *Arabidopsis thaliana* plants.

The *NPR1*, *ERF1*, *MYB75* and *JAR1* genes all showed the expected response with *NPR1*, *ERF1* and *MYB75* increasing in expression at 48 hpi. This confirmed that the genes were suitable for further analyses of gene expression during this study. A genome-wide characterization on of ISR induction in *Arabidopsis* plants, post *B. cinerea* infection (Mathys

et al., 2012). Although *MYC2* also exhibited increased expression at 48 hpi, the band was very faint and possibly indicates very low expression. *JAR1* expression was highest 24 hpi, corresponding with the assumption that it acts as signalling mechanism to induce subsequent ET and *NPR1* expression (Glazebrook, 2005). Over the past 10 years, accumulating evidence has indicated the involvement of both JA and ET in ISR regulation (Van Wees et al., 2008). For *PR2* and *PDF1.3* genes, the expected expression profiles were found. For future qRT-PCR analysis, it would be better to rather employ the original marker gene, *PDF1.2* as it is an established gene and is routinely used during immune-related studies as an indication of ISR elicitation. The inoculated leaves exhibited the brightest band at  $T_0$ , but any up-regulation for the un-inoculated leaves was only found after 24 hours. This is an indication that the ISR-response is present more quickly in the inoculated leaves than in the un-inoculated leaves. The ISR-response is generally present throughout the plant, starting in the infected leaves and spreading over time to the un-inoculated (or un-infected) parts. The results of the study support the hypothesis that ISR is a quick response (within 48 h of pathogen attack) which has now become generally accepted (Loon et al., 1998; Van Wees et al., 2008; Mathys et al., 2012).

*PR1*, *PR2* and *PR5* are indicators of systemic acquired resistance (SAR) defence responses (van Loon, et al., 2006). The expression of pathogenesis-related (*PR*) genes have been identified as important hallmarks for SA accumulation and the induction of SAR (Rudrappa et al., 2010). Thus for subsequent infection of the transgenic lines, *PR2* expression could be employed in the study to indicate the involvement of SAR involvement. Previous studies have already indicated the involvement of SA-dependent SAR, alongside ISR elicitation during infection (Van der Ent et al., 2009; Pieterse et al., 2014b). However, in the study mock inoculated leaves had no consistent expression for *PR2*, *JAR1* or *ERF1*. The difference in expression between the different mock inoculated leaves did, however, indicate that the growth environment the plant was placed in, i.e. the propagation boxes and high humidity, might have a stressful, negative influence on the plants during their 48 h incubation. The difference in expression was, however, not present for all seven genes. No effect was observed for the *PDF1.3*, *MYB75*, *MYC2* or *NPR1* genes. Attempts should be made to provide the plant with a less stressful environment. To try and limit the stress endured by the plant, shorter incubation periods might be tested. The gene expression could be tested for example at 0 h, 6h, 12h and 24 h instead. Another alternative would be to investigate more genes and then choose hallmark genes that are not affected by the growth conditions, like *PDF1.3*, *MYB75*, *MYC2* or *NPR1*.

From the sqRT-PCR results obtained, it was decided to include all but *VSP2* in any further analysis. The seven remaining hallmark genes would still allow for a wide description of

responses activated and involved in the defence response elicited from *B. cinerea* infection, including the JA/ET-signalling pathway, the SA-signalling pathway and the phenylpropanoid-signalling pathway. In addition, *MYC2* and *JAR1* are sufficient indicators, together with *PDF1.3* and *NPR1* analysis, of ISR-priming and ISR induction by JA-signalling (Glazebrook, 2005; Van der Ent et al., 2009; Mathys et al., 2012).

### **3.4.3 Exposure to Acetoin and 2,3-butanediol prime certain defence related genes**

Three separate studies have identified the positive effects PGPR produced VOCs, acetoin (AC) and 2,3-butanediol (2,3-BD) has on plant defence. Originally, protection against the bacterial pathogen *Erwinia carotovora* subsp. *carotovora* was illustrated (Ryu et al., 2004a). It was exhibited when *Arabidopsis* plants exposed to the (RR)- and (SS)-isomers of 2,3-BD showed a triggered ISR response. Findings were further supported when PGPR mutants, producing reduced levels of 2,3-BD, did not elicit the same level of resistance against infection (Ryu et al., 2004a). When AC was exogenously applied to *A. thaliana* plants, subsequent infection with *P. syringae* DC3000 was stunted (Rudrappa et al., 2010). Interestingly, this Master's study concluded that 2,3-BD treatment was not able to protect plants against infection. When AC and 2,3-BD were exogenously applied to the plants, prior to *B. cinerea* infection, similar results were obtained in terms of an increased resistance present for AC treatment but nothing significant for 2,3-BD treatment. From drop-inoculated leaves, it was evident that lesion development was stunted in the AC treated plants, but not the plants exposed to 2,3-BD. Although it was tried to be objective during the photographing of detached leaves, the results show different aged leaves at each time point, since separate plants were used for each measurement to prevent the measuring process having any effect on further lesion development (Figure 3.8). For future studies, it would be therefore advisable to conduct a separate experiment focused on lesion development. In this experimental design, care should be taken to inoculate leaves of the same age and to monitor lesion development for a longer time period on one single leaf. It is also advised that more than one repeat is included, to gain a better idea of consistency regarding this result.

It was previously shown that PGPR strain *Bacillus subtilis* GB03 specifically triggered ISR in response to pathogen challenge (Ryu et al., 2004a). Further study revealed that when acetoin was exogenously applied to *Arabidopsis* plants, certain SA-, ET- and JA-related genes were upregulated, prior to pathogen infection (Kwon et al., 2010). It is now thought that the VOCs



prime the plant to elicit resistance to a greater variety of pathogens. Gene expression for certain ET-biosynthesis and ET-responsive, as well as JA-responsive genes, were shown to be upregulated post acetoin exposure (Kwon et al., 2010; Mathys et al., 2012). To further investigate the possibility of plant priming before pathogen attack, six-week-old *A. thaliana* plants were treated with AC and 2,3-BD (separately), 24 h prior to *B. cinerea* challenge. Gene expression profiles for seven hallmark genes were then compiled. AC exposure prior to infection with *B. cinerea* primes the JA-signalling pathway in the plant for an ISR response. When plants were treated with acetoin 24 h prior to infection, *JAR1* was expressed earlier when compared to the water-treated control (Figure 3.7). This supports the hypothesis that the VOCs elicit a JA-dependent response in *A. thaliana* plants (Ryu et al., 2004a; Kwon et al., 2010; Rudrappa et al., 2010). Both *MYC2* and *JAR1*, linked to JA-signalling, were expressed at  $T_0$ . This acts as additional support that the response is JA-dependent. It also supports the suggested signalling pathway described in Mathys et al. (2012), where JA-signalling leads to *MYC2* up-regulation (present at  $T_{24}$  and  $T_{48}$ ) when the ISR is primed/induced (Figure 3.7). The expression of *MYC2* then signals *VSP2* expression (Mathys et al., 2012), which might explain why the *VSP2* expression levels were so low during the optimization process. In future studies it would be advisable to include an additional time point 12 or 24 h past the  $T_{48}$  time point, to investigate *VSP2* expression during infection. Expression of *JAR1*, *MYC2* and *VSP2* is important, because genes are thought to be responsible for the ISR-boost post infection. Also, *JAR1* can act as a transducer for JA-signalling (Glazebrook, 2005). *JAR1* activation might also acts as signal for JA-responses and through subsequent *MYC2* and *VSP2* activation an ISR-boost post *B. cinerea* infection occurs. If the AC is able to elicit this response prior to infection, it would cut short the process and allow the plant to fight infections more quickly and more intensely.

A more significant level of up-regulation was present when sqRT-PCR analysis was conducted on 2,3-BD treated plants. This suggests that this particular VOC is more effective in priming the plant. Previous reports of 2,3-BD treated plants did not include gene analysis. It was reported that this VOC was not as effective at reducing disease symptoms in plants when compared to AC (Rudrappa et al., 2010). The original study done with the PGPR *B. subtilis* strains, GB03 and IN937a, showed that the strains elicit different immune responses. The IN937a strain triggered a response which was ET-independent and the GB03 strain elicited a response that was ET-dependent (Ryu et al., 2004a). Further studies focussed on the GB03 strain and on the VOC, acetoin. The results presented in this MSc study indicate that 2,3-BD alone, without the presence of AC, was not as effective against pathogen attack. Both AC and 2,3-BD were present in the volatile blends released by GB03 and IN937a (Ryu et al., 2004a). The sqRT-PCR results from this study also showed that treatment with 2,3-BD primes the *PR2*

gene, which is a traditional hallmark for the SA-regulated SAR-response. No priming was evident for *NPR1*, *JAR1*, *ERF1* or *PDF1.3*, the traditional hallmarks for ISR, following 2,3-BD treatment. In combination with the results from the study conducted by Rudrappa et al., (2010), and the results presented for this study, it appears that the real elicitor of ISR could possibly be AC and not 2,3-BD.

The sqRT-PCR results presented in this study suggest that the 2,3-BD is linked to a SAR response and that acetoin is responsible for the ISR response. This suggestion will, however, require future detailed analysis of the expression profiles present in plants post VOC treatment. Future studies should also focus on determining the immune response elicited by each VOC (acetoin or 2,3-BD) separately. Also the effect on gene expression has to be determined when plants are treated with both VOCs simultaneously (Ryu *et al.*, 2004). Once a profile has been established for each VOC in Arabidopsis, research could be expanded to further investigate if the response is similar in different plant species, e.g. tobacco or tomato plants. Care should also be taken to determine whether the response elicited and the gene profile remains the same when plants are challenged with different types of pathogens, for example a bacterial (e.g. *P. syringae*) or fungal (e.g. *B. cinerea*) pathogen. Thereby, more information towards the specific signalling pathways involved in ISR (as well as the hallmark genes) is accumulated.

#### **3.4.4 Double transgenic plants exhibit lower resistance**

Results obtained from the chemically-treated plant infection trial prompted further investigation into the hypothesis that acetoin is responsible for increased disease resistance. Transgenic lines AB2 (containing both the *ALDC* and *BDH1* genes) and A3 (a single transgenic line containing only the *ALDC* gene), were inoculated with *B. cinerea* to compile a genetic profile for the transgenic plants during infection. Disease resistance was monitored by measuring lesion development and scoring disease symptoms. The A3 line responded slightly better to infection than WT plants, but the difference was not significant. This lack of statistical significance may be related to the small number of replicates used in this study. AB2 lines further had decreased disease resistance, but again the difference was not statistically significant. However, the trends observed correlated was similar to chemically treated plants. *ALDC* expression was further extremely low in the AB2 line, compared to *BDH1*. This suggests that very low acetoin amounts were present in the plant.



Phenotypic comparison between the AB2, A3 and B8 lines provided a qualitative comparison of *B. cinerea* resistance between the different lines. To my knowledge, none of the previous studies conducted (Ryu et al., 2004a; Kwon et al., 2010; Rudrappa et al., 2010) with acetoin and 2,3-BD focused on the type of lesion that developed during infection, since none of the other studies used a necrotrophic pathogen to investigate disease resistance. Previous studies have reported that the PGPR-mediated form of resistance varies between the plant tested and the type of pathogen it is being infected with (van Loon et al., 2006; Mathys et al., 2012; Pieterse et al., 2014a; Pieterse et al., 2014b). In this MSc study it was found that AB2 and A3 lines abscised the infected leaves before a mycelia could develop on the leaf (Figures 3.8 to Figure 3.10). This could represent a mechanism through which the plant prevents the infection spreading further through the plant. Another interesting phenotype observed was a glassy area around the point of infection (described in the scoring system as Grade 2, Figure 3.3). This type of development is very likely a hypersensitive-type response in the leaf, where necrosis is induced around the point of infection preventing it from spreading further. Future studies could investigate this phenomenon further with lactophenol-trypan blue staining (Thomma et al., 1998; Denby et al., 2004), to visualise the infection and its spread throughout the leaf in more detail. It will provide valuable information on whether the leaves respond similarly in the WT plants compared to the transgenic lines.

*JAR1*, *PR2*, *MYC2* and *MYB75* genes were primed in this study in the single transgenic A3 plants. This fits the model that expression of JA-response genes are the first step in ISR elicitation (Glazebrook, 2005) and that the ISR response, triggered by acetoin, is *NPR1*-dependent (Ryu et al., 2004b). It additionally indicates the involvement of a SA-mediated response due to the up-regulation of the *PR2* gene. The *PR2* gene acts as a hallmark for a SA-mediated SAR response (Rudrappa et al., 2010; Mathys et al., 2012). This also supports the findings in recent studies that elicitation of ISR is not SA-independent as originally hypothesized (Mathys et al., 2012; Pieterse et al., 2014a; Pieterse et al., 2014b). Still confusing is that only few of the chosen genes in AB2 plants showed any priming (*NPR1* and only a low level for *JAR1*). *PR2* expression was present at a high level at 0 and 24 hpi, completely different to WT with expression at 48 hpi. Conversion of most acetoin to 2,3-BD, might have occurred thereby eliciting a SAR response rather than an ISR response (at lower levels). It has yet also to be confirmed that the transgenic lines do actually produce any detectable level of volatile (Dempers, 2014) despite that both genes are present and transcribed. With expression of *ALDC* and/or *BDH1*, certain immune responses might be triggered, but not sufficient to protect the plant in comparison when VOCs are exogenously added to the plant (Ryu et al., 2004a; Kwon et al., 2010; Rudrappa et al., 2010).

### **3.5 CONCLUSIONS**

*Arabidopsis* transgenic AB2 lines challenged with *B. cinerea* showed no significant increase in disease resistance. The A3 line, expressing the *ALDC* gene, exhibited an interesting phenotypic response in the infected leaves 48 hours post inoculation with the fungal spore suspension. A form of programmed cell death (or a heightened hypersensitive response) was observed around the point of infection in the A3 line, which was not present in the inoculated B8 (containing only the *BDH1* gene) or the inoculated WT leaves. Additional observations were made that the infected leaves were prematurely abscised before further spread of infection could occur. The observed abscission was not present in the B8 line or the WT plant, which rather exhibited the formation of large amounts of *B. cinerea* mycelia on the infected leaves that spread to the surrounding leaves.

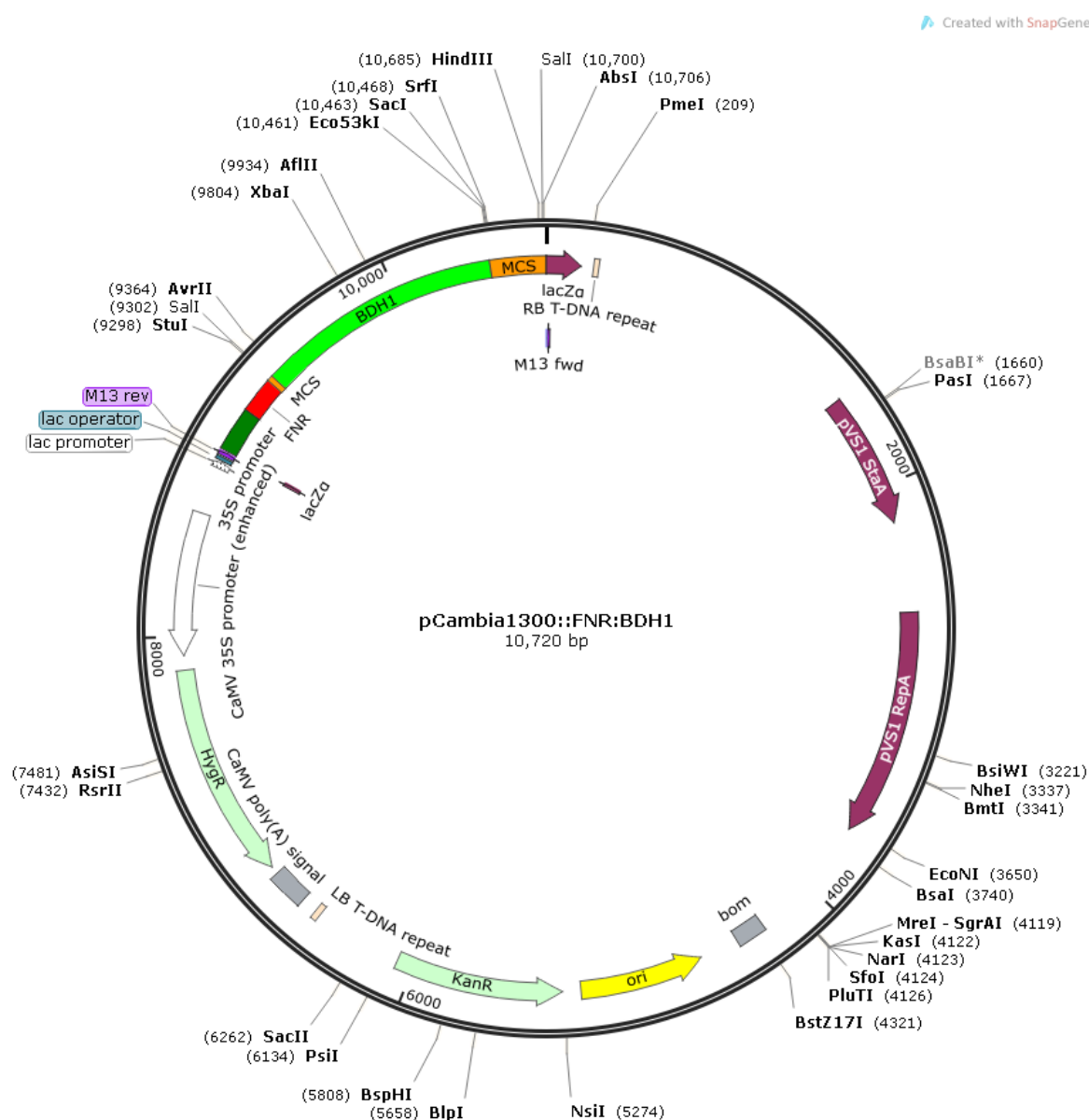
Analysis on a transcriptomic level with sqRT-PCR indicated that *Arabidopsis* A3 line was ISR-primed before *B. cinerea* infection. This priming phenomenon was not present in the AB2, B8 or WT lines. It was, however, also observed when *Arabidopsis* WT plants were treated with synthetic acetoin and 2,3-butanediol exogenously. The addition of the volatile prior to *B. cinerea* infection caused an up-regulation of certain immune-related genes. Treatment with 2,3-butanediol triggered priming of the *PR2*, *MYC2* and *ERF1* genes, while acetoin treatment indicated up-regulation in the *JAR1* and *MYC2* genes. The A3 line indicated priming in four separate genes including *JAR1*, *MYC2*, *MYB75* and *PR2*. It was additionally observed from the sqRT-PCR that JA-related, *JAR1*, and SA-related, *PR2*, genes were up-regulated during the first 48 hours post infection. The transcriptomic data therefore indicated that the immune response elicited in both the volatile treated and the A3 line, was not SA-independent.

Future studies need to investigate whether the transgenic plants release any volatiles and whether acetoin and 2,3-BD are indeed present in transgenic plants. To also obtain any statistical significance, a larger sample size might be tested and a statistical analysis with ANNOVA applied. For this study measurement only included three biological repeats per transgenic line due to limited seed availability. In future studies, it would also be beneficial to include more than one line for each genotype (i.e A, B or AB lines). Further increasing sample size might also include inoculating more than five leaves per plant. The experiment could be transferred to an *in vitro* environment where detached leaves are monitored individually, instead of whole plants in the propagation boxes. Using detached leaves is common practise and was used in previous studies to show disease development on a quantitative level (Thomma et al., 1998; Denby et al., 2004; AbuQamar et al., 2006).

### **3.6 ANNEXURES**

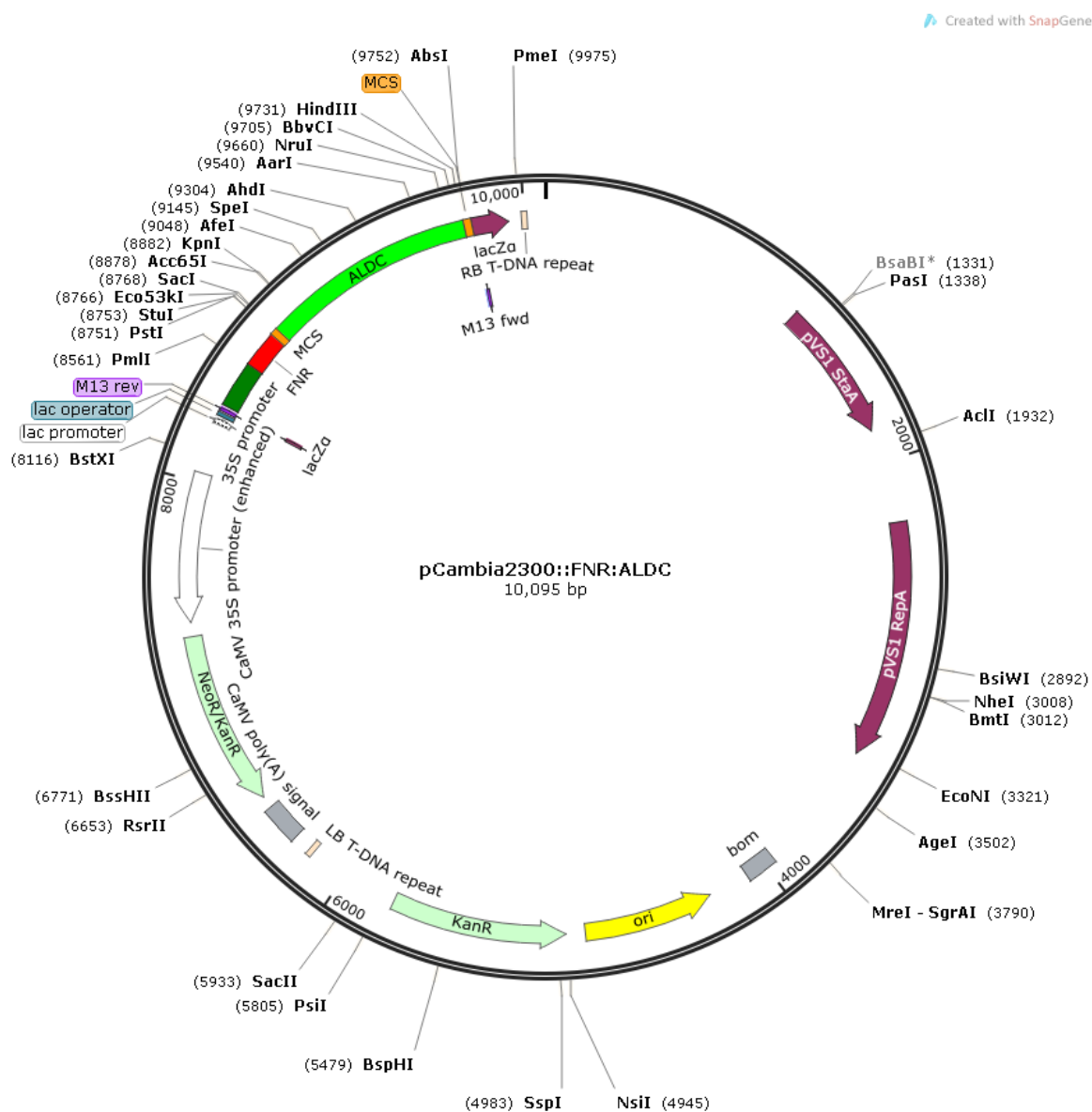
## Annexure A

Vector map of plant transformation vector *pCambia1300::FNR:BDH1* as created by D. Dempers (2014).



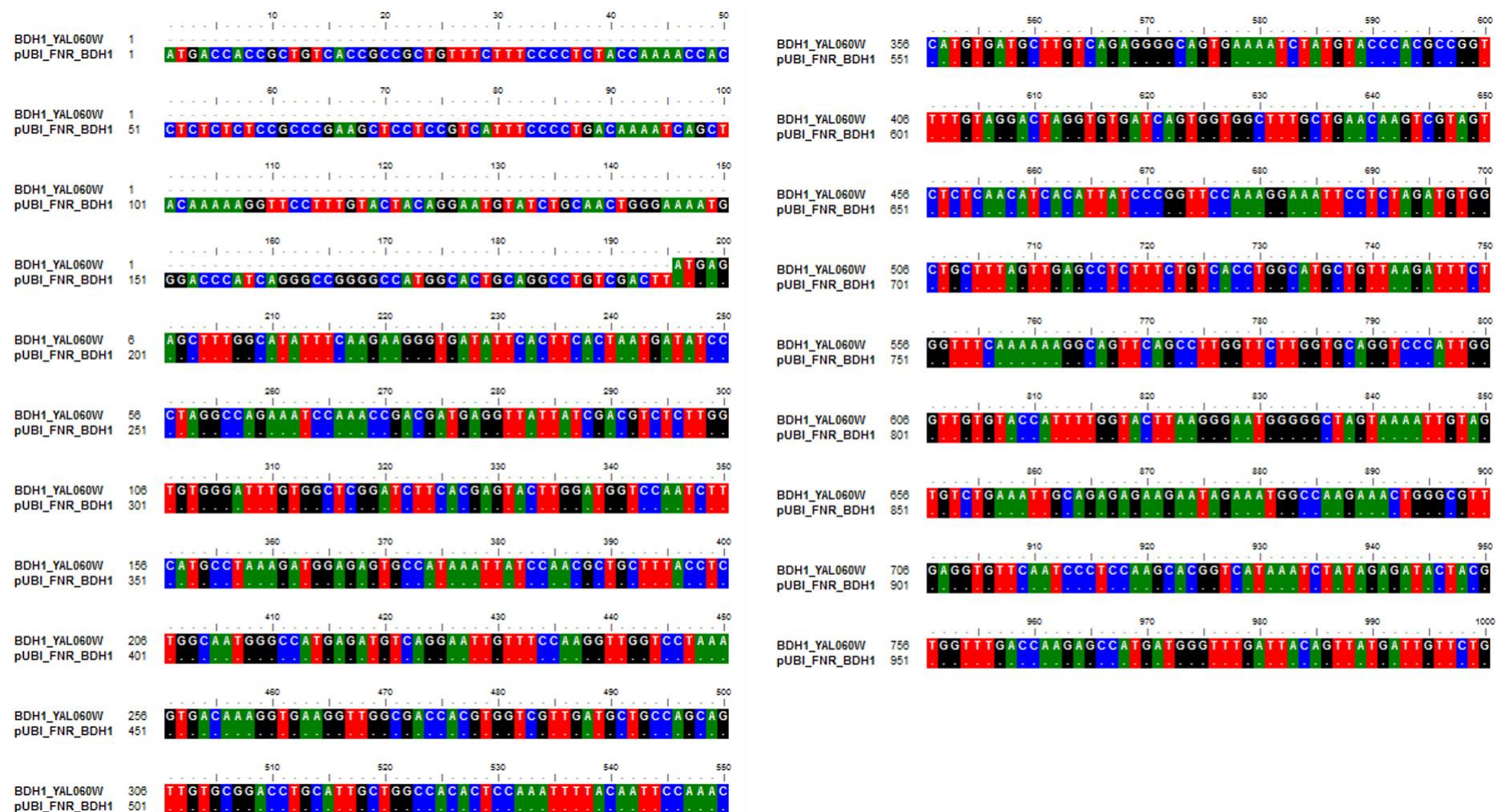
## Annexure B

Vector map of plant transformation vector *pCambia2300::FNR:ALDC* as created by D. Dempers (2014).



## Annexure C

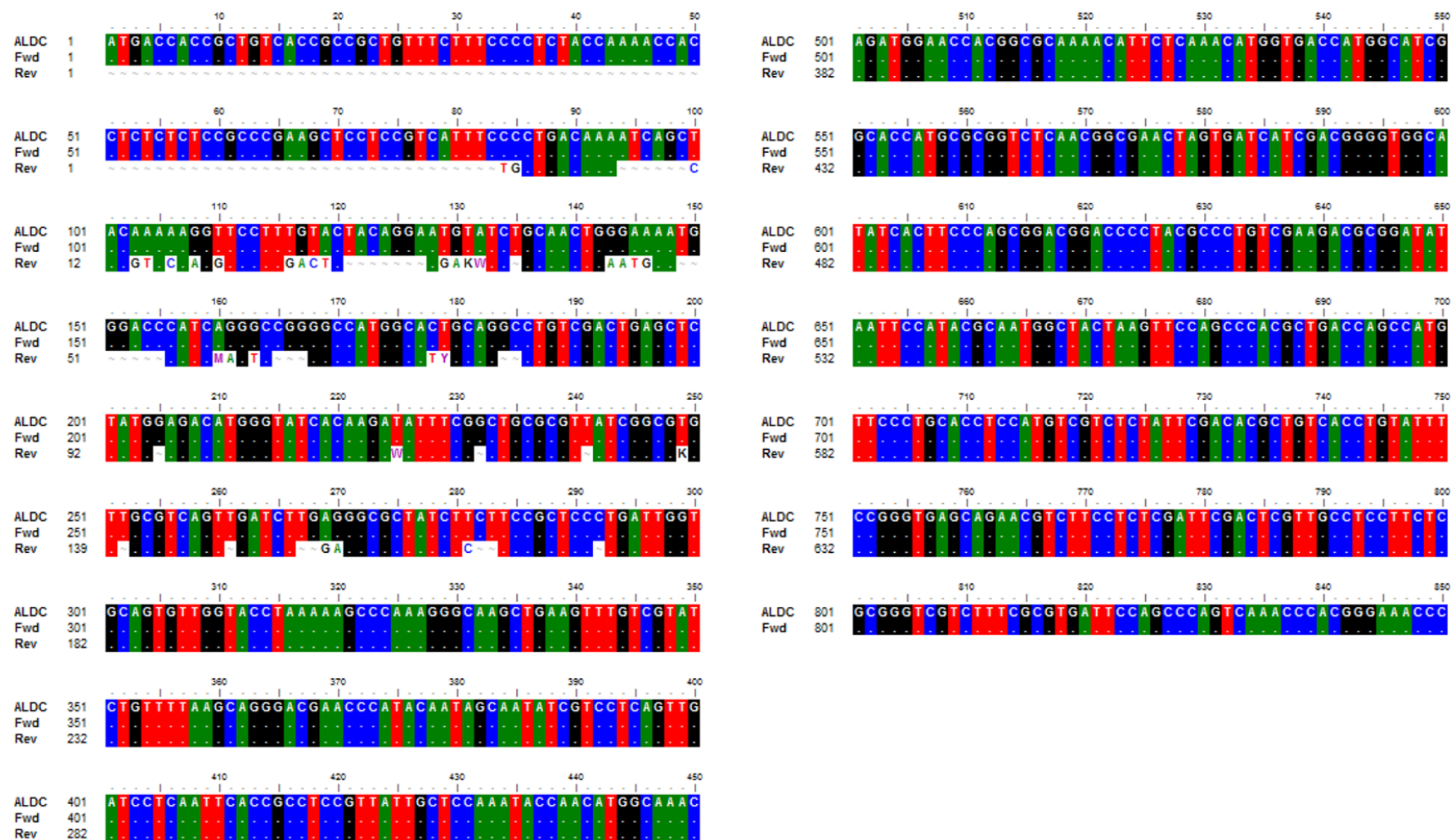
Full sequence data for the sugarcane transformation vector pUBI::FNR:BDH1





## Annexure D

Full sequence data for the sugarcane transformation vector *pUBI::FNR:ALDC*



## **CHAPTER 4**

### **General Conclusions and Future Prospects**



In this study RNA-interference (RNAi) based technology was employed to attempt the silencing of the *cytokinin oxidase/dehydrogenase* (*CKX*) gene family, present in sugarcane. The gene family transcribed for the CKX enzyme is known to break down cytokinin in plants and maintain the cytokinin homeostasis. It was hypothesized that silencing one or a number of the *CKX* genes, it would result in increased plant growth. This postulated growth increase was observed in a previous study, where the transgenic barley indicated increased root and shoot mass (Zalewski et al., 2010). To repeat these results in sugarcane, an RNAi construct had to be created. An area of high homology within the *CKX* gene family was, however, first determined with a multiple sequence alignment and subsequent phylogenetic analysis. The alignment and analysis aided in identifying a conserved gene region. The identified conserved area, approximately 300 bp in size, was cloned into the pUBI510+ transformation vector and an RNAi construct applying the newly optimized isothermal *in vitro* recombination system (IR-hpRNAi) developed by Jiang et al., (2013), was successfully optimized during this Master's study. This was done with the ultimately goal of silencing multiple *CKX* genes to obtain growth promoting low cytokine levels in transgenic sugarcane.

Optimization identified in particular two important steps to create a silencing construct with the IR-hpRNAi system. The first important consideration was the design of primer pairs to amplify sense and antisense strands. The complementary areas included in the primer design should not exceed 20 to 30 bp, for optimum recombination to occur. An additional important factor is the design of a primer within the intron area included in the hairpin. This will allow for PCR identification of potential positive constructs, because it aids to prevent the self-annealing of sense and anti-sense strands within the hairpin construct during PCR analysis. Due to difficulties experienced during optimization of the IR-hpRNAi process, a GATEWAY® cloning system was also used successfully to create a second hairpin construct with the monocot transformation vector, pHb7GW-I-WG-UBIL, acting as destination vector. The constructed RNAi vectors will subsequently be employed in follow-up studies, where sugarcane is transformed and resulting transgenic plants are assessed in regards to *CKX* gene expression and plant growth.

For the second part of the study disease resistance due to *ALDC* and *BDH1* expression was evaluated, as an alternative strategy to improve sugarcane growth. Results indicated an increased pathogen resistance in transgenic *A. thaliana* A3 lines. The AB2 line contained both the *ALDC* and *BDH1* gene, responsible for acetoin and 2,3-butanediol production and no conclusive result could be obtained for these transgenic plants in regards to disease resistance. The increased pathogen resistance observed in the A3 line was very likely due to an induced systemic response (ISR), elicited by the PGPR-produced volatile organic compounds. Both the AB2 and A3 lines exhibited an interesting phenotypic response to *B.*

*cinerea*, with an increased level of necrosis around the point of infection. Further transcriptomic analysis conducted with sqRT-PCR indicated the possible involvement of salicylic acid (SA)-mediated immune responses in *B. cinerea* challenged A3 and AB2 lines.

An interesting observation was that the AB2 line showed a decrease in resistance when lesion size and the scoring of lesion development in particular was considered. Three possibilities might explain this phenomena. The decrease in resistance is possibly caused by metabolic strain from the *ALDC* and *BDH1* genes that it is then unable to protect itself from pathogen attack. The second possibility might be that acetoin and 2,3-butanediol volatiles are required to elicit the full ISR-response. The third possibility is that the acetoin produced in the AB2 line is converted to 2,3-BD at such a quick rate, that it fails to elicit a full ISR-response in the plant. However, supporting evidence for these possibilities will be investigated in future research.

To confirm the phenomenon of increased resistance observed in the A3 line, more than one single transgenic line should be tested, as confirmation that the increased resistance is a consistent result. More detailed studies might also be conducted with different plant pathogens to see if resistance remains. An important suggestion for future studies is also to include qRT-PCR results and not only semi-quantitative results to more exactly determine gene expression. This technique is known to be more reliable for RNA quantification (Bustin and Mueller, 2005) and will enable the use of smaller genes such as *PDF1.2*. This suggestion is made because of the inconsistent results obtained from *PDF1.3*. Since measuring the disease development in infected transgenic, as well as VOC treated plants, was challenging, future studies might employ alternative pathogens like *P. syringae*. Such pathogens have been routinely employed in previous studies and provide more reliable methods for quantifying disease instance (Ryu *et al.*, 2004; Kwon *et al.*, 2010; Rudrappa *et al.*, 2010). Alternatively, *B. cinerea* lesion development might be monitored with additional lactophenol-trypan blue staining and subsequent counting of conidiospores (Govrin and Levine, 2002; Meng *et al.*, 2013). This technique allows for an in-depth analysis of how the *B. cinerea* infection spreads throughout the leaf.

In order to confirm the lower resistance observed in the AB2 line, most important will be to test more double transgenic lines in the future. It will also help to obtain more quantitative data for lesion measurements to carry out a better statistical analysis. If indeed statistically significant higher sensitivity to *B. cinerea* attack is found with more lines other model plant species (e.g. tobacco) might be tested in addition to different types of plant pathogens.

To assess the hypothesised hypersensitive response in the A3, and possibly the AB2 line, it would be wise to include hallmark genes to indicate the involvement of programmed cell death

in the leaf of the elicitation of a SA-mediated hypersensitive response in the leaf, post inoculation. The lactophenol-trypan blue staining will for example indicate the cellular response on a phenotypic level and the additional hallmark genes on a transcriptomic level.

## **LITERATURE CITED**

- AbuQamar S, Chen X, Dhawan R, Bluhm B, Salmeron J, Lam S, Dietrich R, Mengiste T** (2006) Expression profiling and mutant analysis reveals complex regulatory networks involved in Arabidopsis response to Botrytis infection. *Plant J* **48**: 28–44
- Aitken KS, McNeil MD, Hermann S, Bundock PC, Kilian A, Heller-Uszynska K, Henry RJ, Li J** (2014) A comprehensive genetic map of sugarcane that provides enhanced map coverage and integrates high-throughput Diversity Array Technology (DART) markers. *BMC Genomics* **15**: 152
- Armstrong DJ, Firtel RA** (1989) Cytokinin oxidase activity in the cellular slime mold, *Dictyostelium discoideum*. *Dev Biol* **136**: 491–499
- Ashikari M, Sakakibara H, Lin S, Yamamoto T** (2014) Cytokinin Oxidase Regulates Rice Grain Production. *Science* **309**: 741–745
- Auer CA** (1997) Cytokinin conjugation : recent advances and patterns in plant evolution. *Plant Growth Regul* **23**: 17–32
- Avalbaev M, Somov K, Yuldashev R, Shakirova FM** (2012) Cytokinin oxidase is key enzyme of cytokinin degradation. *Biochem Biokhimiia* **77**: 1354–61
- Bashan Y, de-Bashan LE, Prabhu SR, Hernandez JP** (2014) Advances in plant growth-promoting bacterial inoculant technology: Formulations and practical perspectives (1998-2013). *Plant Soil* **378**: 1–33
- Bhattacharyya PN, Jha DK** (2012) Plant growth-promoting rhizobacteria (PGPR): Emergence in agriculture. *World J Microbiol Biotechnol* **28**: 1327–1350
- Bilyeu KD, Cole JL, Laskey JG, Riekhof WR, Esparza TJ, Kramer MD, Morris RO** (2001) Molecular and biochemical characterization of a cytokinin oxidase from maize. *Plant Physiol* **125**: 378–386
- Booth IR** (1985) Regulation of cytoplasmic pH in bacteria. *Microbiol Rev* **49**: 359–378
- Bostock RM** (2005) Signal crosstalk and induced resistance: straddling the line between cost and benefit. *Annu Rev Phytopathol* **43**: 545–580
- Burch LR, Horgan R** (1989) The purification of cytokinin oxidase from *Zea mays* kernels. *Phytochemistry* **28**: 1313–1319

- Bustin SA, Mueller R** (2005) Real-time reverse transcription PCR (qRT-PCR) and its potential use in clinical diagnosis. *Clin Sci* **109**: 365–379
- Celińska E, Grajek W** (2009) Biotechnological production of 2,3-butanediol—Current state and prospects. *Biotechnol Adv* **27**: 715–725
- Choudhary DK, Johri BN** (2009) Interactions of *Bacillus* spp. and plants—with special reference to induced systemic resistance (ISR). *Microbiol Res* **164**: 493–513
- Cook RJ, Misono KS, Wagner C** (1984) Identification of the covalently bound flavin of dimethylglycine dehydrogenase and sarcosine dehydrogenase from rat liver mitochondria. *J Biol Chem* **259**: 12475–80
- Crespi M, Vereecke D, Temmerman W, Van Montagu M, Desomer J** (1994) The *fas* operon of *Rhodococcus fascians* encodes new genes required for efficient fasciation of host plants. *J Bacteriol* **176**: 2492–501
- Delaney TP** (1997) Genetic dissection of acquired resistance to disease. *Plant Physiol* **113**: 5–12
- Dempers D** (2014) Overexpression of  $\alpha$ -acetolactate decarboxylase and acetoin reductase/2,3-butanediol dehydrogenase in *Arabidopsis thaliana*. Masters thesis. Stellenbosch University, South Africa.
- Denby KJ, Kumar P, Kliebenstein DJ** (2004) Identification of *Botrytis cinerea* susceptibility loci in *Arabidopsis thaliana*. *Plant Journal* **38**: 473–486
- Duijff BJ, Pouhair D, Olivain C, Alabouvette C, Lemanceau P** (1998) Implication of systemic induced resistance in the suppression of fusarium wilt of tomato by *Pseudomonas fluorescens* WCS417r and by nonpathogenic *Fusarium oxysporum* Fo47. *Eur J Plant Pathol* **104**: 903–910
- Ellis T, Adie T, Baldwin GS** (2011) DNA assembly for synthetic biology: from parts to pathways and beyond. *Integr Biol (Camb)* **3**: 109–118
- Van der Ent S, Van Wees SCM, Pieterse CMJ** (2009) Jasmonate signaling in plant interactions with resistance-inducing beneficial microbes. *Phytochemistry* **70**: 1581–1588
- Falco MC, Tulmann Neto a., Ulian EC** (2000) Transformation and expression of a gene for herbicide resistance in a Brazilian sugarcane. *Plant Cell Rep* **19**: 1188–1194

- Farag MA, Ryu C-M, Sumner LW, Paré PW** (2006) GC–MS SPME profiling of rhizobacterial volatiles reveals prospective inducers of growth promotion and induced systemic resistance in plants. *Phytochemistry* **67**: 2262–2268
- Farmer EE** (2001) Surface-to-air signals. *Nature* **411**: 854–856
- Forlani G, Mantelli M, Nielsen E** (1999) Biochemical evidence for multiple acetoin-forming enzymes in cultured plant cells. *Phytochemistry* **50**: 255–262
- Frebort I, Kowalska M, Hluska T, Frebortova J, Galuszka P** (2011) Evolution of cytokinin biosynthesis and degradation. *J Exp Bot* **62**: 2431–2452
- Frébort I, Sebela M, Galuszka P, Werner T, Schmölling T, Pec P** (2002) Cytokinin oxidase/cytokinin dehydrogenase assay: optimized procedures and applications. *Anal Biochem* **306**: 1–7
- Galuszka P, Frébortová J, Werner T, Yamada M, Strnad M, Schmölling T, Frébort I** (2004) Cytokinin oxidase/dehydrogenase genes in barley and wheat. *Eur J Biochem* **271**: 3990–4002
- Gibson DG** (2011) Enzymatic Assembly of Overlapping DNA Fragments. **498**: 349–361
- Glazebrook J** (2005) Contrasting Mechanisms of Defense Against Biotrophic and Necrotrophic Pathogens. *Annu Rev Phytopathol* **43**: 205–227
- Glick BR** (2012) Plant growth-promoting bacteria: mechanisms and applications. *Scientifica (Cairo)* **2012**: 1-15
- Govrin EM, Levine A** (2002) Infection of Arabidopsis with a necrotrophic pathogen, *Botrytis cinerea*, elicits various defense responses but does not induce systemic acquired resistance (SAR). *Plant Mol Biol* **48**: 267–276
- Groenewald JH, Botha FC** (2008) Down-regulation of pyrophosphate: Fructose 6-phosphate 1-phosphotransferase (PFP) activity in sugarcane enhances sucrose accumulation in immature internodes. *Transgenic Res* **17**: 85–92
- Hauge B, Oggero C, Nguyen N, Fu C, Dong F** (2009) Single tube, high throughput cloning of inverted repeat constructs for double-stranded RNA expression. *PLoS One* **4**: 1-10
- Houba-Hérin N, Pethe C, d'Alayer J, Laloue M** (1999) Cytokinin oxidase from *Zea mays*: purification, cDNA cloning and expression in moss protoplasts. *Plant J* **17**: 615–26
- Hwang I, Sheen J, Müller B** (2012) Cytokinin Signaling Networks. *Annu Rev Plant Biol* **63**:

353–380

- Ingelbrecht IL, Post JE, Mirkov. I and TE** (1999) Post transcriptional gene silencing in transgenic sugarcane. Dissection of homology-dependent virus resistance in a monocot that has a complex polyploid genome. *Plant Physiol* **119**: 1189–1198
- Iyer LM, Kumpatla SP, Chandrasekharan MB, Hall TC** (2000) Transgene silencing in monocots. *Plant Mol Biol* **43**: 323–346
- Ji X-J, Huang H, Ouyang P-K** (2011) Microbial 2,3-butanediol production: A state-of-the-art review. *Biotechnol Adv* **29**: 351–364
- Jiang Y, Xie M, Zhu Q, Ma X, Li X, Liu Y, Zhang Q** (2013) One-step cloning of intron-containing hairpin RNA constructs for RNA interference via isothermal *in vitro* recombination system. *Planta* **238**: 325–330
- Jones ML, Barnard RT** (2005) Chimerization of multiple antibody classes using splice overlap extension PCR. *Biotechniques* **38**: 181–182
- Joyce P, Hermann S, O’Connell A, Dinh Q, Shumbe L, Lakshmanan P** (2014) Field performance of transgenic sugarcane produced using *Agrobacterium* and biolistics methods. *Plant Biotechnol J* **12**: 411–424
- Jung JH, Vermerris W, Gallo M, Fedenko JR, Erickson JE, Altpeter F** (2013) RNA interference suppression of lignin biosynthesis increases fermentable sugar yields for biofuel production from field-grown sugarcane. *Plant Biotechnol J* **11**: 709–716
- Kaneko T, Nakamura Y, Wolk CP, Kuritz T, Sasamoto S, Watanabe A, Iriguchi M, Ishikawa A, Kawashima K, Kimura T, et al** (2001) Complete genomic sequence of the filamentous nitrogen-fixing cyanobacterium *Anabaena* sp. strain PCC 7120. *DNA Res* **8**: 205–253
- Karimi M, Depicker A, Hilson P** (2007) Recombinational Cloning with Plant Gateway Vectors. *Plant Physiol* **145**: 1144–1154
- Van Kast C a, Laten HM** (1987) Cytokinin Utilization by Adenine-Requiring Mutants of the Yeast *Saccharomyces cerevisiae*. *Plant Physiol* **83**: 726–7
- Kloepper JW** (1980) Effects of Rhizosphere Colonization by Plant Growth-Promoting Rhizobacteria on Potato Plant Development and Yield. *Phytopathology* **70**: 1078
- Kojima M, Kamada-Nobusada T, Komatsu H, Takei K, Kuroha T, Mizutani M, Ashikari**

- M, Ueguchi-Tanaka M, Matsuoka M, Suzuki K, et al** (2009) Highly Sensitive and High-Throughput Analysis of Plant Hormones Using MS-Probe Modification and Liquid Chromatography-Tandem Mass Spectrometry: An Application for Hormone Profiling in *Oryza sativa*. *Plant Cell Physiol* **50**: 1201–1214
- Kunkel BN, Brooks DM** (2002) Cross talk between signaling pathways in pathogen defense. *Curr Opin Plant Biol* **5**: 325–331
- Kwon YS, Ryu CM, Lee S, Park HB, Han KS, Lee JH, Lee K, Chung WS, Jeong MJ, Kim HK, et al** (2010) Proteome analysis of *Arabidopsis* seedlings exposed to bacterial volatiles. *Planta* **232**: 1355–1370
- Laloue M, Fox JE** (1989) Cytokinin oxidase from wheat: partial purification and general properties. *Plant Physiol* **90**: 899–906
- Lee B, Farag M a., Park HB, Kloepper JW, Lee SH, Ryu CM** (2012) Induced Resistance by a Long-Chain Bacterial Volatile: Elicitation of Plant Systemic Defense by a C13 Volatile Produced by *Paenibacillus polymyxa*. *PLoS One* **7**: 1–11
- Lina B a R, Jonker D, Kozianowski G** (2002) Isomaltulose (Palatinose??): A review of biological and toxicological studies. *Food Chem Toxicol* **40**: 1375–1381
- van Loon LC** (2007) Plant responses to plant growth-promoting rhizobacteria. *Eur J Plant Pathol* **119**: 243–254
- Loon LC Van, Bakker PAHM, Pieterse CMJ** (1998) Systemic resistance induced by rhizosphere bacteria. *Phytopathology* **36**: 453–483
- van Loon LC, Geraats BPJ, Linthorst HJM** (2006) Ethylene as a modulator of disease resistance in plants. *Trends Plant Sci* **11**: 184–191
- Malito E, Coda A, Bilyeu KD, Fraaije MW, Mattevi A** (2004) Structures of Michaelis and product complexes of plant cytokinin dehydrogenase: implications for flavoenzyme catalysis. *J Mol Biol* **341**: 1237–1249
- Massonneau A, Houba-Hérin N, Pethe C, Madzak C, Falque M, Mercy M, Kopecny D, Majira A, Rogowsky P, Laloue M** (2004) Maize cytokinin oxidase genes: differential expression and cloning of two new cDNAs. *J Exp Bot* **55**: 2549–57
- Mathys J, De Cremer K, Timmermans P, Van Kerckhove S, Lievens B, Vanhaecke M, Cammue BP a., De Coninck B** (2012) Genome-Wide Characterization of ISR Induced in *Arabidopsis thaliana* by *Trichoderma hamatum* T382 Against *Botrytis cinerea*



Infection. Front Plant Sci **3**: 1–25

- Maurhofer M, Reimann C, Schmidli-Sacherer P, Heeb S, Haas D, Défago G** (1998) Salicylic Acid Biosynthetic Genes Expressed in *Pseudomonas fluorescens* Strain P3 Improve the Induction of Systemic Resistance in Tobacco Against Tobacco Necrosis Virus. *Phytopathology* **88**: 678–84
- Miller CO, Skoog F, Okumura FS, Von Saltza MH, Strong FM** (1956) Isolation, Structure and Synthesis of Kinetin, a Substance Promoting Cell Division<sup>1,2</sup>. *J Am Chem Soc* **78**: 1375–1380
- Mok DWS, Mok MC** (2001) Etabolism and. 89–118
- Mok MC, Martin RC, Mok DWS, In S, Cellular V, Plant DB, Apr NM** (2015) Cytokinins : Biosynthesis , Metabolism and Perception Published by : Society for In Vitro Biology. **36**: 102–107
- Morris RO, Bilyeu KD, Laskey JG, Cheikh NN** (1999) Isolation of a gene encoding a glycosylated cytokinin oxidase from maize. *Biochem Biophys Res Commun* **255**: 328–33
- Murai N** (2014) Review: Plant growth hormone cytokinins control the crop seed yield. *Am J Plant Sci* **5**: 2178–2187
- Murashige T und Skoog F** (1962) A Revised Medium for Rapid Growth and Bio Assays with Tobacco Tissue Cultures. *Physiol Plant* **15**: 473–497
- Nakashimada Y, Srinivasan K, Murakami M, Nishio N** (2000) Direct conversion of cellulose to methane by anaerobic fungus *Neocallimastix frontalis* and defined methanogens. *Biotechnol Lett* **22**: 223–227
- Naylor M, Murphy AM, Berry JO, Carr JP** (1998) Salicylic Acid Can Induce Resistance to Plant Virus Movement. *Mol Plant-Microbe Interact* **11**: 860–868
- Nehra V, Choudhary M** (2015) A review on plant growth promoting rhizobacteria acting as bioinoculants and their biological approach towards the production of sustainable agriculture. *Journal of Appl Natural Science* **7(1)**: 540-556
- Nicander B, Bjorkman PO, Tillberg E** (1995) Identification of an N-Glucoside of cis-Zeatin from Potato Tuber Sprouts. *Plant Physiol* **109**: 513–516
- Noguera A, Enrique R, Perera MF, Ostengo S, Racedo J, Costilla D, Zossi S, Cuenya**

- MI, Filippone MP, Welin B, et al** (2015) Genetic characterization and field evaluation to recover parental phenotype in transgenic sugarcane: a step toward commercial release. *Mol Breed* **35**: 115
- Osabe K, Mudge S, Graham M, Birch R** (2009) RNAi Mediated Down-Regulation of PDS Gene Expression in Sugarcane (*Saccharum*), a Highly Polyploid Crop. *Trop Plant Biol* **2**: 143–148
- Otsuka M, Harada N, Itabashi T, Ohmori S** (1999) Blood and urinary levels of ethanol, acetaldehyde, and C4 compounds such as diacetyl, acetoin, and 2,3-butanediol in normal male students after ethanol ingestion. *Alcohol* **17**: 119–24
- Pastori GM, Wilkinson MD, Steele SH, Sparks CA, Jones HD, Parry MAJ** (2001) Age-dependent transformation frequency in elite wheat varieties. *J Exp Bot* **52**: 857–863
- Pieterse CMJ** (1998) A Novel Signaling Pathway Controlling Induced Systemic Resistance in *Arabidopsis*. *Plant Cell* **10**: 1571–1580
- Pieterse CMJ, Wees SCM Van, Pelt JA Van, Knoester M** (2014a) A Novel Signaling Pathway Controlling Induced Systemic Resistance in *Arabidopsis* Ramon Laan , Han Gerrits , Peter J . Weisbeek and Leendert C . van Loon Published by : American Society of Plant Biologists ( ASPB ) *Science* **10**: 1571–1580
- Pieterse CMJ, Zamioudis C, Berendsen RL, Weller DM, Van Wees SCM, Bakker PAHM** (2014b) Induced Systemic Resistance by Beneficial Microbes. *Annu Rev Phytopathol* **52**: 347–375
- Pimentel D, Patzek TW** (2005) Ethanol Production Using Corn, Switchgrass, and Wood; Biodiesel Production Using Soybean and Sunflower. *Nat Resour Res* **14**: 65–76
- Press CM, Loper JE, Kloepper JW** (2001) Role of iron in rhizobacteria-mediated induced systemic resistance of cucumber. *Phytopathology* **91**: 593–598
- Qin H, Gu Q, Zhang J, Sun L, Kuppu S, Zhang Y, Burow M, Payton P, Blumwald E, Zhang H** (2011) Regulated expression of an isopentenyltransferase gene (IPT) in peanut significantly improves drought tolerance and increases yield under field conditions. *Plant Cell Physiol* **52**: 1904–14
- Rapulana T, Bouwer G** (2013) Toxicity to *Eldana saccharina* of a recombinant *Gluconacetobacter diazotrophicus* strain carrying a truncated *Bacillus thuringiensis* cry1Ac gene. *African J Microbiol Res* **7**: 1207–1214

- Robert-Seilanianantz A, Navarro L, Bari R, Jones JD** (2007) Pathological hormone imbalances. *Curr Opin Plant Biol* **10**: 372–379
- Ronquist F, Teslenko M, van der Mark P, Ayres DL, Darling A, Hohna S, Larget B, Liu L, Suchard MA, Huelsenbeck JP** (2012) MrBayes 3.2: Efficient Bayesian Phylogenetic Inference and Model Choice Across a Large Model Space. *Syst Biol* **61**: 539–542
- Rudrappa T, Biedrzycki ML, Kunjeti SG, Donofrio NM, Czymmek KJ, Paré PW, Bais HP** (2010) The rhizobacterial elicitor acetoin induces systemic resistance in *Arabidopsis thaliana*. *Commun Integr Biol* **3**: 130–138
- Ryals J, Uknes S, Ward E** (1994) Systemic Acquired Resistance. *Plant Physiol* **104**: 1109–1112
- Ryu C-M, Farag M a, Hu C-H, Reddy MS, Wei H-X, Paré PW, Kloepper JW** (2003) Bacterial volatiles promote growth in *Arabidopsis*. *Proc Natl Acad Sci U S A* **100**: 4927–4932
- Ryu CM, Farag MA, Hu C, Reddy MS, Kloepper JW, Pare PW** (2004a) Bacterial Volatiles Induce Systemic Resistance in *Arabidopsis*. *Plant Physiol* **134**: 1017–1026
- Ryu C-M, Hu C-H, Locy RD, Kloepper JW** (2005) Study of mechanisms for plant growth promotion elicited by rhizobacteria in *Arabidopsis thaliana*. *Plant Soil* **268**: 285–292
- Ryu C-M, Murphy JF, Mysore KS, Kloepper JW** (2004b) Plant growth-promoting rhizobacteria systemically protect *Arabidopsis thaliana* against *Cucumber mosaic virus* by a salicylic acid and NPR1-independent and jasmonic acid-dependent signaling pathway. *Plant J* **39**: 381–392
- Sambrook J, MacCallum P** (2013) Molecular cloning: a laboratory manual. 4<sup>th</sup> Edition. Cold Spring Harbour Laboratory Press.
- Saurabh S, Vidyarthi AS, Prasad D** (2014) RNA interference: concept to reality in crop improvement. *Planta* **239**: 543–564
- Schmülling T, Werner T, Riefler M, Krupková E, Bartrina Y Manns I** (2003) Structure and function of cytokinin oxidase/dehydrogenase genes of maize, rice, *Arabidopsis* and other species. *J Plant Res* **116**: 241–252
- Schreiber K, Ckurshumova W, Peek J, Desveaux D** (2008) A high-throughput chemical screen for resistance to *Pseudomonas syringae* in *Arabidopsis*. *Plant J* **54**: 522–531

- Smehilová M, Galuszka P, Bilyeu KD, Jaworek P, Kowalska M, Sebela M, Sedlářová M, English JT, Frébort I** (2009) Subcellular localization and biochemical comparison of cytosolic and secreted cytokinin dehydrogenase enzymes from maize. *J Exp Bot* **60**: 2701–12
- Smith JL, De Moraes CM, Mescher MC** (2009) Jasmonate- and salicylate-mediated plant defense responses to insect herbivores, pathogens and parasitic plants. *Pest Manag Sci* **65**: 497–503
- Song G, Ryu C-M** (2013) Two Volatile Organic Compounds Trigger Plant Self-Defense against a Bacterial Pathogen and a Sucking Insect in Cucumber under Open Field Conditions. *Int J Mol Sci* **14**: 9803–9819
- Spíchal L** (2012) Cytokinins - Recent news and views of evolutionally old molecules. *Funct Plant Biol* **39**: 267–284
- Sun J, Rao B, Zhang L, Shen Y, Wei D** (2012) Extraction of Acetoin From Fermentation Broth Using an Acetone/Phosphate Aqueous Two-Phase System. *Chem Eng Commun* **199**: 1492–1503
- Suttle JC, Mornet R** (2005) Mechanism-based irreversible inhibitors of cytokinin dehydrogenase. *J Plant Physiol* **162**: 1189–96
- Thomma BPHJ, Eggermont K, Penninckx IAMA, Mauch-Mani B, Vogelsang R, Cammue BPA, Broekaert WF** (1998) Separate jasmonate-dependent and salicylate-dependent defense-response pathways in *Arabidopsis* are essential for resistance to distinct microbial pathogens. *Proc Natl Acad Sci U S A* **95**: 15107–15111
- Timmusk S, Nicander B, Granhall U, Tillberg E** (1999) Cytokinin production by *Paenibacillus polymyxa*. *Soil Biol Biochem* **31**: 1847–1852
- Ton J, Davison S, Van Wees SC, Van Loon L, Pieterse CM** (2001) The *arabidopsis* ISR1 locus controlling rhizobacteria-mediated induced systemic resistance is involved in ethylene signaling. *Plant Physiol* **125**: 652–661
- Verhagen BWM, Glazebrook J, Zhu T, Chang H-S, van Loon LC, Pieterse CMJ** (2004) The transcriptome of rhizobacteria-induced systemic resistance in *arabidopsis*. *Mol Plant Microbe Interact* **17**: 895–908
- Vyroubalova S, Vaclavikova K, Tureckova V, Novak O, Smehilova M, Hluska T, Ohnoutkova L, Frebort I, Galuszka P** (2009) Characterization of New Maize Genes

- Putatively Involved in Cytokinin Metabolism and Their Expression during Osmotic Stress in Relation to Cytokinin Levels. *Plant Physiol* **151**: 433–447
- Wang KL, Li H, Ecker JR** (2002) Ethylene Biosynthesis and Signaling Networks. *Plant Cell* **14**: S131–S152
- Van Wees SC, Van der Ent S, Pieterse CM** (2008) Plant immune responses triggered by beneficial microbes. *Curr Opin Plant Biol* **11**: 443–448
- Weller D** (1988) the Rhizosphere With Bacteria. *Ann Rev Phytopathol* **26**: 379–407
- Werner T, Motyka V, Strnad M, Schmülling T** (2001) Regulation of plant growth by cytokinin. *Proc Natl Acad Sci U S A* **98**: 10487–92
- Wesley S V, Helliwell C a, Smith N a, Wang MB, Rouse DT, Liu Q, Gooding PS, Singh SP, Abbott D, Stoutjesdijk P a, et al** (2001) Construct design for efficient, effective and high-throughput gene silencing in plants. *Plant J* **27**: 581–590
- Wu L, Birch RG** (2007) Doubled sugar content in sugarcane plants modified to produce a sucrose isomer. *Plant Biotechnol J* **5**: 109–117
- Xiao Y-H, Yin M-H, Hou L, Pei Y** (2006) Direct amplification of intron-containing hairpin RNA construct from genomic DNA. *Biotechniques* **41**: 548–552
- Xiao Z, Xu P** (2007) Acetoin Metabolism in Bacteria. *Crit Rev Microbiol* **33**: 127–140
- Yang SH, Yu H, Goh CJ** (2003) Functional characterisation of a cytokinin oxidase gene DSKX1 in *Dendrobium* orchid. *Plant Mol Biol* **51**: 237–248
- Yuldashev R, Avalbaev A, Bezrukova M, Vysotskaya L, Khripach V, Shakirova F** (2012) Cytokinin oxidase is involved in the regulation of cytokinin content by 24-epibrassinolide in wheat seedlings. *Plant Physiol Biochem* **55**: 1–6
- Zablotowicz RM, Tipping EM, Lifshitz R, Kloepper JW** (1991) Plant growth promotion mediated by bacterial rhizosphere colonizers. *Rhizosph Plant Growth Beltsv Symp Agric Res* **14**: 315–326
- Zalewski W, Galuszka P, Gasparis S, Orczyk W, Nadolska-Orczyk A** (2010) Silencing of the HvCKX1 gene decreases the cytokinin oxidase/dehydrogenase level in barley and leads to higher plant productivity. *J Exp Bot* **61**: 1839–1851
- Zalewski W, Gasparis S, Boczkowska M, Rajchel IK, Kała M, Orczyk W, Nadolska-Orczyk A** (2014) Expression Patterns of HvCKX Genes Indicate Their Role in Growth

and Reproductive Development of Barley. PLoS One **9**: e115729

**Zalewski W, Orczyk W, Gasparis S, Nadolska-Orczyk A** (2012) HvCKX2 gene silencing by biolistic or Agrobacterium-mediated transformation in barley leads to different phenotypes. BMC Plant Biol **12**: 206

**Zhang X, Henriques R, Lin S-S, Niu Q-W, Chua N-H** (2006) Agrobacterium-mediated transformation of *Arabidopsis thaliana* using the floral dip method. Nat Protoc **1**: 641–646

**Zhou D, Guo J, Xu L, Gao S, Lin Q, Wu Q, Wu L, Que Y** (2014) Establishment and application of a loop-mediated isothermal amplification (LAMP) system for detection of cry1Ac transgenic sugarcane. Sci Rep **4**: 4912